KINETICS AND BENEFITS OF EMPLOYING UV LIGHT FOR THE TREATMENT OF AQUEOUS AMMONIA IN WASTEWATER

by

John Bergese

Submitted in partial fulfilment of the requirements
for the degree of Master of Applied Science

at

Dalhousie University
Halifax, Nova Scotia
August 2013

DEDICATION PAGE

Dedicato alla famiglia e alla mia Patria.

TABLE OF CONTENTS

LIST OF TABLES

LIST OF FIGURES

ABSTRACT

Nitrogen compounds, such as aqueous ammonia, are a widespread problem in the wastewater industry as they are toxic to numerous aquatic life, cause eutrophication, and contribute to various environmental concerns. Environment Canada has mandated new wastewater regulations, limiting un-ionized ammonia discharge to 1.25 mg/L, expressed as nitrogen. This study provides insight into methods for removing nitrogen compounds, specifically aqueous ammonia, from wastewater. Two wastewater treatment technologies were compared: Ultra Violet light and an electrochemical process. These treatments were evaluated individually, as well as in combination, to determine potential synergistic effects.

The UV light experiments were conducted with a collimated beam apparatus and evaluated the effects of pH, UV fluence, initial concentration of nitrogen, and different chloride concentrations on nitrogen removal. Electrochemical experiments, using a Ti/RuO_2 anode with a Ti cathode, evaluated the effects of pH and current density, at two different chloride concentrations on treatment efficacy. The photoelectrochemical process was evaluated in parallel with the electrochemical process to evaluate synergistic effects. All of the treatment technologies were used to treat secondary wastewater effluent obtained from a municipal wastewater plant, Mill Cove Water Pollution Control Centre, Bedford, Nova Scotia.

Results from UV experiments indicated that pH had an impact on removal efficiency. At pH=8.0, no significant removal of total nitrogen was observed, whereas 47.6% and 59.5% removals were observed at pH=10.0 and pH=12.0, respectively. The degradation of total nitrogen was attributed to the removal of aqueous ammonia from the system. Different chloride concentrations did statistically affect removal efficiency. Increased initial contaminant concentration resulted in higher removal efficiencies, which suggests the underlying removal mechanism is proportional to the amount of contaminant present. In order to develop a kinetic model for the degradation of nitrogen compounds, the presence of hydroxyl radicals was confirmed via the degradation of para-chlorobenzoic acid.

Results from the electrochemical experiments demonstrated that both initial pH, and current density had an effect on treatment efficiency. At both chloride concentrations, the system with the highest current density (15 mA/cm^2 at $[Cl^-]$=530 mg/L and 40 mA/cm^2 at $[Cl^-]$=5300 mg/L) at pH=9.7, resulted in the highest efficiency compared to pH=5.7. The production of DBPs (TTHMs and THAAs) was monitored when electrochemically treating municipal wastewater.

Experiments conducted with both a UV light and an electrochemical cell resulted in no synergistic treatment benefits. However, lower levels of chlorine residual were observed in the photoelectrochemical process, which may result in lower DBPs. The photoelectrochemical treatment of municipal wastewater resulted in lower levels of THAAs compared to the electrochemical process.

LIST OF ABBREVIATIONS AND SYMBOLS USED

AOP	Advanced Oxidation Process
Cl^-	Chloride Ion
$Cl\cdot$	Chlorine Radical
Cl_2	Chlorine
COD	Chemical Oxygen Demand
DBP	Disinfection By-Product
DC	Direct Current
e^-	Electron
GC	Gas Chromatography
$h\nu$	Electromagnetic Wave
H^+	Hydrogen Ion
H_2	Hydrogen
H_2O_2	Hydrogen Peroxide
H_2SO_4	Sulfuric Acid
H_3O^+	Hydronium Ion
HAA	Haloacetic Acid
HPLC	High Pressure Liquid Chromatography
HOCl	Hypochlorous Acid
IC	Ion Chromatography
ICP-MS	Inductively Coupled Plasma Mass Spectrometry
LP	Low Pressure
MCWPCC	Mill Cove Water Pollution Control Centre
MDL	Minimum Detection Limit
N_2	Nitrogen Gas
NCl_3	Trichloramine
NH_2	Amidogen
NH_2OH	Hydroxylamine
$NHCl_2$	Dichloramine
NH_2Cl	Monochloramine

NH_3	Ammonia
NH_4^+	Ammonium
NH_4Cl	Ammonium Chloride
NO_2^-	Nitrite Ion
NO_3^-	Nitrate Ion
NO	Nitrogen Monoxide
HNO	Nitroxyl
NS	Nova Scotia
NaCl	Sodium Chloride
NaOH	Sodium Hydroxide
O_2	Oxygen Molecule
O_2^-	Superoxide
O_3	Ozone
$O(^1D)$	Excited Oxygen
OCl^-	Hypochlorite Ion
$OH\cdot$	Hydroxyl Radical
OH^-	Hydroxide Ion
pCBA	Para-chlrobenzoic Acid
pH	Potential Hydrogen
R^2	Coefficient of Determination
Ru	Ruthenium
THAAs	Total Haloacetic Acids
THM	Trihalomethane
TTHMs	Total Trihalomethanes
Ti	Titanium
TiO_2	Titanium Dioxide
TN	Total Nitrogen
TOC	Total Organic Carbon
US EPA	United States Environmental Protection Agency
UV	Ultra Violet
QC	Quality Control

ACKNOWLEDGEMENTS

I would like to thank my supervisors, Dr. Graham Gagnon and Dr. Jennie Rand, for their support and technical advice through my graduate studies. Thank you for giving me the opportunity to conduct this research. Your guidance and various opportunities beyond my research have been very beneficial for my professional development. It has been an honour to work with you and will remember fondly my time in Halifax and Wolfville.

I would like to acknowledge the Industrial Research Chair (IRC) of the Centre for Water Resources Studies (CWRS) for funding this research.

I would also like to thank my committee members, Dr. Mysore Satish and Dr. George Jarjoura, for being part of my committee and providing valuable feedback. Your external view of the research has been very valuable.

Additionally, I would like to thank many people in Dr. Gagnon's research group. I would like to thank Heather Daurie, Shelley Oderkirk and Elliott Wright for all their help in the laboratory. Heather has been a great mentor in the laboratory over the years, thank you for all the help and patience with my endless questions. Sarah Jane Payne, I cannot begin to describe your support through the journey. Thank you so much for everything! I would also like to thank Tarra Chartrand for all the organizational help she provided over the years. I would also like to acknowledge the research group as a whole, you are all awesome and it has been great working with you over the years. The help of staff members at Dalhousie University, the Irving Centre at Acadia University, and Mill Cove Water Pollution Control Centre was appreciated.

Last, but not least, I would like to thank my friends. Some of you are close, others many kilometers away, but you have always supported and encouraged me. For the ones who are away, you have showed me that the vastness of spacetime is just an illusion!

Chapter 1: Introduction

Fresh water bodies are limited throughout the world and their preservation is critical. A monitoring report prepared by the US EPA (2009) indicated that 44% of the assessed rivers and streams in the United States of America are contaminated. The same report listed 64% of the assessed lakes and 30% of the assessed bays and estuaries as contaminated. The cause of these contaminated water bodies was mainly a product of untreated municipal, agricultural, or industrial discharges (US EPA, 2009).

In order to prevent the deterioration of quality of the receiving waters, and to minimize the interference with the water's ecology, discharges from various industrial or municipal processes have to be treated before being released into the environment (Hammer and Hammer, 2012). Nitrogen compounds are typically found in wastewater effluents, and ammonia is considered the most problematic of such compounds (Mousavi et al., 2011). High levels of ammonia increase bacteria population, cause eutrophication, and lead to the depletion of dissolved oxygen (Moazed, 2008; Vohra et al., 2010). Even at low levels, ammonia is toxic to most marine life forms as it blocks oxygen transfer in the gills of fishes (Rezakazemi et al., 2012; Khuntia et al., 2013). The removal of ammonia in wastewater effluents prior to discharge to water bodies is therefore essential in order to preserve the environment.

Traditional methods for the removal of ammonia include: biological nitrification, air stripping, ion exchange, and break point chlorination (Pressley et al., 1972; Adams, 1974). These methods have their respective disadvantages however. Biological nitrification and air stripping are pH and temperature sensitive, while break point chlorination may leave chlorine in the treated water causing disinfection by-products (Adams, 1974; Yang et al., 2012; Khuntia et al., 2013). Therefore, new methods for the removal of aqueous ammonia have to be investigated.

1.1 Project Objectives

The overall aim of this research was to provide further insight into methods for removing nitrogen compounds, specifically aqueous ammonia, from wastewater. Two specific technologies were investigated: ultra violet (UV) light and an electrochemical process. The research was divided into four tasks in order to achieve the overall objective:

1. Investigate the removal efficiency of the direct photolysis of nitrogen compounds with UV light.
2. Develop an electrochemical cell at a bench-scale level and investigate the effectiveness of treatment in removing nitrogen compounds.
3. Investigate synergistic effects of employing UV light with an electrochemical process for the removal of nitrogen compounds.
4. Determine the effectiveness of treatment for each technology with secondary wastewater effluent obtained from a wastewater treatment plant.

1.2 Organization of Thesis

Each result chapter was written with an introduction, a materials and methods section listing specific methods used for that chapter, discussion of results, and a conclusion. Listed below is a brief description of the content of each chapter:

- Chapter 2 provides a literature review of the chemistry and sources of ammonia, and the various treatment options available. An overview of regulatory wastewater guidelines for ammonia in Canada is also provided.
- Chapter 3 describes the methods and materials used in this current research. A description of the municipal wastewater treatment plant from which the wastewater was obtained is also provided.
- Chapter 4 presents findings on the direct photolysis of nitrogen compounds with UV light. Synthetic wastewater was used in order to investigate factors affecting the treatment efficiency, and the optimized condition was used to treat secondary wastewater effluent from a municipal treatment plant.
- Chapter 5 presents findings on the electrolysis of nitrogen compounds. Synthetic wastewater was used to investigate various factors affecting treatment, and the optimized conditions were used to treat secondary wastewater effluent obtained from a municipal treatment plant.
- Chapter 6 presents findings from the synergistic use of UV technology with an electrochemical cell. Synthetic wastewater and secondary wastewater effluent were used to investigate synergistic effects.
- Chapter 7 provides a synthesis and conclusions from the findings of this research. It also recommends future research opportunities in the field.

Chapter 2: Literature Review

2.1 Chemistry of Ammonia

Total nitrogen is composed of organic nitrogen (amino sugars, amino acids, or proteins), nitrate, nitrite, and aqueous ammonia (Hammer and Hammer, 2012). Aqueous ammonia, expressed as NH_3/NH_4^+, can be present in either the un-ionized form (ammonia: NH_3) or the protonated form (ammonium: NH_4^+). The sum of the concentration of NH_3 and NH_4^+ is referred to as total ammonia, usually expressed as 'total ammonia-nitrogen'.

Ammonia is a colorless alkaline gas at ambient temperature and pressure; with a penetrating odour (Constable et al., 2003). It has a melting point of -77.7 °C and a boiling point of -33.5 °C and is very soluble in water, with a solubility of 895 g/L at 0 °C and 101 kPa (NRC, 1977; Environment Canada and Health Canada, 2001).

In various aqueous environments, total ammonia exists in either the NH_3 or NH_4^+ form. The presence of each form depends on the pH and temperature of the solution, in accordance with Equation 2.1 (Rezakazemi et al., 2012):

$$NH_3 + H_2O \leftrightarrow NH_4^+ + OH^- \tag{2.1}$$

From Equation 2.1, the equilibrium constants, K_a and K_b, are yielded according to Equations 2.2 and 2.3 (Rezakazemi et al., 2012):

$$K_a = \frac{[NH_3][H^+]}{[NH_4^+]} = 5.6 \times 10^{-10} \qquad (2.2)$$

$$K_b = \frac{[NH_4^+][OH^-]}{[NH_3]} = 1.8 \times 10^{-5} \qquad (2.3)$$

Ammonia and ammonium are in equilibrium at pH=9.25. Therefore, when pH is above 9.25, NH_3 is the dominant form of total ammonia. Whereas when pH is below 9.25, NH_4^+ becomes the dominant form of total ammonia. Table 2-1 lists the percentage of ammonia in fresh water for various temperatures and pH levels.

Table 2-1 Percent of NH_3 species in total ammonia (Adapted from Environment Canada and Health Canada, 2001).

Temp (°C)	pH					
	6.0	7.0	8.0	9.0	9.5	10.0
0	0.008	0.082	0.82	7.64	20.7	45.3
5	0.012	0.125	1.23	11.1	28.3	55.6
10	0.018	0.186	1.83	15.7	37.1	65.1
15	0.027	0.273	2.67	21.5	46.4	73.3
20	0.039	0.396	3.82	28.4	55.7	79.9
25	0.056	0.566	5.38	36.3	64.3	85.1

Accordingly, at 25 °C and pH of 8.0, only 5.38% of total ammonia is in the NH_3 form whereas at pH of 10.0, over 85% of total ammonia is in the NH_3 form. The relationship between pH and ammonia species is illustrated in Figure 2-1.

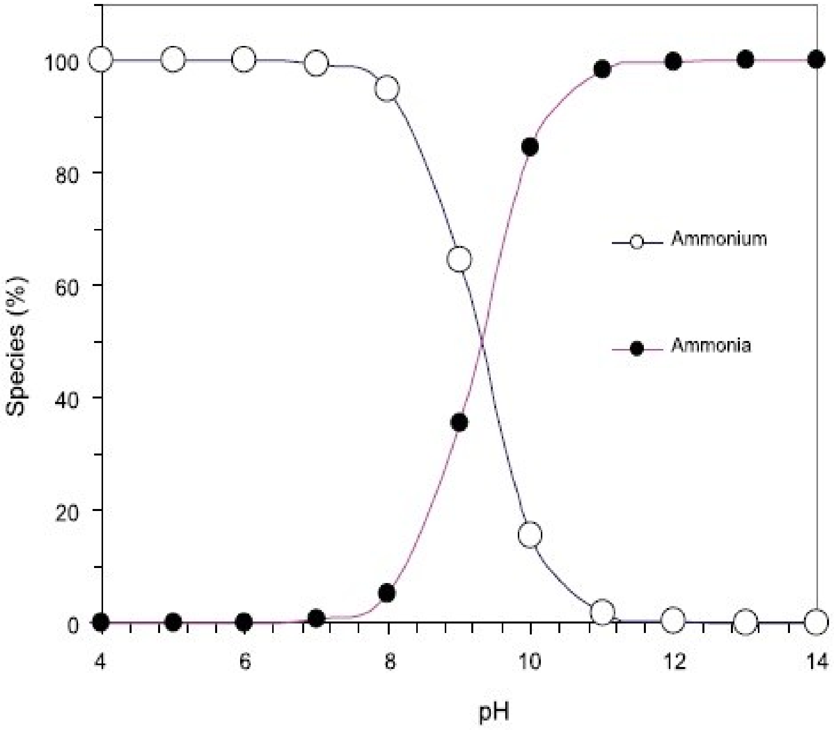

Figure 2-1 Relationship between pH and NH_3/NH_4^+ species (Vohra et al., 2010).

2.2 Sources of Ammonia

Ammonia is naturally found in the environment as plants and animals excrete it, or it can be the produced by the decomposition of organisms (Randall and Tsui, 2002). Point and nonpoint sources of pollution can also contribute to the concentration of ammonia in the environment. As a point source, ammonia is released into the environment from a variety of wastewater effluents (municipal, industrial, aquaculture, and agricultural) (Wicks et al., 2002). Nonpoint sources of ammonia include runoffs from agricultural and industrial practices. Rainfall, land use, vegetation, and various human activities affect the severity of pollution impact from these nonpoint sources (Liang et al., 2008).

The composition of municipal wastewater has changed over the past century, where an increase in human activities has caused an increase in quantity and variety of pollutants in municipal wastewater that require treatment (Brown et al., 2011). Wastewater is typically a mixture of pollutants (natural and synthetic hormones, pharmaceuticals, and industrial chemicals), liquid wastes, debris, organic compounds (polycyclic aromatic hydrocarbons, nonylphenols, dioxins, and furans) and inorganic compounds (aqueous ammonia, nitrate, nitrite, chloramines) (Holeton et al., 2011; Roberts et al., 2011; Tetreault et al., 2011).

The concentration of ammonia in municipal wastewaters varies on average from 10 to 200 mg/L (Ashrafizadeh and Khorasani, 2010). Comeau et al. (2008) reported the concentration of ammonia in the effluent of three municipal wastewater treatment plants and their respective receiving watersheds (Halifax, Pictou, and Cocagne) in Atlantic Canada. Concentration of ammonia was typically low (<1 mg/L) in all samples (wastewater effluent samples as well as samples from the watersheds), except in the final effluent from Mill Cove (NH_3 average concentration was 30.42 mg/L) (Comeau et al., 2008). Holeton et al. (2011) reported on a Canadian national survey (for some provinces between 2003 and 2008) of wastewater releases (which included spills, leaks, and discharges) and the subsequent impact on the receiving waters. The authors reported an increase in ammonia concentration release in the provinces of Quebec (4.2×10^6 Kg-N) and Newfoundland ($<1 \times 10^6$ Kg-N). Carlson et al. (2013) have reported an ammonia concentration of 8 mg/L in the Dead Horse Creek in Manitoba, downstream of Winkler's lagoons outfall. Environment Canada and Health Canada (2001) reported a national survey of ammonia concentration in municipal wastewater effluents, with a national average concentration of NH_3 of 13.89 mg/L.

Industrial wastewater is characterized as any type of wastewater discharged from industrial practices. Compared to municipal wastewater, industrial wastewater typically has a higher organic strength (>1000 mg-COD/L), extreme temperature or pH (non-neutral), high concentration of salt, and may contain synthetic or natural hazardous substances (Lin et al., 2012). Industrial wastewater can also contain varying concentrations of aqueous ammonia (either as NH_3 or NH_4^+ form). The concentration of aqueous ammonia has been reported for different industrial wastewater effluents: assorted agricultural practices, metal-plating, coking, petroleum or oil refining, and liquid crystal factories (Kim et al., 2005; Nemoto et al., 2007; Miladinovic and Weatherley, 2008; Ashrafizadeh and Khorasani, 2010; Vohra et al., 2010; Rezakazemi et al., 2012). Table 2-2 lists different industrial practices, their location and corresponding aqueous ammonia concentration in the effluent.

Table 2-2 Concentration of aqueous ammonia in industrial wastewater effluents.

Type of industrial wastewater	Location	NH_3-N/NH_4^+-N (mg/L)	Reference
Landfill leachate	Italy	5210	Lopez et al., 2004
Landfill leachate	China	700	Zhao et al., 2010
Landfill leachate	China	642-895	Ye et al., 2011
Landfill leachate	China	2910	Liu et al., 2012
Landfill leachate	Greece	1500	Urtiaga et al., 2012
Nutrition (cheese whey)	Turkey	58-150	Farizoglu et al., 2004
Nutrition (pet food)	Canada	797-1400	Kurian et al., 2005
Nutrition (Coca Cola plant)	China	2400-11000	Lin et al., 2009
Pharmaceutical	Spain	4.8	Melero et al., 2009
Pharmaceutical	India	56-132	Saravanane and Sundararaman, 2009
Refinery	China	56-125	Xianling et al., 2005
Refinery	Brazil	25-55	Souza et al., 2011
Textile	Algeria	5-18	Badani et al., 2005
Tannery	Korea	228	Chung et al., 2004
Tannery	Korea	886	Min et al., 2004
Tannery	Italy	80-160	De Gisi et al., 2009
Tannery	Italy	118	Munz et al., 2009

2.3 Wastewater Guidelines

Prior to 2012, each province in Canada had developed their respective wastewater regulations and this resulted in an inconsistent regulatory benchmark and considerable differences in wastewater treatment levels achieved by each utility (Environment Canada, 2012). In order to address this issue, a new regulating document developed in 2012 under the Fisheries Act and sponsored by Environment Canada was implemented for most wastewater utilities throughout Canada. The only utilities not required to comply with these new set of regulations are those located in the far north of the country (Nunavut, Northwest Territories, northern regions of Quebec, and Newfoundland & Labrador).

Compliance with the new regulations is on a risk-based timeline for each wastewater utility. Wastewater systems that are categorized as high, medium, or low risk must comply by 2020, 2030, and 2040, respectively (Environment Canada, 2012). This set of standards is the new benchmark for wastewater effluent quality, in effort to reduce the negative impact untreated wastewater has on the environment. Table 2-3 lists the wastewater parameters and limit of acceptable concentration for discharge.

Table 2-3 List of wastewater guidelines (Environment Canada, 2012).

Parameter	Acceptable concentration (mg/L)	Remark
Carbonaceous Biochemical Oxygen Demand (CBOD)	<25	Not Applicable
Suspended solids	<25	Not Applicable
Total chlorine residual	<0.02	If chlorine used in treatment
Un-ionized ammonia	<1.25 as Nitrogen	At 15 °C ± 1 °C

The concentration of un-ionized ammonia is computed from Equations 2.4 - 2.6 (Environment Canada, 2012):

$$Un-ionized\ Ammonia = Total\ Ammonia \times \left[\frac{1}{\left(1+10^{(pK_a - pH)}\right)} \right] \tag{2.4}$$

where:

$$\text{Total Ammonia} = NH_3 + NH_4^+ \tag{2.5}$$

$$pK_a = 0.09018 + \frac{2729.92}{T} \tag{2.6}$$

where temperature (T) is in Kelvin.

In addition to proposing limits of acceptable concentrations for key parameters, the regulatory benchmark also dictates monitoring, recording, and sample grabbing. Continuous monitoring and recording of the influent and effluent volumes of the treatment facility is required. Effluent samples are also to be collected and analyzed for the specified parameters (along with determining whether or not they are acutely lethal) on a monthly or quarterly frequency determined based on the average daily volume deposited annually by the facility (Environment Canada, 2012).

2.4 Treatment Options

A variety of treatment options have been investigated for the removal of aqueous ammonia in various types of waters. Traditional methods for the treatment of aqueous ammonia include: air stripping, biological nitrification-denitrification, and break point chlorination (Pressley, 1972;

Adams, 1974). These methods, however, have several disadvantages. For example, nitrification is energy intensive while denitrification requires a high quantity of carbon sources (Nishimura et al., 2012). Furthermore, both air stripping and nitrification-denitrification are not effective in low winter temperatures (Du et al., 2005). New methods for the treatment of aqueous ammonia have therefore been explored.

2.4.1 Advanced Oxidation Processes

Advanced Oxidation Processes (AOPs) are any type of process that generates sufficient amount of hydroxyl radicals (OH·) to oxidize contaminants and result in water purification (Glaze et al. 1987; Cooper et al., 2009). These processes have been used in the water industry as an application for both potable water and wastewater treatment. AOPs have been researched because they offer a promising alternative to conventional treatment methods. For example, photocatalytic AOPs result in low amounts of waste by-products, operate at ambient temperatures, and could utilize the sun as an energy source (Vohra et al., 2010).

Reactive Oxygen Species (ROS) consist of free radicals (superoxide radical ($O_2\cdot$), hydroperoxyl radical ($HO_2\cdot$), hydroxyl radical (OH·), and alkoxyl radical (RO·)) and non-radicals (hydrogen peroxide (H_2O_2), singlet oxygen ($^1O_2$), and hypochlorous acid (HOCl)) (Tai et al., 2002; Gomes et al., 2005). Free radicals, as defined by Gomes et al. (2005), are “atoms or molecules, capable of independent existence, that possess one or more unpaired electrons”. These radicals are very short-lived and stable compared to non-radicals because the electrons are not paired in orbitals as they have different spin directions (Gomes et al., 2005).

In the water industry, the hydroxyl radical is considered to be the most important free radical generated via AOPs. It is a strong and powerful non-selective oxidant that reacts with a wide range of contaminants and degrades them (Anjaneyulu et al., 2005; Chu and Chan, 2007; Liu et al., 2007; Teel et al., 2007). Once the OH· radical is generated, the overall mechanism for the degradation of contaminant "R" is in accordance with Equations 2.7 - 2.9 (Stasinakis, 2008):

$$R + OH\cdot \rightarrow ROH \tag{2.7}$$

$$R + OH\cdot \rightarrow R\cdot + H_2O \tag{2.8}$$

$$R^n + OH\cdot \rightarrow R^{n-1} + OH^- \tag{2.9}$$

Depending on the nature of the contaminant, the hydroxyl radical degrades the contaminant by various pathways. The hydroxyl radical can either bind to the contaminant (as a radical addition in accordance to Equation 2.7), abstract a hydrogen atom from the contaminant (Equation 2.8) or it can transfer an electron to the contaminant (Equation 2.9).

Table 2-4 lists studies with AOPs that investigated the removal of aqueous ammonia. The table lists the type of process and wastewater used, range of the concentration of aqueous ammonia, factors investigated, and findings from the research.

Table 2-4 Review of AOPs for the removal of aqueous ammonia in wastewater.

Type of process	Type of water	Range of NH_3/NH_4^+ concentration	Factors investigated	Findings	Reference
UV/TiO_2	Synthetic	1.7 mg/L	TiO_2 concentration, and pH	pH>9.25 was beneficial for photocatalytic oxidation. Increase in TiO_2 concentration resulted in higher removal rates.	Zhu et al., 2005
UV/H_2O_2	Synthetic	31, 102, 1006 mg-N/L	pH, and initial concentration	pH>9.25 was beneficial for removal. Removal rate increased with an increase in initial concentration. Removal rates were low overall.	Huang et al., 2008
UV/TiO_2/H_2O_2	Synthetic	38 mg/L	pH, addition of H_2O_2, and TiO_2 concentration	Degradation of NH_3-NH_4^+ occurred at pH>7. Addition of H_2O_2 increased the efficiency of the photocatalytic process. Increase in TiO_2 concentration was beneficial for removal up to 0.3 mg/L.	Zhang et al., 2009
UV/H_2O_2	Landfill leachate	432.01 - 446.67 mg/L	Light bulb power, temperature, and treatment time	Removal rates increased with an increase in light bulb intensity, temperature, and treatment time. 97% removal was observed at optimized conditions.	De Brito et al., 2010
UV/TiO_2	Synthetic	850 mg/L	Addition of air, and/or silver nitrate	Addition of oxygen and silver nitrate increased removal rate.	Mikami et al., 2010
UV/TiO_2	Synthetic	10 mg/L	pH, presence/absence of $S_2O_3^{2-}$ and p-cresol at various concentrations	Alkaline pH was beneficial for removal. At pH=7 and 12, presence of $S_2O_3^{2-}$ increase removal. At pH=10.0, presence of $S_2O_3^{2-}$ and p-cresol increase removal.	Vohra et al., 2010
UV/ZnO/ Electrochemical Process	Synthetic	100 - 188 mg/L	Effects of employing a photocatalytic process with an electrochemical process	Combined photocatalytic and electrochemical processes resulted in the highest removal rates compared to each individual process.	Rezaee et al., 2012

UV/H_2O_2

Hydrogen peroxide (H_2O_2) is a strong oxidizer that is used in the water industry. H_2O_2 can also be used in combination with a UV light source as an AOP. The UV/H_2O_2 process results in the generation of the OH· radical, and enhances degradation efficiency compared to the singular use of H_2O_2. This is because H_2O_2 has a lower standard redox potential (E°=+1.78 V) compared to the OH· radical (E°=+2.8 V) (Kusic et al., 2006).

With a wavelength of 254 nm, the radiation from the light source can photo-activate the H_2O_2 according to Equation 2.10 (Buxton et al., 1988; Crittenden et al., 1999):

$$H_2O_2 + h\nu \rightarrow 2OH\cdot \tag{2.10}$$

Two hydroxyl radicals are produced from the photolysis of the H_2O_2 molecule. In theory, a higher concentration of H_2O_2 would result in a higher concentration of OH· radical. However, Kusic et al. (2006) observed that an increase in H_2O_2 dose does enhance oxidation before plateauing. The propagation reaction of the UV/H_2O_2 process is in accordance to Equation 2.11, where the OH· radical can further react with H_2O_2 to form the less active $HO_2\cdot$ (Crittenden et al., 1999; Kusic et al., 2006):

$$OH\cdot + H_2O_2 \rightarrow HO_2\cdot + H_2O \tag{2.11}$$

Some factors should be considered when employing a UV/H_2O_2 process, including initial concentration of the contaminant, the dose of the hydrogen peroxide, pH, reaction time, and whether other co-pollutants are present (Stasinakis, 2008). The disadvantages of employing a UV/H_2O_2 based AOP include the poor UV absorption characteristic of the H_2O_2 molecule, the residual of H_2O_2 that needs to be addressed in the process, and the inability of solar light to dissociate the H_2O_2 molecule (Crittenden et al., 1999; Stasinakis, 2008).

UV/O_3

Ozone (O_3) is a strong oxidant that is used in the water industry for disinfection and degradation of organic matter (Tanaka and Matsumura, 2002). O_3 has conventionally a low reactivity with many contaminants (Reisz et al., 2003). Therefore, O_3 is generally used in combination with another oxidant (H_2O_2) or process (UV, TiO_2) in order to increase its oxidation strength (Reisz et al., 2003).

The use of UV/O_3 results in the production of the hydroxyl radical and other radical species. The production of the hydroxyl radical is in accordance with Equations 2.12 - 2.14 (Reisz et al., 2003; Tezcanli-Guyer and Ince, 2004; Song et al., 2008):

$$O_3 + h\nu \rightarrow O_2 + O(^1D) \qquad (2.12)$$

$$O(^1D) + H_2O \rightarrow H_2O_2 \qquad (2.13)$$

$$H_2O_2 + h\nu \rightarrow 2OH\cdot \qquad (2.14)$$

Under light irradiation, in accordance to Equation 2.12, O_3 decomposes into oxygen (O_2) and excited oxygen ($O(^1D)$). The $O(^1D)$ atom further reacts with the bulk water to produce H_2O_2 (Equation 2.13). The photo-activation of hydrogen peroxide further produces two hydroxyl radicals, in accordance to Equation 2.14. From Equations 2.12 and 2.13, it appears that the use of UV/O_3 is therefore an expensive way of producing H_2O_2, which is then further dissociated into OH· radicals (Munter, 2001). However, because of the low UV absorption of the H_2O_2 molecule, the production of OH· radicals is more effective via the UV/O_3 process (Munter, 2001).

UV/TiO$_2$

Titanium dioxide (TiO_2) is widely available and used as a catalyst in the water industry (Stasinakis, 2008; Rengifo-Herrera et al., 2009). Overall, employing a photo-catalytic process for water or wastewater treatment has the advantage of producing minimal waste, low operating cost, operation at ambient or low temperatures, and the possible use of sunlight for light irradiation (Bhatkhande et al., 2002; Stasinakis, 2008; Vohra et al., 2010).

The general process involved in the production of hydroxyl radicals in a UV/TiO_2 based AOP is illustrated in Figure 2-2. The production of the OH· radicals in a UV/TiO_2 based AOP is in accordance with Equations 2.15 - 2.17 (Chen et al., 2005; Song et al., 2007):

$$TiO_2 + h\nu \rightarrow e_{cb} + h^+ \tag{2.15}$$

$$e_{cb} + O_2 \rightarrow O_2^- \tag{2.16}$$

$$h^+ + H_2O \rightarrow (H_2O)^+ \rightarrow H^+ + OH\cdot \tag{2.17}$$

As the semiconductor absorbs the radiation from the light source, the conduction band electrons (e_{cb}) and valence band holes (h^+) are produced in accordance to Equation 2.15. The produced electrons in the conduction band further react with the oxygen molecule to produce superoxide radical anions (O_2^-) (Equation 2.16). On the other hand, the produced valence band holes from Equation 2.15 interact with the bulk water to subsequently produce OH· radicals (Equation 2.17).

Some factors are to be considered when employing a UV/TiO_2 process, including initial contaminant concentration, amount of catalyst, treatment time, temperature, pH, intensity of the light source, and whether other ionic species are present (Stasinakis, 2008).

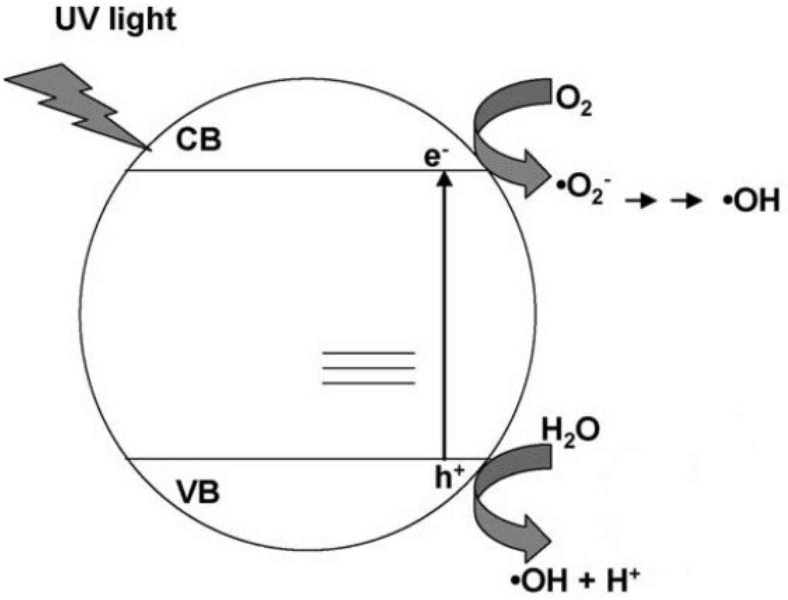

Figure 2-2 Photocatalytic production of OH· radicals on a TiO_2 surface (Adapted from Rengifo-Herrera et al., 2009).

2.4.2 Electrochemical Process

In the past decade, electrochemical treatment has attracted wide attention for the treatment of various wastewaters (municipal and industrial wastewaters, aquaculture, landfill leachate, and tannery effluent). Electrochemical treatment is a simple technology, has remote control capabilities and low maintenance, does not produce sludge, and it works well with different pollutants at various concentrations (Vanlangendonck et al., 2005; Diaz et al., 2011; Huang et al., 2012). The presence of toxic agents (detergents, pesticides, and phenols) does not interfere with the electrochemical process either (Vlyssides et al., 2002). In addition, electrochemical treatment generates minimal secondary wastes and the final product of treatment is nitrogen gas, which is harmless and does not require further treatment (Liu et al., 2009; Diaz et al., 2011).

Alternatively, electrochemical treatment has a high operating cost due to the energy required for operation and corrosion of the electrodes may result in excessive metal release (Anglada et al., 2009; Kapalka et al., 2010). Furthermore, not all types of wastewaters have enough naturally occurring conductivity required for electrochemical treatment and therefore, additional electrolytes may have to be supplemented (Anglada et al., 2009).

Various factors must be considered when electrochemically treating wastewaters. Physico-chemical characteristics (pH, temperature, and chloride concentration) of the wastewater have an effect on the efficiency of treatment (Chen et al., 2007; Li and Liu, 2009; Liu et al., 2009; Wang et al., 2012). The current density (the intensity of the current per unit area of the electrode, expressed as mA/cm^2), controls the reaction rate and also influences the energy consumption of the process (Chen et al., 2007; Hu et al., 2009; Liu et al., 2009). The choice in electrode material and their corresponding distance, is important because it affects the efficiency process (Hu et al., 2009; and Kapalka et al., 2010). Furthermore, choice in electrode material is important because the release of metals could occur throughout the treatment process (Anglada et al., 2009), and this should not result in health implications for humans, or be poisonous to the ecosystem.

The electrochemical treatment of pollutants can take place through direct oxidation (occurring at the surface of the anode) or through indirect oxidation (in the bulk), illustrated in Figure 2-3 (Anglada et al., 2009). Table 2-5 lists studies conducted on the electrochemical removal of aqueous ammonia in various wastewaters, including type of wastewater used, factors investigated, and respective findings.

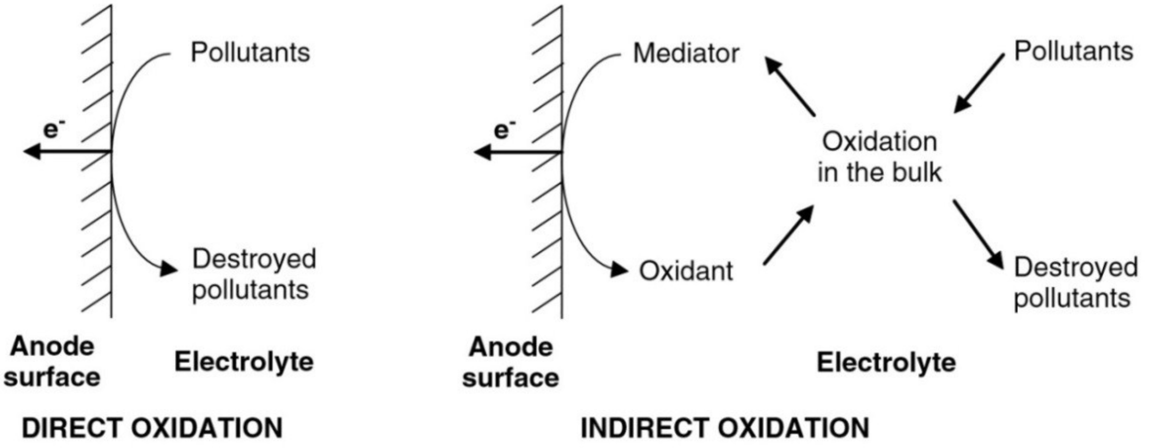

Figure 2-3 Direct and indirect oxidation of contaminants in an electrochemical process (Anglada et al., 2009).

Table 2-5 Review of the electrochemical research treating aqueous ammonia in wastewater.

Cathode & Anode	Type of Wastewater	Range of NH_3/NH_4^+ Concentration	Factors Investigated	Findings	NH_3/NH_4^+ Kinetics Order	Reference
Stainless steel & Ti/Pt	Municipal	150 mg-N/L	pH	Alkaline pH was beneficial for removal. 72% removal after 120 minutes.	Not reported	Vlyssides et al., 2002
Stainless steel & BDD	Raw and pre-treated landfill leachate	859.4, 1934 mg/L	Chloride concentration and current density	High chloride concentration and current density increased removal rates. Total removal observed with 90 mA/cm^2 after 360 min.	Not reported	Cabeza et al., 2007
Ti & RuO_2-IrO_2-TiO_2/Ti	Synthetic	40 mg/L	pH, chloride concentration, and current density	Removal efficiency increased with chloride concentration and current density. Neutral and alkaline pH was beneficial for removal.	First-order	Chen et al., 2007
Ti & RuO_2/TiO_2	Produced water	103 mg/L	Current density	Higher current density increased removal. Total removal with 17.78 mA/cm^2 after 30 minutes.	Not reported	De Lima et al., 2009
Ti & Ti/RuO_2-Pt	Synthetic & municipal	40, 60 mg/L	Current density, distance between electrodes, and chloride concentration	Removal rates increased with an increase in current density and chloride concentration. Smaller electrode spacing was beneficial for removal.	First-order	Hu et al., 2009
Stainless steel & Ti/RuO_2	Synthetic & municipal	10, 32, 51, 103 mg-N/L & 19 mg-N/L	Current density, chloride concentration, pH, and initial concentration	Increase in chloride concentration and current density resulted in higher removals. Neutral and alkaline pH were beneficial for removal.	Zero-order	Li and Liu, 2009
Stainless steel & Ti/IrO_2	Synthetic & municipal	32 mg-N/L & 15-25 mg-N/L	pH, chloride concentration, and current density	Degradation was independent of pH. Higher current density and chloride concentration resulted in higher removals.	Zero-order	Liu et al., 2009
Ti & Ti/RuO_2, Ti/IrO_2	Synthetic	700 mg/L	Not Applicable	Similar performance for both anodes; >97% of total nitrogen removed with 40 mA/cm^2.	Zero-order	Xiao et al., 2009

The electrochemical treatment of ammonia has been reported as direct oxidation on the surface of the anode or as indirect oxidation occurring in the bulk (Feng et al., 2003). Direct oxidation of a pollutant occurs when the pollutant diffuses from the bulk to the surface of the anode and it is oxidized (Anglada et al., 2009). Two pathways can be followed for the direct oxidation of a pollutant: electrochemical conversion and electrochemical combustion (Deng and Englehardt, 2007; Huang et al., 2012). The direct oxidation of ammonia has been reported with low removal rates for various anodes (Ru_2O-Ir_2O-Ti_2O/Ti, Ti/RuO_2, Ti/IrO_2, Ti/RuO_2-Pt) (Chen et al., 2007; Hu et al., 2009; Li and Liu, 2009; Liu et al., 2009; Wang et al., 2012). Therefore, the indirect oxidation of ammonia is usually the main removal mechanism attributed to the electrochemical treatment.

In the electrochemical treatment of ammonia, indirect oxidation can occur by hydroxyl radicals or by HOCl formed in the process (Chen et al., 2007; Li and Liu, 2009). The indirect oxidation of ammonia by hydroxyl radicals has been reported to have minimum, or negligible, contribution to the removal efficiency of ammonia (Feng et al., 2003; Li and Liu, 2009; Liu et al., 2009). Therefore, HOCl formed in the process is mainly responsible for the indirect oxidation of ammonia (following breakpoint chlorination), in accordance to Equations 2.15 - 2.21 (Liu et al., 2009; Li and Liu, 2009; Gendel and Lahav, 2012; Wang et al., 2012):

At the cathode:

$$2H^{+} + 2e^{-} \rightarrow H_{2} \qquad (2.15)$$

At the anode:

$$2Cl^{-} \rightarrow Cl_{2} + 2e^{-} \qquad (2.16)$$

In the solution:

$$Cl_2 + H_2O \rightarrow HOCl + H^+ + Cl^- \quad (2.17)$$

$$HOCl \rightarrow H^+ + OCl^- \quad (2.18)$$

$$3HOCl + 2NH_3 \rightarrow N_2 + 3H_2O + 3H^+ + 3Cl^- \quad (2.19)$$

$$3HOCl + 2NH_4^+ \rightarrow N_2 + 3H_2O + 5H^+ + 3Cl^- \quad (2.20)$$

$$4HOCl + NH_4^+ \rightarrow NO_3^- + H_2O + 6H^+ + 4Cl^- \quad (2.21)$$

According to breakpoint chlorination, no nitrite should theoretically be formed (Hu et al., 2009). Nitrate is formed in the electrochemical process (Equation 2.21), although it can also be reduced to nitrogen gas at the cathode, in accordance to Equation 2.22 (Kim et al., 2005):

$$NO_3^- + 3H_2O + 5e^- \rightarrow \frac{1}{2}N_2 + 6OH^- \quad (2.22)$$

Nitrogen gas is the final product when ammonia is treated electrochemically, in accordance to Equations 2.19 and 2.20. Previous research has reported the conversion of degraded ammonia to nitrogen gas with various anodes and cathodes in their respective electrochemical systems (Kim et al., 2005; Li and Liu, 2009; Liu et al., 2009; Xiao et al., 2009).

An unintended consequence of using an electrochemical process is the corrosion of the electrode, particularly the anode. The choice in electrode material is therefore important as the release of the metal could be toxic to the ecosystem.

In an electrochemical process, galvanic corrosion is the principal corrosion process involved as the anode and cathode are in a common electrolyte solution (Ahmad, 2006). As corrosion occurs, the anode is sacrificed whereas the cathode is protected. Equations 2.23 and 2.24 represent the corrosion processes in an electrochemical process, where the anode (M_1) undergoes oxidation and the cathode (M_2) undergoes reduction (Droste, 1997):

$$M_1 \rightarrow M_1^{(n)+} + (n)e^- \tag{2.23}$$

$$M_2^{(n)+} + (n)e^- \rightarrow M_2 \tag{2.24}$$

In Equation 2.23 and 2.24, 'n' is the number of electrons released by the metal. As the anode corrodes, the metal's ions are released into the solution and the electrons migrate to the cathode, reducing the cathode's oxidizing state.

2.4.3 Photoelectrochemical Process

Several studies have investigated the effectiveness of treating various contaminants (aqueous ammonia and landfill leachate) with a combination of UV light and an electrochemical process (photoelectrochemical). The photoelectrochemical treatment of contaminants is considered more efficient compared to electrochemical treatment, as the photolysis of HOCl produced in the electrochemical process produces different radicals, in accordance to Equation 2.25 (Xiao et al., 2009; Soltani et al., 2013):

$$HOCl + h\nu \rightarrow OH\cdot + Cl\cdot \tag{2.25}$$

Xiao et al. (2009) reported on the treatment of nitrogen compounds (aqueous ammonia) with an electrochemical cell (Ti/RuO_2 or Ti/IrO_2 anodes) supplemented with a UV light with an intensity of 1.36 mW/cm^2. The authors observed the ammonia pseudo zero-order constant increase by 1.5 times in the photoelectrochemical process compared to the electrochemical process (for both anodes). Treatment of landfill leachate has also been reported with a photoelectrochemical process, where Xiao et al. (2013) observed an improved 33% removal of ammonia in a photoelectrochemical process compared to an electrochemical process. Zhao et al. (2010) have also reported on a faster degradation rate when landfill leachate was treated with a photoelectrochemical process (41.6% TOC removal) compared to an electrochemical process (28.3% TOC removal).

2.4.4 Other Processes

Several other processes have also been investigated for the removal of aqueous ammonia in the literature. Several studies have reported the removal of aqueous ammonia using zeolite (Du et al., 2005; Sarioglu, 2005; Ashrafizadeh et al., 2008; Khosravi et al., 2012), membrane contactors (Ashrafizadeh and Khorasani, 2010; Hasanoglu et al., 2010; Rezakazemi et al., 2012) , and ozone (Khuntia et al., 2013). Table 2-6 lists some of the other processes utilized for the removal of aqueous ammonia in wastewater. The table lists the process utilized, the type of wastewater used, the range of aqueous ammonia concentration, the factors investigated, and respective findings.

Table 2-6 Review of other processes for the removal of aqueous ammonia in wastewater.

Type of process	Type of wastewater	Range of NH_3/NH_4^+ concentration	Factors investigated	Findings	Reference
Ozone	Synthetic	75 mg/L	pH	Removal >90% at pH=8.0. Chloride concentration did not have an effect on removal.	Tanaka and Matsumura, 2002
Ion exchange	Synthetic	2.1, 8.4, 18.3, 36.5, 56.4, 94.2 mg/L	pH, contact time, and initial ammonia concentration	Contact time, pH, and initial ammonia concentration had an effect on removal efficiency.	Du et al., 2005
Ion exchange	Synthetic	8.8 - 885 mg-N/L	pH, flow rate, and initial ammonium concentration	Increased removal efficiencies were obtained with low flow rate and increase in initial concentration. Low pH was beneficial for removal.	Sarioglu, 2005
Microwave radiation	Industrial Wastewater	2400 - 11000 mg/L	Temperature, flow rate, aeration condition, and initial ammonia concentration	High temperature and low flow rate resulted in higher removals. Aeration and initial concentration had negligible effect on removal.	Lin et al., 2009
Hollow-fiber membrane contactor	Synthetic	50, 200, 400, 800 mg/L	pH, initial ammonia concentration, feed velocity, and chloride concentration	Higher removal efficiencies observed with elevated pH and increase in feed velocity. Initial concentration and presence of chloride ions had no effect on removal efficiency.	Ashrafizadeh and Khorasani, 2010
Membrane contactor	Synthetic	250 - 500 mg/L	Temperature, initial ammonia concentration, acid concentration, and flow rate	Increase in temperature, acid concentration, and flow rate resulted in higher removals. Initial concentration had no effect.	Hasanoglu et al., 2010
Ozone	Synthetic	100 mg/dm^3	pH, rate of ozone regeneration, and presence of bromide ions	High pH and ozone generation rate resulted in higher removals. Bromide ions contributed to higher removals.	Khuntia et al., 2013
Partial nitrification and anammox	Synthetic	150 mg-N/L	Solids retention time	80-90% removal of inorganic nitrogen.	Nishimura et al., 2012
Radiation/H_2O_2	Synthetic	2250 mg/L	Peripheral water level, pH, radiation	Optimal removal occurred at a peripheral water level of 1.5 times the inner water height. Highest removal (90.4%) was achieved at pH=11.0.	Wenjun et al., 2012

Chapter 3: Materials & Methods

Experiments were conducted in two laboratories for this research: the Clean Water Laboratory at the Centre for Water Resources Studies, Dalhousie University, Halifax, and the Drinking Water Quality Laboratory at the Irving Centre, Acadia University, Wolfville. Experiments utilizing the UV light beam (photooxidation and photoelectrochemical experiments) were conducted at Acadia University, whereas the electrochemical experiments were conducted at Dalhousie University. The samples were analyzed in either laboratory, depending on where the specific instrument was situated.

Analytical Procedures

Various parameters were measured throughout this research: pH, chlorine residual (total and free), anions (chloride, nitrate, and nitrite) and cations (ammonium) concentrations, total organic carbon (TOC), total nitrogen (TN), para-chlorobenzoic acid (pCBA), disinfection by-products (DBPs), and metal concentrations (titanium and ruthenium).

Glassware Preparation and Stock Preparation

Milli-Q was used as water throughout the research, obtained from an ultrapure water purification system (Millipore Corporation, MA) with typical resistance of ≈18.2 MΩ.cm at 25 °C. All glassware was washed and triple rinsed with Milli-Q prior to experiments. Chemical grade laboratory solutions obtained from Fischer Scientific (ON) were used throughout the research. Stock solutions of sodium chloride (NaCl, Fisher Scientific, ON), ammonium chloride (NH_4Cl, Fisher Scientific, ON), and pCBA (Sigma-Aldrich, MO) were made fresh prior to experiments.

Synthetic wastewater was made by mixing NH_4Cl and NaCl stock solutions in 1000 mL Milli-Q to achieve the desired concentration. For saline experiments where a higher concentration of chloride was required, additional NaCl (Fisher Scientific, ON) stock was added to the solution. pH adjustment was achieved with the addition of 0.1 M H_2SO_4 (Fisher Scientific, ON), 0.1 M or 10.0 M NaOH (Fisher Scientific, ON).

Experimental Design

Synthetic wastewater used in this research was produced by mixing NH_4Cl (Fisher Scientific, ON), NaCl (Fisher Scientific, ON), and Milli-Q. All experiments were conducted in batches. Batch experiments with synthetic wastewater were conducted in order to investigate factors affecting removal efficiency. All experiments were conducted at room temperature (20-23 °C), in duplicates, and in randomized order. Optimized conditions from the synthetic wastewater experiments were used to treat secondary wastewater effluent obtained from Mill Cove Water Pollution Control Centre (MCWPCC), Bedford, Nova Scotia.

pH

The pH probe was standardized each time prior to conducting experiments. An Accumet XL50 (Fisher Scientific, ON) with the respective probe was used. A calibration curve with laboratory standards (Fisher Scientific, ON) was obtained each time. The probe was rinsed with Milli-Q between sample measurements.

Concentration of Cations

The concentration of cations (NH_4^+) was analyzed using Ion Chromatography (IC). Samples were filtered through a 0.45 μm polysulfone filter membrane (GE Water & Process

Technologies) that was previously rinsed with at least 400 mL of Milli-Q. Samples were stored in the dark at 4 °C until analysis. A 850 Professional IC (Metrohm, Switzerland) equipped with a 858 Professional sample processor and a Metrosep C4-150/4.0 column was used. The eluent consisted of 1.7 mM HNO_3 (Fisher Scientific, ON) and 0.7 mM Dipicolinic Acid (Acros Organics, NJ) with a flow of 0.9 mL/min. Before analysis, the pH of the samples was lowered to 2-3 with a 10.0 M H_2SO_4 (Fisher Scientific, ON) solution in order to convert all of the aqueous ammonia into ammonium form. A calibration curve was obtained each time prior to analysis of samples. The precision of the instrument was validated with quality control (QC) samples (Milli-Q spiked with a known concentration of IC standard (Fisher Scientific, ON)). Washes and QC samples were prepared for every 10 samples. Recovery testing was performed and results accepted only if recovery was between 70 and 130%. The minimum detection limit (MDL) for NH_4^+ was 0.5 mg/L.

Concentration of Anions

The concentration of anions (chloride, nitrate, and nitrite) was monitored using IC according to Standard Methods 300.1 (US EPA, 1999). Samples were prepared and stored according to the same procedure outlined for cation samples. A 761 Compact IC (Metrohm, Switzerland) was used, equipped with a Metrosep-A-Supp-5 column, a suppressor module, and a 788 filtration sample processor. The eluent consisted of 3.2 mM Na_2CO_3 and 1.0 mM $NaHCO_3$ at 0.7 mL/min. A calibration curve was obtained each time prior to analysis of samples. The precision of the instrument and recovery testing were conducted as previously described. The MDL was 0.6 mg/L, 0.8 mg/L, 0.7 mg/L for chloride, nitrate, and nitrite, respectively.

Chlorine residual

Total and free chlorine were measured using a DR-500 UV-VIS spectrophotometer (HACH Co., CO, USA) or a DR-2800 spectrophotometer (HACH Co., CO, USA), both at a wavelength of 254 nm. The DPD colorimetric method was used. All samples that were over the limit of the instrument were diluted and reported at their final concentration. The concentration of monochloramine was determined by the difference between total and free chlorine.

Organic Carbon

Total organic carbon (TOC) samples were collected in 40 mL clean vials with no head space and preserved by dropping pH<2 with concentrated phosphoric acid (Fisher Scientific, ON). Samples were stored in the dark at 4 °C until analysis. Samples were analyzed with a TOC-V CPH (Shimadzu Corporation, Kyoto, Japan) equipped with a Shimadzu ASI-V autosampler, and a catalytically aided combustion oxidation nondispersive infrared detector (NDIR). The injection volume was 50 µL, at an operating temperature of 720 °C with a gas flow of 150 mL/min. A calibration curve, with hydrogen phthalate standard (National Institute of Standards and Technology (NIST), MD), was obtained each time prior to analysis of the samples. Precision of the instrument was validated (with washes and QC samples) as previously detailed. The MDL was 0.6 mg-C/L for TOC.

Total Nitrogen

Total nitrogen (TN) was analyzed with a Shimadzu Total Nitrogen (Shimadzu Corporation, Kyoto, Japan) measuring unit mounted on a Shimadzu TOC-V CPH (Shimadzu Corporation, Kyoto, Japan). The injection volume was 50 µL, at an operating temperature of 50 °C with a gas flow of 150 mL/min. A calibration curve, with potassium nitrate standard (Wako, Japan), was obtained each time prior to analysis of samples. Samples were collected, preserved, and stored as previously described with TOC samples. Accuracy of the instrument was validated (with washes and QC samples) as previously described. The MDL was 0.2 mg-N/L for TN.

Metal Concentration

Analysis of metals, titanium (Ti) and ruthenium (Ru), was carried out using an X-Series II ICP-MS (Thermo Scientific, ON). As samples had a turbidity over 1 NTU, a nitric acid digestion (105 °C for two hours in 5% nitric acid) was conducted in accordance to Standard Methods 3030E (APHA, 2009). Samples were then preserved with couple of drops nitric acid (Fisher Scientific, ON) to drop pH below 2, and stored in the dark at 4 °C until analysis. The MDL was 0.5 μg/L and 0.4 μg/L for Ti and Ru, respectively.

pCBA Analysis

Hydroxyl radicals (OH·) are short-lived radicals and therefore the direct measurement of such radicals is not possible. pCBA is an established and known probe used to detect the formation of hydroxyl radicals in various water systems (Elovitz and Gunten, 1999; Cho et al., 2004; Park et al., 2004; Watts and Linden, 2007; Brunet et al., 2009). In this research, pCBA was used as a probe compound to evaluate the production of OH· radicals. pCBA degradation was monitored by high pressure liquid chromatography (HPLC) (Series 200, Perkin Elmer, Milford, MA) as described by Brunet et al. (2009). A C18 reverse-phase column (Nova-Pak C18, 3.9 mm by 150 mm, Waters, Milford, MA) was employed with a UV detector (Series 200, Perkin Elmer, Waltham, MA) at a wavelength of 232 nm. The mobile phase utilized was 50% Milli-Q and 50%

acetonitrile (Fisher Scientific, ON) at a flow rate of 0.4 mL/min. Prior to analysis, all samples were filtered through a 0.45 μm polysulfone filter membrane (GE Water & Process Technologies) that had been previously rinsed with at least 400 mL of Milli-Q. All samples were taken in triplicates: two for data acquisition, while the third was spiked with additional pCBA in order to magnify the corresponding peak. A calibration curve was obtained each time prior to analysis. The accuracy of the instrument was checked as previously described.

Disinfection By-Products

Disinfection by-products (DBPs) of interest in this research were trihalomethanes (THMs) and haloacetic acids (HAAs). Four main THM compounds were detected in this research: chloroform, bromodichloromethane, chlorodibromomethane, and bromoform. HAA compounds of interest were bromoacetic acid, dibromoacetic acid, dichloroacetic acid, tribromoacetic acid, trichloroacetic acid, bromochloroacetic acid, bromodichloroacetic acid, and chlorodibromoacetic acid. THMs and HAAs were detected by liquid-liquid extraction and gas chromatography (GC), according to US EPA Methods 551.1 and 552.2.

THM and HAA samples were sampled in 20 mL vials. Prior to sampling, the vials were washed, rinsed with Milli-Q, allowed to dry, and baked in an oven at 105 °C for approximately five hours. Caps for the vials were also washed, rinsed with Milli-Q, and allowed to air dry. Duplicate samples were taken in 20 mL vials. The vials were filled headspace free and then preserved; HAA samples were preserved with 1 drop of 50 g/L NH_4Cl, whereas THM samples were preserved with 1 drop of 50 g/L NH_4Cl, 2 drops of 8 g/L $Na_2S_2O_3$, and 3 drops of 0.1 N HCl. Samples were then stored in the dark at 4 °C until extraction. After extraction, samples were processed with GC using a Varian CP-3800 GC equipped with a VF-5 column, a Varian CP-8400 auto sampler, and coupled with an electron capture detector (GC-ECD).

THM samples were extracted within 14 days of collection. Samples were extracted at room temperature. The samples were transferred to 40 mL amber extraction vials, and one scoop of $Na_2S_2O_3$ and 4 mL of pentane was added to each. The samples were capped and shaken for 30 seconds. Samples were then placed in a vial tray and shaken for an additional two minutes. Samples were left for 10 minutes to allow the layers to separate. The know aliquot of extract from the sample was collected and placed in a 2 mL GC vial. 40 µL of internal standard (1 mg/L of 1, 2-dichloropropane) was spiked into each sample's extract. Extract of the samples were stored in the dark at -20 °C until analysis. GC operating conditions were an injector temperature of 220 °C, a detector temperature of 320 °C, 1 µL injection volume with a flow rate of 1 mL/min. The sample was injected at 50 °C and held for seven minutes, while the temperature increased to 115 °C (at a rate of 5 °C/min) with no holding time, and further increased to 295 °C (at a rate of 50 °C/min) with 30 seconds of holding time. The MDL was 1.5 µg/L for THM compounds.

HAA samples were extracted within 14 days. Samples were extracted at room temperature. Samples were transferred to a 40 mL amber vial, and one tablespoon of $Na_2S_2O_3$, two drops of Na_2SO_3, 1 mL of concentrated H_2SO_4, and 4 mL of methyl tertiary butyl ether (MTBE) was added to each. Samples were capped and shaken for 30 seconds. A styrofoam tray was used to further shake the samples for two minutes. Samples were left for three minutes to allow layers to separate. The known aliquot of extract from the sample was collected and placed into 2 mL GC vials. 20 µL of internal standard (1 mg/L of 1, 2-dibromopropane) and 1 mL of diazomethane was added to each sample. Extract of samples were stored in the dark at -20 °C until analysis. GC operating conditions were an injector temperature of 200 °C, a detector temperature of 300 °C, 1 µL injection volume with a flow rate of 1 mL/min. The sample was injected at 35 °C and held for 10 minutes, while the temperature increased to 65 °C (at a rate of 2.5 °C/min) with no holding time, and further increased to 205 °C (at a rate of 20 °C/min) with a seven minutes holding time. The MDL was 0.9 µg/L, 2.1 µg/L, 0.3 µg/L, 0.2 µg/L, 1.2 µg/L, 1.0 µg/L, 1.5 µg/L, 1.3 µg/L for bromoacetic acid, dichloroacetic acid, trichloroacetic acid, bromochloroacetic acid, dibromoacetic acid, bromodichloroacetic acid, chlorodibromoacetic acid, and tribromoacetic acid, respectively.

Light Source

A low pressure (LP) collimated UV beam (Trojan Technologies, London, ON) was used as the light source, illustrated in Figure 3-1. The light was directed from the center of the lamp, through a transparent window, down an encased tunnel and onto a stirrer. The lamp emitted at a wavelength of 253.7 nm. Standards, as described by Kuo et al. (2003), were followed when conducting experiments. Fluence values were obtained as described by Bolton and Linden (2003) with an ILT 1400-A radiometer photometer (International Light Technologies, Peadoby, MA). The method uses the reading from the radiometer at the centre of the stirrer, the distance from the surface of the solution to the lamp, the absorption coefficient of the solution, and the volume of the solution in order to calculate various exposure times based on the desired fluence.

Figure 3-1 Collimated UV beam used in the research.

Electrochemical Cell

The set-up for the electrochemical experiments, illustrated in Figure 3-2, consisted of a power source, electrodes (anode and cathode), and an electrolysis cell. A direct current (DC) power source (GW Instek, Taiwan) supplied a constant current (0-3 A) by constantly changing the voltage (0-30 V). A titanium (Ti, Grade 2, commercially pure titanium, 98.9%) electrode was used as the cathode (BioSurface Technologies Corp, MT), with size 100 mm x 60 mm x 3 mm. An alloy of titanium and ruthenium dioxide (Ti/RuO_2) was used as the anode (Baoki Changli Special Metal Co. Ltd., China), with size 100 mm x 60 mm x 2 mm. The distance between the electrodes in the electrolysis cell was 6.0 cm, and each had a surface area of 60 cm^2. 300 mL of solution was added to each batch, which resulted in a contact surface area of 30 cm^2 for the electrodes. The electrolysis cell was placed on a stir plate and the solution was constantly stirred with a stir bar. As the electrodes were places in the electrolysis cell, some dead zones were created. To ensure that the solution was homogenous at the end of treatment, the solution was further stirred when the electrodes were removed.

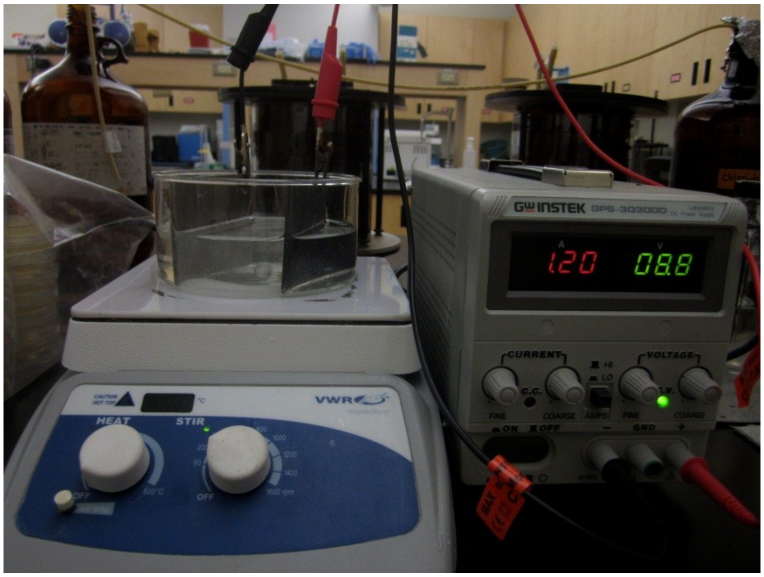

Figure 3-2 Electrochemical cell set-up.

Wastewater Source

The Mill Cove Water Pollution Control Centre (MCWPCC) in Bedford (Nova Scotia, Canada) is the largest municipal secondary treatment facility in Atlantic Canada. Halifax Water operates the plant that services the communities of Bedford and Sackville, with a population of 55000 (Halifax Water, 2013). MCWPCC was originally constructed in 1969 and upgraded in 1997, with a maximum daily flow capacity of 7.5 million imperial gallons per day (MImpGa/day) (Hu and Gagnon, 2006). The plant consists of grit removal, primary clarification, pure oxygen activated sludge biological treatment, secondary clarification, and UV light for disinfection (Hu and Gagnon, 2006; Comeau et al., 2008; Halifax Water, 2013). The plant is situated in a residential area and odour control is achieved by covering the primary and pure oxygen processes, and adding a two stage air scrubbing system (a wet phase followed by an activated carbon phase) that is situated in the grit removal room (Halifax Water, 2013). The effluent is discharged to the Bedford Basin (in the North-Western end of the Halifax Harbor) through an underwater pipe that runs for couple of kilometers (Crouse et al., 2012). A process diagram of the plant is presented in Figure 3-3. For this research, secondary wastewater effluent (prior to UV disinfection) was collected from the plant. The characteristics of the collected wastewater are detailed in Table 3-1.

Table 3-1 Characteristics of secondary wastewater effluent obtained from MCWPCC.

Parameter	Average ± Standard Deviation
pH	6.86 ± 0.02
TN (mg/L)	19.34 ± 0.22
NH_4^+ (mg/L)	37.84 ± 0.55
[Cl^-] (mg/L)	188.88 ± 38.61
TOC (mg/L)	11.45 ± 1.10
Ti (µg/L)	8.61 ± 1.35
Ru (µg/L)	0.12 ± 0.025

Statistical analysis

Statistical analysis was conducted to determine differences between treatments. Basic statistical values were displayed by means and standard deviation. Data was sorted, organized and plotted using Microsoft Excel 2010 ® (Redmond, WA). The Mini-Tab ® 16 software (State College, PA) was used to compute various statistical analyses. All statistical analysis was computed at 95% significance level, unless stated otherwise.

Figure 3-3 MCWPCC process diagram (Halifax Water, 2013).

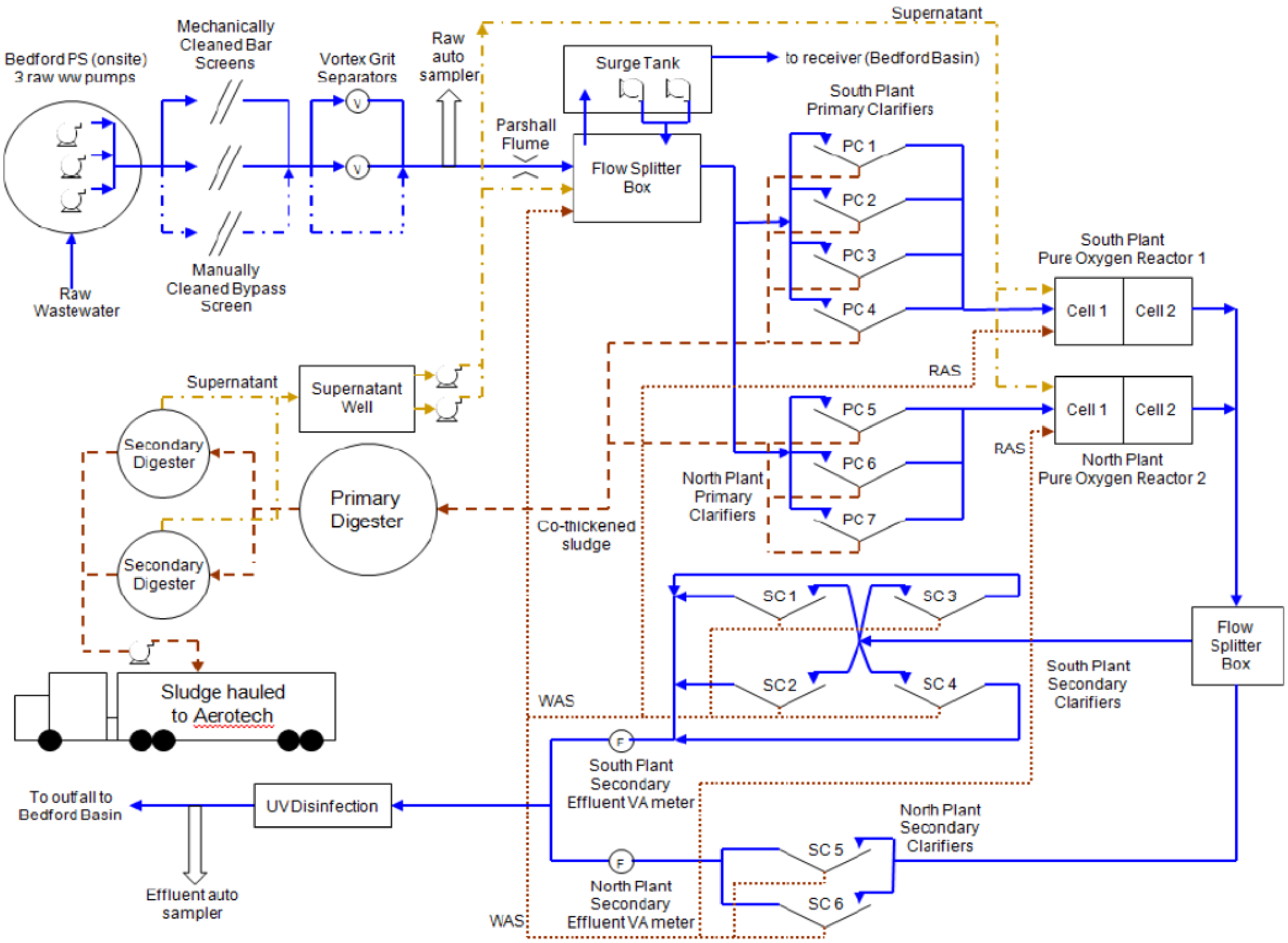

Chapter 4: Direct Photolysis of Nitrogen Compounds in Wastewater by UV Light

4.1 Introduction

Nitrogen compounds are a widespread concern in the wastewater industry and ammonia is considered one of the most problematic of these compounds (Mousavi et al., 2011). The release of wastewaters containing high levels of ammonia cause an increase in bacteria population, eutrophication, depletion of dissolved oxygen (Moazed, 2008; Vohra et al., 2010), and accelerated corrosion of construction materials in receiving waters (Ashrafizadeh and Khorasani, 2010). Ammonia also reduces the efficiency of the final disinfection process of wastewater treatment (Huang et al., 2008). Presence of nitrifying organisms could also bio-oxidize ammonia to nitrite and nitrate, both of which are harmful to humans (Moazed, 2008). Furthermore, ecological concerns are raised as ammonia is toxic to most marine life forms, even at low concentrations (Hued et al., 2006; Rezakazemi et al., 2012). The removal of nitrogen compounds is therefore essential to preserve various ecosystems.

Aqueous ammonia is typically present in either the un-ionized (NH_3) or ionized (NH_4^+) form. In aqueous environments, ammonia is typically found as an ammonium ion (Sarioglu, 2005). Nitrogen compounds (containing aqueous ammonia) are found in municipal, aquaculture, agricultural, and industrial wastewaters. Industrial wastewaters containing aqueous ammonia include soda-plants, oil refineries, coal gasification plants, dairy plants, tanneries, textile plants, and landfill leachate (Jung et al., 2004; Miladinovic and Weatherley, 2008; Hasanoglu et al., 2010; Rezakazemi et al., 2012).

In 2012, Environment Canada mandated a new set of wastewater effluent regulations, which limit the concentration of NH_3 to less than 1.25 mg/L, expressed as nitrogen at 15 °C ± 1 °C, computed from Equations 4.1 - 4.3 (Environment Canada, 2012):

$$Un-ionized\ Ammonia = Total\ Ammonia \times \left[\frac{1}{(1+10^{(pK_a-pH)})} \right] \tag{4.1}$$

where:

$$\text{Total Ammonia} = NH_3 + NH_4^+ \tag{4.2}$$

$$pK_a = 0.09018 + \frac{2729.92}{T} \tag{4.3}$$

where temperature (T) is in Kelvin.

In the literature, nitrogen compounds (in particular ammonia) have been treated with biological processes (Adams, 1974; Fang et al., 1993), anammox (Nishimura et al., 2012), ion exchange (Miladinovic and Weatherley, 2008; Khosravi et al., 2012), ozonation (Khuntia et al., 2013), microwave radiation (Lin et al., 2009), hollow-fiber membrane contactor (Ashrafizadeh and Khorasani, 2010), and electrochemical processes (Hu et al., 2009; Li and Liu, 2009; Liu et al., 2009; Kapalka et al., 2010).

UV based AOPs have also been proven effective in removing aqueous ammonia from wastewater. AOPs such as UV/H_2O_2 (Huang et al., 2008; De Brito et al., 2010) and UV/TiO_2 (Zhu et al., 2005; Vohra et al., 2010) have been investigated. Generation of the hydroxyl radical, a highly reactive and non-selective oxidant, is common in all AOPs.

The direct photolysis of various compounds with UV light has not been reported, as some organic species do not degrade efficiently under UV light (Rosenfeldt et al., 2006). Rand and Gagnon (2008) reported on the degradation of chlorine-based disinfectants (chlorine, monochloramine, and chlorine dioxide) when exposed to UV irradiation, where they observed the degradation of NH_3 to nitrite in chloramine-treated systems. Xiao et al. (2009) have reported on a faster degradation of ammonia in an electrochemical process when supplemented with UV irradiation. However, there is a paucity of literature investigating the effectiveness of UV irradiation for the direct photolysis of nitrogen compounds. Beckles and Diyamandoglu (2006) have reported on the photooxidation of ammonia under UV light in the presence of halide ions (Br^-, Cl^-, and I^-). Zheng et al. (1998) have also reported the photooxidation of ammonia with a UV light ($\lambda > 222.4$ nm) by OH· radicals. This research further investigated the direct photolysis of nitrogen compounds when exposed to a light source with a wavelength of 254 nm.

The aim of this research was to investigate the effectiveness of UV light in removing nitrogen from municipal wastewater. A LP collimated UV beam was utilized as a light source. pCBA was used as an organic probe compound in order to evaluate the production and efficiency of OH· radicals to degrade nitrogen compounds. Various factors affecting nitrogen removal efficiency were investigated, and a possible pathway for the direct photolysis of nitrogen is also presented. The optimized experimental conditions were further used to treat secondary wastewater effluent collected from MCWPCC in Bedford, NS.

4.2 Materials & Methods

Experimental Design

Synthetic wastewater was produced by mixing NH_4Cl and NaCl stock solutions with Milli-Q water. Batch experiments with synthetic wastewater were conducted in order to investigate the effects of pH, chloride concentration, and initial nitrogen concentration on the removal efficiency of nitrogen. Samples were taken prior to and after UV light irradiation at various fluence (100, 500, and 1000 mJ/cm^2 representing on average 16, 80, and 155 minutes), and analyzed for the respective wastewater parameters (pH, aqueous ammonia, total nitrogen, nitrate, nitrite, and pCBA). All experiments were conducted in duplicates, at room temperature (20-23 °C), in a randomized order. Optimized conditions were used to treat secondary wastewater effluent from MCWPCC in Bedford, NS. Figure 4-1 illustrates a schematic of the experimental set-up.

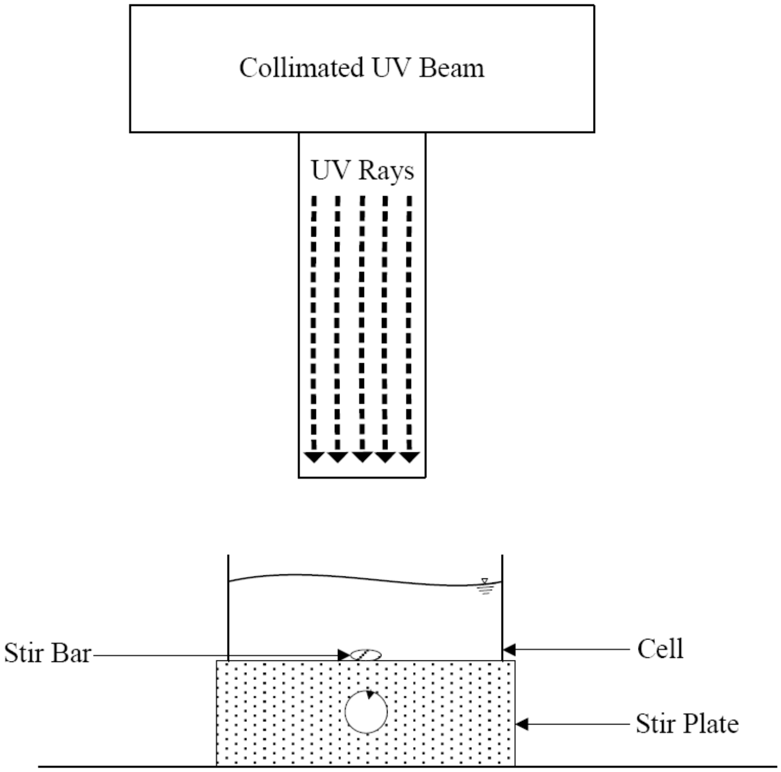

Figure 4-1 Experimental set-up for direct photolysis experiments.

Light Source

A LP UV collimated beam (Trojan Technologies, London, ON) was employed as the light source, emitting at a wavelength of 253.7 nm. UV fluence values were obtained as described by Bolton and Linden (2003) with an ILT 1400-A radiometer photometer (International Light Technologies, Peadoby, MA). The method used the UV irradiance reading from the radiometer at the center of the stirrer, the distance from the surface of the solution to the lamp, the absorption coefficient of the solution, and the volume of the solution in order to calculate various exposure times based on desired UV fluence.

Chemical Preparation

All chemical solutions were prepared with ultrapure Milli-Q (18.2 MΩ.cm, Millipore Corporation, MA) water. All glassware was washed with laboratory grade detergent and triple-rinsed with Milli-Q prior to experimentation. NH_4Cl and NaCl stock solutions were mixed with Milli-Q to produce synthetic wastewater. For saline experiments, additional NaCl stock solution was added to achieve the desired chloride concentration. pCBA was spiked into the solutions to evaluate OH· radical production. Adjustment of pH was achieved with the addition of 1.0 M NaOH and 0.1 M H_2SO_4.

Analytical Methods

As detailed in the Materials & Methods chapter.

Wastewater Collection

As detailed in the Materials & Methods chapter.

Statistical Analysis

Data was organized and plotted using Microsoft Excel 2010® (Redmond, WA). The Mini-Tab ® 16 software (State College, PA) was used to compute statistical analyses; paired t-test and independent t-test. All statistical analysis was computed at a 95% significance level, unless stated otherwise.

4.3 Results & Discussion

Effect of pH

The influence of pH on total nitrogen degradation was investigated at three pH levels (8, 10, 12), illustrated in Figure 4-2. The initial average concentration of total nitrogen was 26 mg/L. All of the samples were irradiated at three UV fluence conditions of 100, 500, and 1000 mJ/cm^2.

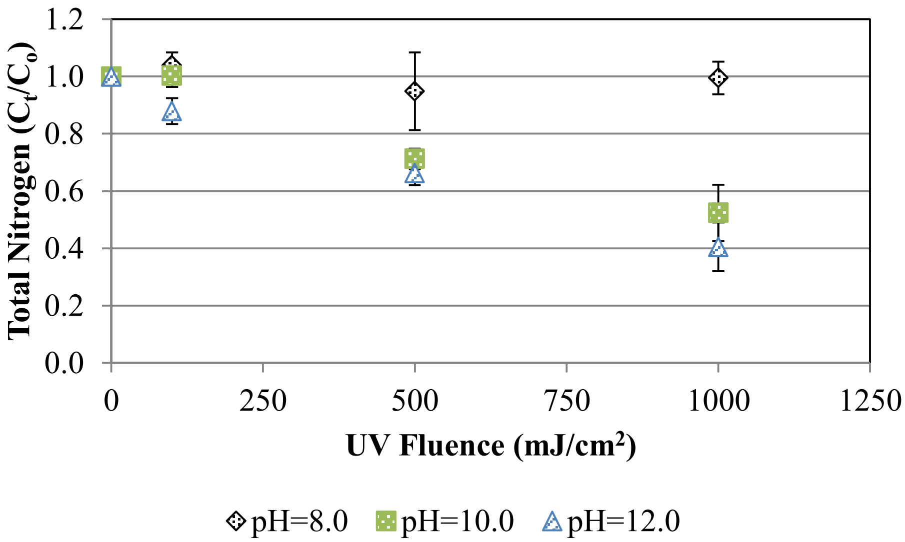

Figure 4-2 Effects of pH on the photolysis of total nitrogen (Error bars represent standard deviation).

At initial pH of 8.0, no significant total nitrogen removal (<0.5%) was observed regardless of the UV fluence employed (p=0.959). With an initial pH of 10.0 or 12.0, a decrease in concentration for total nitrogen was observed. At a UV fluence condition of 1000 mJ/cm^2 and initial pH=10.0, the total nitrogen concentration dropped to 13.2 mg/L (resulting in 47.6% removal). With an initial pH=12.0 and UV fluence of 1000 mJ/cm^2, total nitrogen removal was even greater compared to pH=10.0, with 59.5% removal of total nitrogen.

The dependence of aqueous ammonia removal on pH was been reported in the literature for various systems (Nemoto et al., 2007; Zhu et al., 2007; Huang et al., 2008; Vohra et al., 2010). At pH above 9.25, aqueous ammonia is present primarily in NH_3 form, whereas NH_4^+ is the dominant form at pH<9.25 (Figure 2-1). The dissociative equilibrium of ammonia in water is in accordance with Equation 4.4 (Huang et al., 2008):

$$NH_4^+ + H_2O \rightarrow NH_3 + H_3O^+ \qquad \mathrm{p}K_a=9.246 \qquad (4.4)$$

Ammonium is in equilibrium with ammonia at a $\mathrm{p}K_a$ of 9.25. Accordingly at pH=10.0, NH_3 is 85% of total N (on molar basis) and at pH=12.0, NH_3 is over 99% of total N (on a molar basis). Thus, the decrease of total nitrogen observed in the system was from the removal of aqueous ammonia that was oxidized by OH· or potentially through volatilization. For this research, the experimental dish used was not enclosed; however the loss of aqueous ammonia due to volatilization was investigated by control experiments at two pH levels (8.0 and 10.0). The results showed that there was negligible loss of aqueous ammonia, also confirmed by other research (Huang et al., 2008; Zhu et al., 2008; Mikami et al., 2010). However, it is suspected that at the high pH level (12.0) some of the aqueous ammonia was removed through volatilization as ammonia is typically found in the gas form at high pH levels (Idelovitch and Michail, 1981).

Aqueous ammonia, measured as ammonium and reported as ammonium nitrogen, was also monitored for the experiments. The results confirmed the removal of aqueous ammonia at pH levels higher than 9.25 (Figure 4-3). The removal efficiencies of aqueous ammonia were in the same range of the photochemical (Zhu et al., 2005) and photocatalytic (Vohra et al., 2010) systems, but greater compared to the hydrogen peroxide photooxidation system reported by Huang et al. (2008).

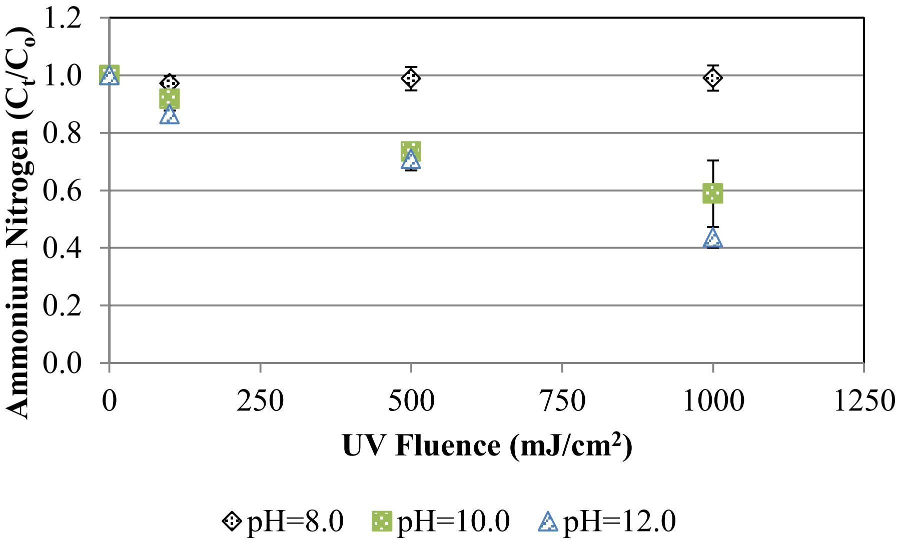

Figure 4-3 Effect of pH on the photolysis of ammonium nitrogen (Error bars represent standard deviation).

A decrease in pH occurred in all water matrices (Figure 4-4). For the water matrix with [TN]=26 mg/L and $[Cl^-]$=500 mg/L, with an initial pH=10.0 the pH did not decrease lower than 9.04; whereas with an initial pH=12.0, the pH stayed above 11.45. Zhu et al. (2005) and Huang et al. (2008) have both reported a pH decrease in their respective systems with the degradation of ammonia. Zhu et al. (2005) concluded that the pH decrease in their photocatalytic system was due to the formation of a proton from the oxidation of NH_3.

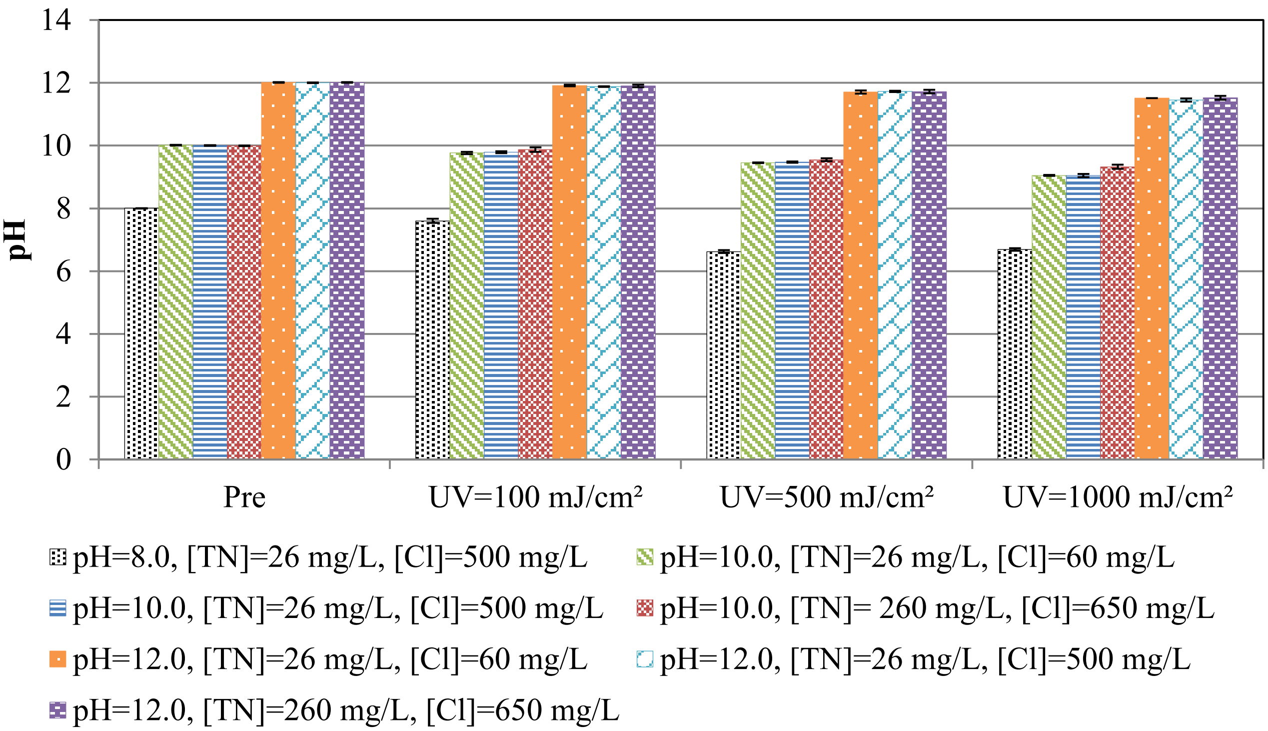

Figure 4-4 pH variation in various water matrices (Error bars represent standard deviation).

At all pH levels (8.0, 10.0, 12.0), little or no nitrite (NO_2^-) and nitrate (NO_3^-) were formed (or close to their respective MDL). Other research has also observed the lack of formation of either NO_2^- or NO_3^- when aqueous ammonia degrades. Vohra et al. (2010) have reported 2 mg/L of NO_3^- formation when NH_4^+-NH_3 undergoes a TiO_2 assisted photocatalytic degradation at pH 12.0 (although no NO_2^- was formed). Zhu et al. (2005) have observed the production of NO_2^- (but not NO_3^-) after six hours of ammonia treatment with UV irradiation at pH=10.2. Zhu et al. (2005) have suggested that UV irradiation on ammonia may have produced other nitrogen products, such as NH_2OH and N_2. The results from this present research suggest that total nitrogen was removed in the system due the conversion of ammonia to other nitrogen compounds, and the formation of NO_2^- or NO_3^- was not quantified in the process.

The results suggest that pH and UV fluence were beneficial for the direct photolysis of nitrogen compounds. The removal of total nitrogen was attributed to the removal of aqueous ammonia in the system. Simple linear regression conducted on the data suggests high correlation (R^2=0.97 at pH=10.0 and R^2=0.98 at pH=12.0) between total nitrogen and UV fluence.

Effect of Chloride Concentration

The influence of chloride ions on total nitrogen degradation was investigated (Figure 4-5). The effects were investigated at two chloride concentrations ($[Cl^-]$=60 mg/L and $[Cl^-]$=500 mg/L) for two pH levels (10.0 and 12.0), with a fixed initial total nitrogen concentration of 26 mg/L. The samples were irradiated at three UV fluence conditions of 100, 500, and 1000 mJ/cm^2.

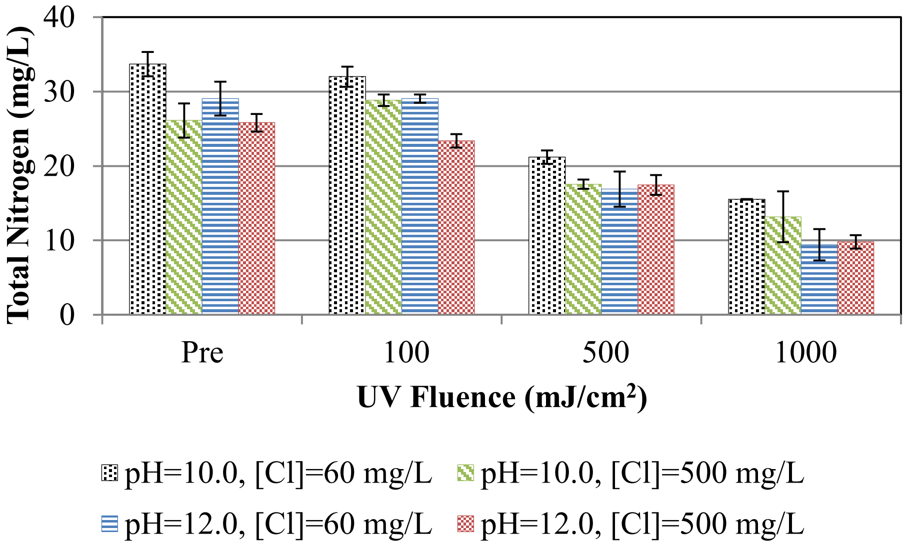

Figure 4-5 Effect of chloride concentration on the photolysis of total nitrogen (Error bars represent standard deviation).

At an initial pH=10.0 and a low chloride concentration ($[Cl^-]$=60 mg/L), a 53.6% removal of total nitrogen was achieved compared to a 47.6% at $[Cl^-]$=500 mg/L, with a UV fluence condition of 1000 mJ/cm^2. An independent t-test concluded that there was no significant difference between treatments (p=0.682). At an initial pH=12.0 and a low chloride concentration ($[Cl^-]$=60 mg/L), 65.4% of total nitrogen was removed compared to 59.5% with a high chloride concentration ($[Cl^-]$=500 mg/L), at a UV fluence of 1000 mJ/cm^2. An independent t-test concluded no difference between treatments (p=0.732).

Although lower chloride concentrations resulted in higher removals in some instances, there was no statistical difference between treatments. The results suggest that an increase in matter particles, from the addition of chloride ions in the solution, does not inhibit the treatment efficiency of the UV light. This is inconsistent with Beckles and Diyamandoglu (2006), who have reported an accelerated photooxidation of ammonia in the presence of Cl^- or Br^-, even in acidic solutions when photolysis of ammonia does not occur. In a different treatment system (by means of ozonation), Tanaka and Matsumura (2002) have reported chloride ions to have little effect on the removal efficiency of ammonia.

Effect of Initial Nitrogen Concentration

The influence of initial nitrogen concentration on removal efficiency was investigated at two nitrogen concentrations (26 mg/L and 260 mg/L) for two pH levels (10.0 and 12.0) (Figure 4-6). The samples were irradiated at three UV fluence conditions of 100, 500, and 1000 mJ/cm^2.

At both pH levels, the amount of total nitrogen removed increased with an increase in initial nitrogen concentration. At pH=10.0 and UV fluence of 1000 mJ/cm^2, the same removal rates were observed (around 47%) for both initial concentrations of nitrogen. However, an independent t-test suggested significant difference between the treatments (p=0.001). At pH=12.0 and UV fluence of 1000 mJ/cm^2, an increase of 3.5% of total nitrogen removal was observed with a higher initial concentration ([TN]=260 mg/L). An independent t-test indicated a significant difference in nitrogen removal with initial nitrogen concentration between the treatments (p=0.003).

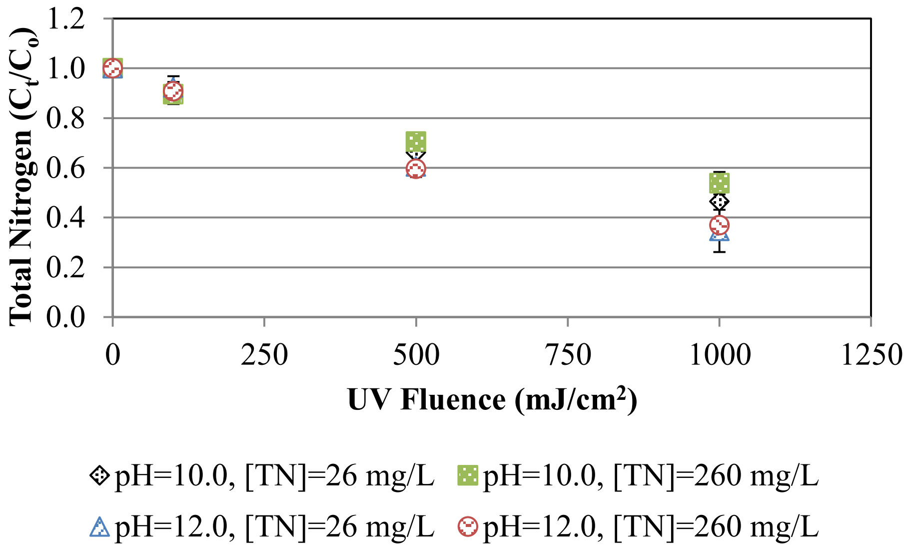

Figure 4-6 Effect of initial concentration on the photolysis of total nitrogen (Error bars represent standard deviation).

The increase in total nitrogen removal was attributed to an increase in aqueous ammonia removal. The results are consistent with findings by Huang et al. (2008), who reported an increase in ammonia removal with an increase in initial ammonia concentration.

The increase in removal at higher initial nitrogen concentration suggests that the removal efficiency is proportional to the initial concentration of contaminant present, suggesting a pseudo-first order reaction. A possible explanation for this is the increase in collision between OH· radicals and NH_3/NH_4^+, as suggested by Huang et al. (2008).

Production of OH· Radicals

OH· radicals can be produced by the photolysis of water at various wavelengths. In this research, UV light irradiation at a wavelength of 253.7 nm was used in order to excite water molecules, which further dissociated into a hydrogen atom and OH· radicals. The direct photolysis of water is in accordance to Equation 4.5, suggested by others at varying wavelengths (Getoff and Schenck, 1968; Legrin et al., 1993; Zheng et al., 1998):

$$H_2O + h\nu \rightarrow (H_2O)^* \rightarrow H + OH\cdot \tag{4.5}$$

pCBA samples were taken at three times through the experiments (at UV fluence values of 100, 500, and 1000 mJ/cm^2). The pCBA degradation in the system and subsequent reaction with the OH· radical, can be expressed by Equation 4.6 (Cho et al., 2004; Watts and Linden, 2007):

$$\frac{-d[pCBA]}{dt} = k_{(OH,pCBA)}[OH]_{SS}[pCBA] \tag{4.6}$$

And solving Equation 4.6 results in:

$$-\ln\left(\frac{[pCBA]}{[pCBA]_{\bullet}}\right) = K_{\text{exp}}t \tag{4.7}$$

Where:

$$K_{\text{exp}} = k_{OH,pCBA}[OH]_{SS} \tag{4.8}$$

The observed rate constant of pCBA (expressed as K_{exp}) was obtained from the slope of the logarithmic plot of pCBA degradation, as dictated by Equation 4.7. The steady state concentration of OH· radicals was further calculated from Equation 4.8, with $k_{OH,pCBA} = 5 \times 10^9$ M^{-1} s^{-1} (Watts and Linden, 2007). The pseudo-steady state assumption for the OH· radical was valid due to the constant degradation of pCBA ($R^2>0.9$) at all exposure times for all water matrices (Elovitz and Gunten, 1999; Cho and Yoon, 2008).

Control experiments were conducted to estimate the production rate of OH· radicals from the photolysis of water. The water matrix for the control experiment did not contain any contaminant, just pCBA spiked into Milli-Q. The results of the control experiments and the steady state concentration of the OH· radicals are illustrated in Figure 4-7 and Figure 4-8, respectively. The concentrations of OH· radicals observed were in the same order of magnitude as research conducted by Watts and Linden (2006) in a different water matrix.

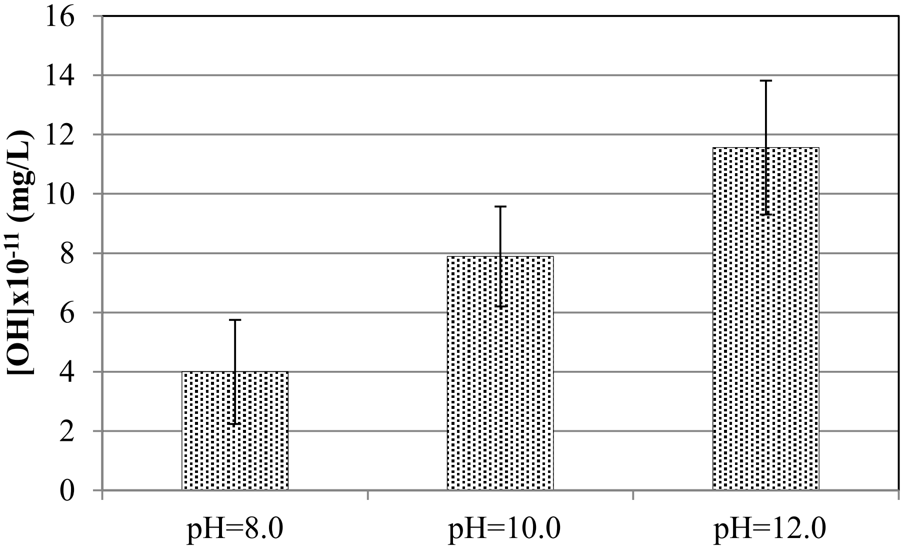

Figure 4-7 Control production of OH· radicals.

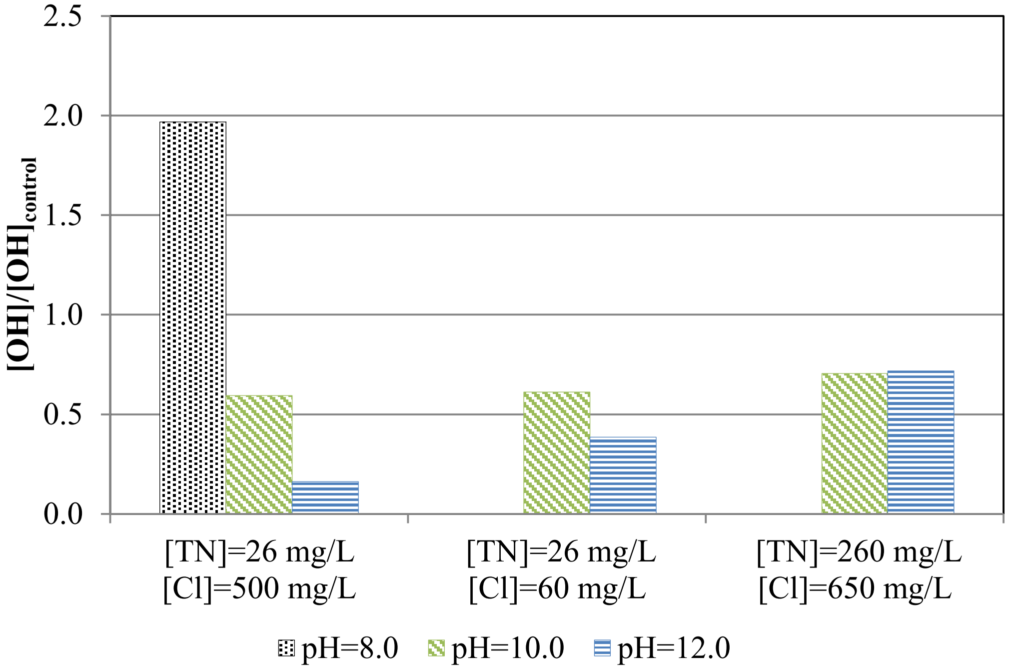

Figure 4-8 Steady state production of OH· radicals in various water matrices.

For the control experiments, production of OH· radicals increased with pH level (R^2=0.99). As in many other AOPs, the major factor that governs the efficiency of OH· radicals to degrade the contaminant is the fraction of OH· radicals that are scavenged by the water matrix compared to the fraction of OH· radicals available for the oxidation of the contaminant (Rosenfeldt et al., 2006). At a chloride concentration of 500 mg/L, the concentration of OH· radicals was greater at pH=8.0 than at pH=10.0 or pH=12.0. The concentration of OH· radicals at pH=10.0 was also greater compared to a pH=12.0. The concentration of OH· radicals was related to the amount of contaminant removed, as none of the contaminant was removed at pH=8.0 and therefore no OH· radical were consumed. The amount of OH· radicals at pH=12.0 was less compared to pH=10.0, suggesting that more OH· radicals were consumed in order to achieve the higher removal rates of nitrogen compounds observed. The same trend of OH· radical concentration was observed at a chloride concentration of 60 mg/L. For the water matrix with an initial total nitrogen concentration of 260 mg/L, the concentration of OH· radicals was equal at both pH levels (10.0 and 12.0). The increased amount of chloride present in the water matrix could have decreased the availability of OH· radicals to oxidize pCBA. Another plausible explanation is an increase in scavenging of OH· radicals by other intermediate products in the process, which reduced the availability of OH· radicals to oxidize the pCBA (Zheng, 1998; Rosenfeldt et al., 2006). Therefore, the pCBA did not degrade and an excess of OH· radicals was observed.

Degradation Pathway

The initial concentration of nitrogen had an effect on removal efficiency. Therefore, rate constants were calculated using pseudo-first order reaction with respect to total nitrogen concentration, as detailed in Equation 4.9:

$$\frac{d[TN]}{dt} = -k_{obs}[TN] \tag{4.9}$$

The reaction rate constant, k_{obs}, was obtained from the slope of the regression line by plotting a logarithmic graph of nitrogen concentration with reaction time, prescribed by Equation 4.10:

$$\ln\left(\frac{[TN]}{[TN]_{\bullet}}\right) = -k_{obs}t \tag{4.10}$$

The values of the rate constants are presented in Table 4-1. The obtained rate constants are small, suggesting low rate constants for aqueous ammonia as well. This is consistent with findings by Huang et al. (2008) who reported the use of other oxidants with OH· radicals for achieving higher ammonia removal efficiency. The rate constants increased with pH level in all water matrices, and the rate constant obtained from the treatment of secondary municipal wastewater was in the same range as other water matrices with the same pH.

Table 4-1 Rate constants and correlation coefficient for the photolysis of total nitrogen in various water matrices.

Water matrix	k (min^{-1})	R^2
[TN]=26 mg/L, [Cl$^-$]=500 mg/L, pH=8.0	0.000145	0.377
[TN]=26 mg/L, [Cl$^-$]=500 mg/L, pH=10.0	0.00398	0.93
[TN]=26 mg/L, [Cl$^-$]=500 mg/L, pH=12.0	0.00579	0.98
[TN]=26 mg/L, [Cl$^-$]=60 mg/L, pH=10.0	0.00506	0.988
[TN]=26 mg/L, [Cl$^-$]=60 mg/L, pH=12.0	0.00682	0.985
[TN]=260 mg/L, [Cl$^-$]=650 mg/L, pH=10.0	0.00408	0.991
[TN]=260 mg/L, [Cl$^-$]=650 mg/L, pH=12.0	0.00649	0.999
Secondary municipal WW effluent (pH=10.0)	0.00426	0.999

The results from this work suggest that nitrogen compounds degraded when exposed to UV irradiation (with a wavelength of 254 nm). The total nitrogen removed was attributed to the removal of aqueous ammonia in the system. It is suspected that the degradation of nitrogen is achieved by collision of OH· radicals with aqueous ammonia. Ammonia is oxidized and reduced to other nitrogen compounds in accordance to either degradation pathway (following Equations 4.11 - 4.13 or 4.14 - 4.15) (Zheng et al., 1998; Huang et al., 2008; Pretzer et al., 2008; Rezaee et al., 2012):

Degradation Pathway 1:

$$NH_3 + OH\cdot \rightarrow NH_2 + H_2O \tag{4.11}$$

$$NH_2 + OH\cdot \rightarrow NH_2OH \tag{4.12}$$

$$NH_2OH \rightarrow HNO \rightarrow NO \rightarrow N_2 \tag{4.13}$$

Degradation Pathway 2:

$$NH_3 + OH\cdot \rightarrow NH_2OH + H^+ \tag{4.14}$$

$$NH_2OH + OH\cdot \rightarrow NO_2^- \rightarrow NO_3^- \tag{4.15}$$

To provide indication for which degradation pathway aqueous ammonia underwent, intermediate products (NO_2^- and NO_3^-) were measured. In this research, concentration of NO_2^- and NO_3^- were low or close to the MDL (MDL was 0.7 mg/L and 0.8 mg/L for nitrite and nitrate, respectively). Therefore it was determined that the degradation pathway which ammonia followed was the degradation pathway 1. It is suspected that ammonia was oxidized and reduced into other nitrogen compounds (amidogen, hydroxylamine, nitroxyl, and nitrogen monoxide), and sequentially to nitrogen gas.

Application to Wastewater

Secondary effluent obtained from MCWPCC was treated at three UV fluence conditions of 100, 500, and 1000 mJ/cm^2 to evaluate the efficiency of treatment with actual wastewater. The wastewater was adjusted to an initial pH of 10.0.

Total nitrogen was removed from the wastewater when irradiated with UV light (Figure 4-9). At a UV fluence of 1000 mJ/cm^2, 70.1% total nitrogen was removed. Simple linear regression was conducted on the data, resulting in a high correlation coefficient (R^2=0.97) between the contaminant removed and UV fluence. The results suggest that UV irradiation can be employed to remove nitrogen compounds in municipal wastewater with pH>9.25.

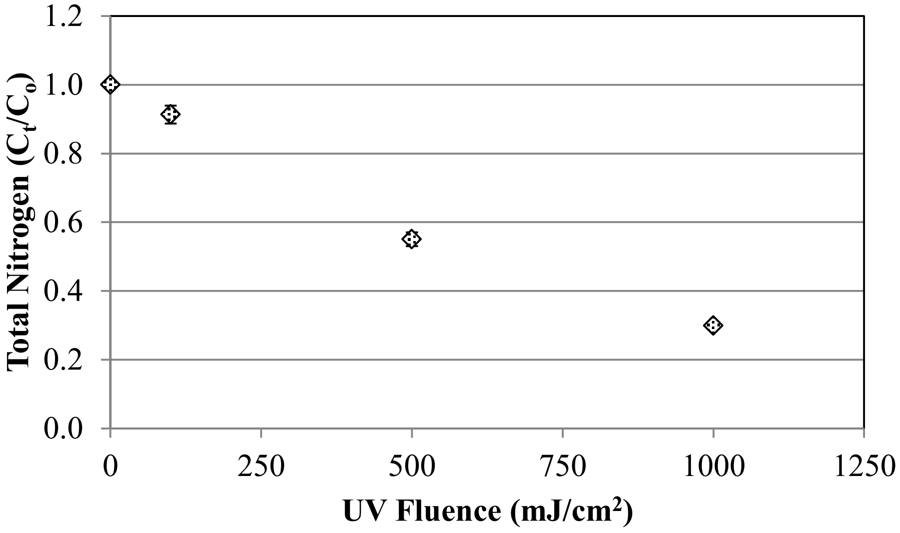

Figure 4-9 Photolysis of total nitrogen in municipal wastewater (Error bars represent standard deviation).

4.4 Conclusion

- The direct photolysis of nitrogen compounds was demonstrated with a UV light.
- The nitrogen removed was attributed to the removal of aqueous ammonia in the system.
- Alkaline pH improved the degradation of total nitrogen, where at pH=12.0 the highest removal was observed (59.5% at a UV fluence of 1000 mJ/cm^2).
- Chloride concentration did not significantly affect treatment efficiency.
- The initial amount of contaminant had an effect on the amount removed, where a higher initial concentration of nitrogen resulted in statistically higher removal rates.
- The kinetics of the process was investigated by monitoring the production of OH· radicals via HPLC, using pCBA as an organic probe compound. The generation of hydroxyl radicals was found to be beneficial for the removal of nitrogen from the solution, photo-

reducing aqueous ammonia to other nitrogen compounds and nitrogen gas as a final product.

- The direct photolysis of nitrogen compounds in secondary wastewater effluent was also observed, where 70.1% was removed at a UV fluence of 1000 mJ/cm^2.
- This research demonstrated the direct photolysis of nitrogen contaminants with a UV light, although removal efficiencies were low. The supplement of other oxidants, such as H_2O_2, O_3, or TiO_2, with UV light would be beneficial for higher removal rates and to possibly meet regulatory standards.

Chapter 5: Mechanism and Kinetics of Electrochemically Treating Aqueous Ammonia

5.1 Introduction

In the past decade, electrochemical treatment of various contaminants has been broadly investigated. Electrochemical treatment is an attractive technology as it is simple, has a small footprint, a rapid start-up time, high treatment efficiency, and does not produce sludge (Dash and Chaudhari, 2005; Li et al., 2009a; Liu et al., 2009). In particular, electrochemical treatment of aqueous ammonia has been previously investigated with various electrode materials (Kim et al., 2005; Hu et al., 2009; Li and Liu, 2009; Liu et al., 2009; Kapalka et al., 2010). Electrochemical treatment of aqueous ammonia offers great potential as the by-product of treatment, which is nitrogen gas in most cases, is harmless (Kim et al., 2005).

Several factors are to be taken into consideration when optimizing an electrochemical process: current density, pH, chloride concentration of the solution, and electrode material (Vlyssides et al., 2002; Vanlangendonck et al., 2005). The electrochemical removal mechanism of ammonia is either through direct oxidation occurring at the surface of the anode, or through indirect oxidation in the solution (Feng et al., 2003). The indirect oxidation of ammonia occurs by hydroxyl radicals produced in the bulk water or by HOCl formed in the process (Chen et al., 2007; Li and Liu, 2009). The electrolytic degradation of ammonia has been reported using pseudo first-order kinetics (Chen et al., 2007; Hu et al., 2009) and pseudo zero-order kinetics (Vanlangendonck et al., 2005; Li and Liu, 2009; Liu et al., 2009). Therefore, the removal mechanism of aqueous ammonia in the electrochemical process is not completely understood. Moreover, the efficiency of electrochemically treating ammonia in actual wastewater has not been reported in detail and there is a paucity of research investigating the formation of DBPs in the process (Cong et al., 2008; Li and Ni, 2012).

The objective of this research was to investigate the removal mechanism of aqueous ammonia in an electrochemical process with varying pH, current density, and chloride concentration. The electrodes used were a Ti cathode with a Ti/RuO_2 anode. The effects of pH and current density on removal efficiency were investigated at two chloride concentrations, and removal kinetics were further investigated at both chloride concentrations. The efficiency of process and the production of DBPs (TTHMs and THAAs) were assessed under optimal operational parameters with secondary effluent wastewater obtained from MCWPCC, Bedford, NS.

5.2 Materials & Methods

Experimental Design

Batch experiments with synthetic wastewater were conducted at two chloride concentrations ($[Cl^-]$=450 mg/L and $[Cl^-]$=4500 mg/L), in order to investigate the effects of pH and current density on the removal efficiency of aqueous ammonia in an electrochemical process. Two pH levels (5.7 and 9.7) and current densities were considered (3.75 and 7.5 mA/cm^2 at the low chloride concentration, and 20 and 40 mA/cm^2 at the high chloride concentration). NH_4Cl, NaCl, and Milli-Q (18.2 MΩ.cm, Millipore Corporation, MA) were mixed to simulate synthetic wastewater. The initial aqueous ammonia concentration was 75 mg/L at a $[Cl^-]$=450 mg/L and 750 mg/L at a $[Cl^-]$=4500 mg/L. Samples were taken prior to and after treatment (20, 40, 60, and 80 minutes), and analyzed for the respective wastewater parameters (pH, aqueous ammonia, total nitrogen, chlorine (total and free), monochloramine, nitrate, nitrite, TTHMs, THAAs, titanium, and ruthenium). Electrolysis treatment at [Cl^-]=450 mg/L was conducted for a maximum of 60 minutes; whereas at [Cl^-]=4500 mg/L the electrolysis treatment was conducted for a maximum of 80 minutes due to the higher concentration of contaminant present. All experiments were conducted in duplicates, at room temperature (20-23 °C), and in a randomized order. Optimized conditions from the synthetic wastewater trials were used to treat secondary wastewater effluent from MCWPCC in Bedford, NS. Figure 5-1 illustrates a schematic of the experimental set-up.

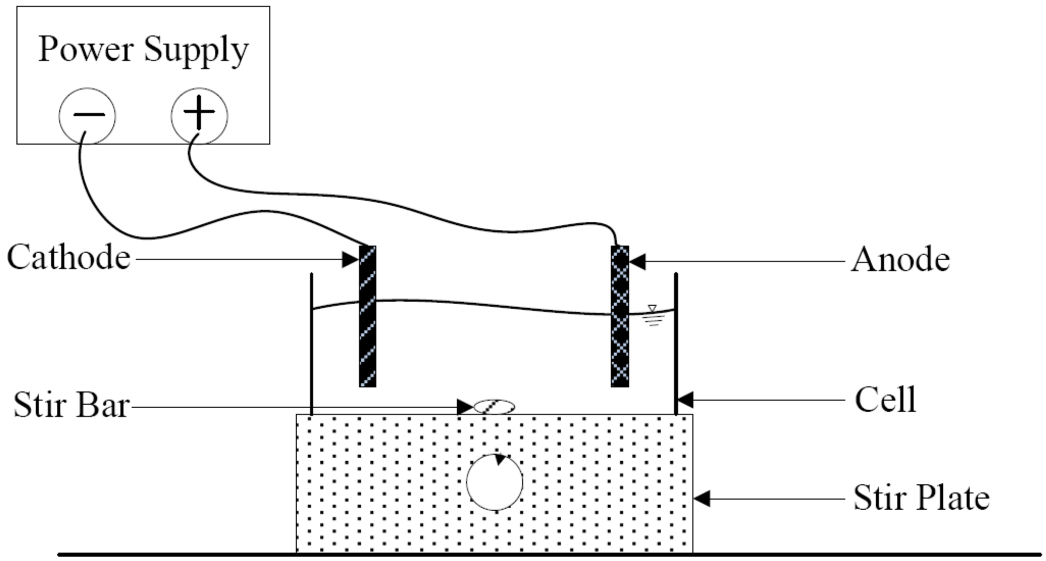

Figure 5-1 Experimental set-up for electrolysis experiments.

Power Supply

A DC power source (GW Instek, Taiwan) supplied a constant current (0-3 A) by constantly changing the voltage (0-30 V). A titanium (Ti, Grade 2, commercially pure titanium, 98.9%) electrode was used as the cathode (BioSurface Technologies Corp, MT), with size 100 mm x 60 mm x 3 mm. An alloy of ruthenium dioxide and titanium (Ti/RuO_2) was used as the anode

(Baoki Changli Special Metal Co. Ltd., China), with size 100 mm x 60 mm x 2 mm. The distance between the electrodes was 6.0 cm, and each had a contact surface area of 30 cm^2.

Chemical Preparation

Chemical solutions used in the research were prepared with ultrapure Milli-Q (18.2 MΩ.cm, Millipore Corporation, MA) water. All of the glassware was washed with laboratory grade detergent and triple-rinsed with Milli-Q prior to start of experiments. NH_4Cl and NaCl stock solutions were mixed with Milli-Q to produce synthetic wastewater at the desired concentrations. Additional chloride was added to the batches with a NaCl stock solution. Adjustment of pH was achieved with a 1.0 M NaOH and 0.1 M H_2SO_4.

Analytical Methods

As detailed in the Materials & Methods chapter.

Wastewater Collection

As detailed in the Materials & Methods chapter.

Statistical Analysis

Data was sorted, organized and plotted using Microsoft Excel 2010 ® (Redmond, WA). Statistical analyses (independent t-test and f-test) were computed with the aid of Mini-Tab ® 16 software (State College, PA). All statistical analysis was computed at 95% significance level, unless otherwise stated.

5.3 Results & Discussion

Electrochemical Treatment of Aqueous Ammonia at [Cl⁻]=450 mg/L

Effect of pH

The effects of pH were investigated at two levels (5.7 and 9.7) for two current densities (3.75 and 7.5 mA/cm^2). Experiments were conducted with an initial ammonium concentration of 75 mg/L. The effects of pH on aqueous ammonia and total nitrogen removal are illustrated in Figure 5-2 and Figure 5-3, respectively.

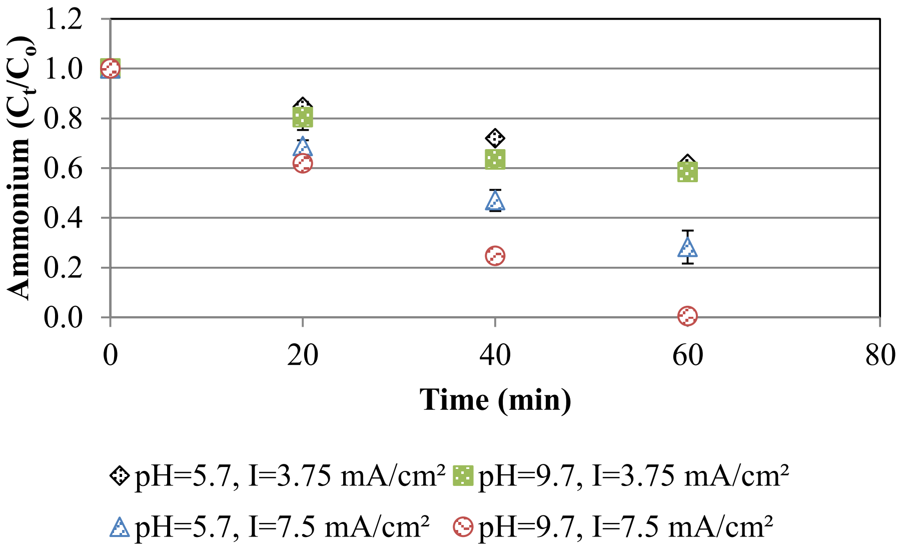

Figure 5-2 Effects of pH and current density on the electrolysis of ammonium at [Cl⁻]=450 mg/L (Error bars represent standard deviation).

Aqueous ammonia and total nitrogen were electrolyzed at higher rates (at both current densities) with an elevated pH of 9.7. After 60 minutes of electrolysis at 3.75 mA/cm^2, 41.56% of aqueous ammonia was removed from the solution with an initial pH=9.7, compared to 38.46% removal at pH=5.7. An independent t-test conducted on the data suggested no statistical difference in treatment efficacy with pH (p=0.59). At a current density of 7.5 mA/cm^2 and after 60 minutes of treatment, 99.5% of aqueous ammonia was removed with an initial pH=9.7, compared to 71.75%

removal at pH=5.7. An independent t-test concluded that there was no significant difference in treatment (p=0.172). The results showed that an elevated pH level was beneficial for the electrolysis of aqueous ammonia using a Ti/RuO_2 anode.

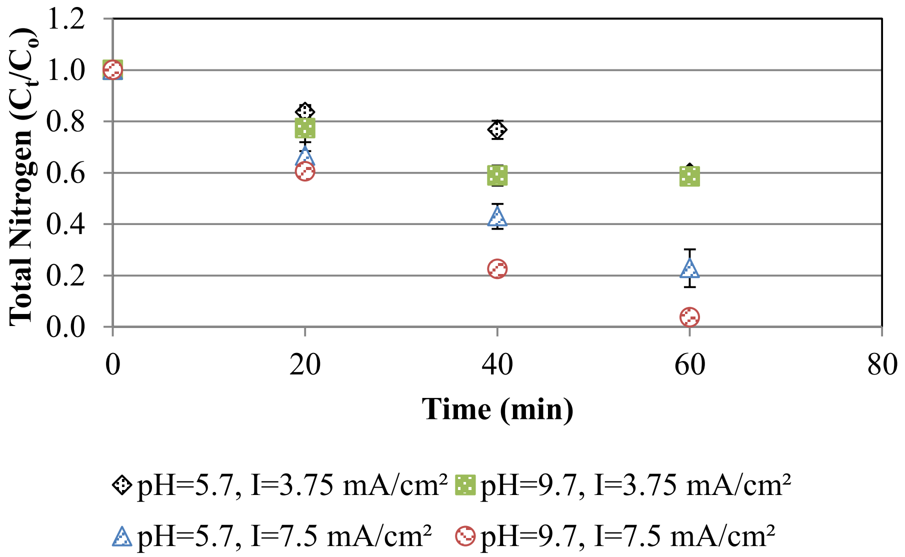

Figure 5-3 Effects of pH and current density on the electrolysis of total nitrogen at [Cl^-]=450 mg/L (Error bars represent standard deviation).

Aqueous ammonia exists in either the ionized (NH_4^+) or the un-ionized (NH_3) form. This is in accordance to the pH of the solution, expressed by Equation 5.1 (Huang et al., 2008):

$$NH_4^+ + H_2O \rightarrow NH_3 + H_3O^+ \qquad pK_a=9.246 \qquad (5.1)$$

At a pH level above 9.25, aqueous ammonia is present mainly in the NH_3 form; whereas at pH level below 9.25, NH_4^+ becomes the dominant form (Figure 5-4). This suggests that NH_3 rather than NH_4^+ is more easily oxidized throughout the electrochemical process (Kim et al., 2005).

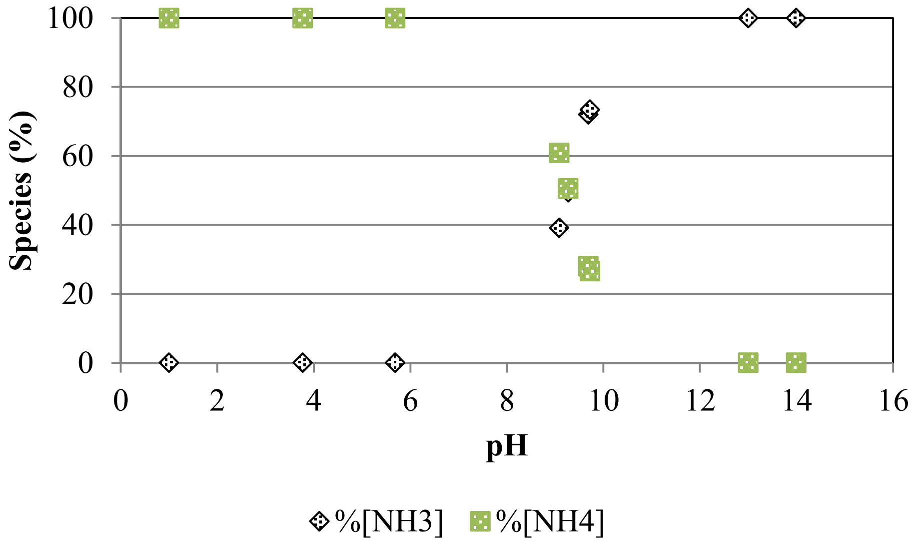

Figure 5-4 Relationship between pH and NH_3/NH_4^+ species.

The results are consistent with findings from Li and Liu (2009) who reported on more efficient ammonia degradation at an alkaline pH with a Ti/RuO_2 anode and stainless steel cathode. Vlyssides et al. (2002) reported a higher reduction of ammonia at pH=9.0 compared to lower pH levels, when using a stainless steel cathode and a Ti/Pt anode. Kim et al. (2005) have also reported a higher removal of ammonia at pH=12.0 compared to pH=7.0, with a Ti cathode and an IrO_2 anode. However, the results from this present study are inconsistent with Liu et al. (2009), who reported pH independence of ammonia removal rate when utilizing a Ti/IrO_2 anode with a stainless steel cathode. The conflicting results suggest that the anode material may alter factors affecting the treatment efficiency. Vanlangendonck et al. (2005) have also reported that pH had no effect (when kept constant in the range 5.5 - 10 through the electrolysis process) on the electrochemical treatment of power plant wastewater effluents containing ammonia when treated with a stainless steel cathode and Ti/RuO_2 anode.

Effect of current density

The influence of current density on aqueous ammonia and total nitrogen removal was investigated at two densities (3.75 and 7.5 mA/cm^2) for two pH levels (5.7 and 9.7), illustrated in Figure 5-2 and Figure 5-3, respectively. With both initial pH levels (5.7 and 9.7), the higher current density (7.5 mA/cm^2) resulted in higher aqueous ammonia and total nitrogen removal. After 60 minutes of electrolysis at pH=5.7 with a current density of 7.5 mA/cm^2, 71.75% of aqueous ammonia was removed from the solution compared to 38.45% removal at 3.75 mA/cm^2. An independent t-test conducted on the data at pH=5.7 suggested significant removal with elevated current density (p=0.024). At an initial pH=9.7 with a current density of 7.5 mA/cm^2, 99.50% of aqueous ammonia was removed after 60 minutes of electrolysis compared to 41.56% removal at 3.75 mA/cm^2. An independent t-test concluded that the higher removal rate for aqueous ammonia with an elevated current density was significant (p=0.016). Total nitrogen removal followed the same trend, with greater removals observed at a higher current density for both pH levels. The results suggest that higher current density removed significantly more aqueous ammonia and total nitrogen from the solution. The results are consistent with other electrochemical research that has reported on elevated contaminant removal at higher current densities with various types of electrodes (Deng and Englehardt, 2007; De Lima et al., 2009; Hu et al., 2009; Li et al., 2009b; Liu et al., 2009).

Contaminant removal at an elevated current density is beneficial as higher currents increase the electron loosing rate from the chloride ion at the anode, in accordance to Equation 5.2 (Kim et al., 2005; De Lima et al., 2009). Furthermore, the produced chlorine is hydrolyzed to produce

HOCl or OCl⁻ (based on the pH of the solution) in accordance to Equations 5.3 and 5.4 (Anglada et al., 2010; Wang et al., 2012), resulting in higher removal rates for the contaminant:

$$2Cl^- \rightarrow Cl_2 + 2e^- \tag{5.2}$$

$$Cl_2 + H_2O \rightarrow HOCl + H^+ + Cl^- \tag{5.3}$$

$$HOCl \rightarrow OCl^- + H^+ \tag{5.4}$$

A decrease in chloride concentration occurred for all the water matrices, as the chloride ions oxidized to chlorine gas in accordance to Equation 5.2 (Figure 5-5). An F-test was conducted on the data to investigate statistical differences. All water matrices resulted in no statistical change in chloride concentration ($F_{cal}<F_{tab}$). This is consistent with findings from other research that reported the chloride ion acts as a catalyst (Equation 5.3), and does not theoretically change in concentration throughout the electrolysis process (Li and Liu, 2009; Liu et al., 2009). However, the drop in chloride observed could be caused by the accumulation of chlorine in the bulk solution (Anglada et al., 2010).

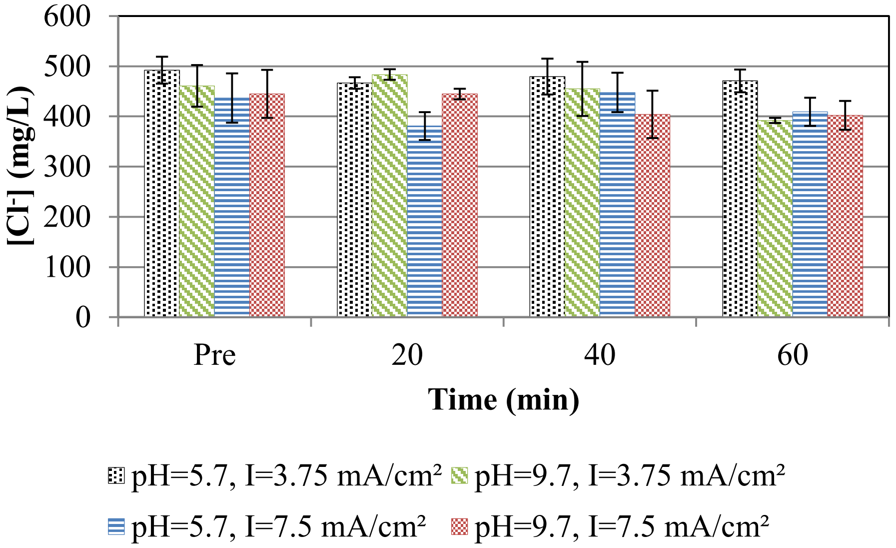

Figure 5-5 Variation in chloride concentration for various water matrices (Error bars represent standard deviation).

Variation in pH and production of chlorine species

The variation of pH throughout the electrolysis process with initial pH levels of 5.7 and 9.7 for both current densities (3.75 and 7.5 mA/cm^2) is illustrated in Figure 5-6. No pH control was conducted throughout the electrolysis process in order to simulate conditions present in the field (Liu et al., 2009). The pH decreased regardless of the initial pH or current density employed, as more H^+ ions were produced in accordance to Equation 5.3. For all water matrices (except at an initial pH=9.7 with 3.75 mA/cm^2), the pH dropped and stabilized at around 3.5. At an initial pH=9.7 with 3.75 mA/cm^2, the pH gradually decreased to 9.1 after 60 minutes of treatment. The results suggest that HOCl is the active chlorine species for all water matrices, except at an initial pH=9.7 and a current density of 3.75 mA/cm^2, where OCl^- is the dominant active chlorine species. This is consistent with the low rate of aqueous ammonia removal observed in the same water matrix (initial pH=9.7 with 3.75 mA/cm^2), as OCl^- is a less potent disinfectant compared to HOCl (Hansen et al., 2012).

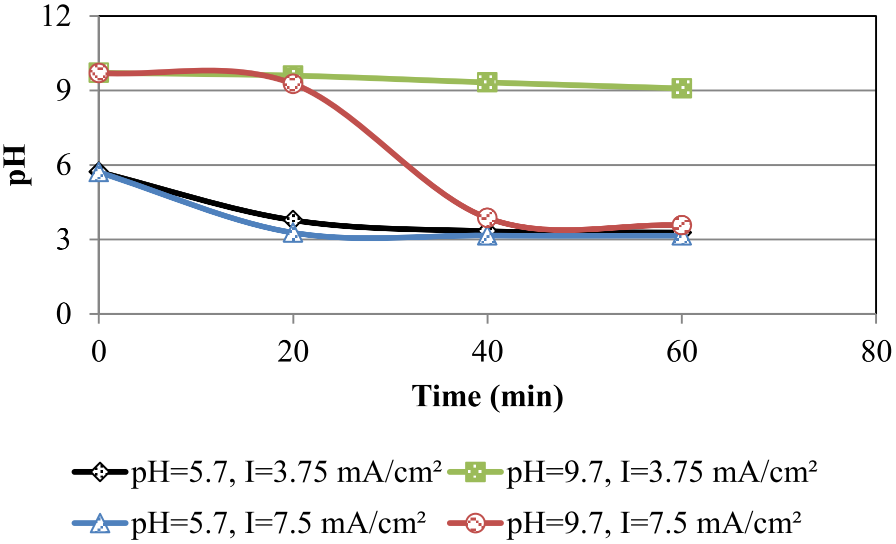

Figure 5-6 Variation of pH in various water matrices at [Cl^-]=450 mg/L (Error bars represent standard deviation).

In water matrices containing ammonia and chlorine, their respective interaction is described by Equations 5.5 - 5.7 (Qiag and Adams, 2004; Gendel and Lahav, 2012):

$$HOCl + NH_3 \rightarrow NH_2Cl + H_2O \qquad (5.5)$$

$$HOCl + NH_2Cl \rightarrow NHCl_2 + H_2O \qquad (5.6)$$

$$HOCl + NHCl_2 \rightarrow NCl_3 + H_2O \qquad (5.7)$$

The production of chlorine (total and free), and monochloramine at both pH levels (5.7 and 9.7) and current densities (3.75 and 7.5 mA/cm^2) is illustrated in Figure 5-7 and Figure 5-8, respectively. Elevated pH level (9.7) resulted in the highest concentration of total chlorine produced. At pH=9.7 with 3.75 mA/cm^2, total chlorine peaked to 60 mg/L after 40 minutes of electrolysis, and then decreased to 47 mg/L at 60 minutes. At pH=9.7 with 7.5 mA/cm^2, total chlorine reached a concentration of 61 mg/L after 60 minutes of electrolysis. Elevated pH level did not contribute to higher free chlorine concentrations. The highest concentration of free chlorine observed was 16.25 mg/L, with pH=9.7 and 7.5 mA/cm^2 after 60 minutes of electrolysis. No pattern was evident in total and free chlorine concentrations. It is suspected that the drop in chlorine is due to the formation of chloramines or chlorine gas, quantified in other research (Li and Liu, 2009). Chloramines were produced in the first 20 minutes of treatment and either stabilized or decreased in concentration subsequently. In the water matrix at pH=5.7 with 3.75 mA/cm^2, monochloramine concentration gradually increased to 40.8 mg/L after 60 minutes of treatment. The highest concentration of monochloramine (46.3 mg/L) was observed at pH=9.7 with 3.75 mA/cm^2, after 40 minutes of treatment. Dichloramine ($NHCl_2$) and trichloramine (NCl_3) were not measured in this research, but it is suspected that they converted to non-toxic nitrogen gas as observed by Xiao et al. (2009).

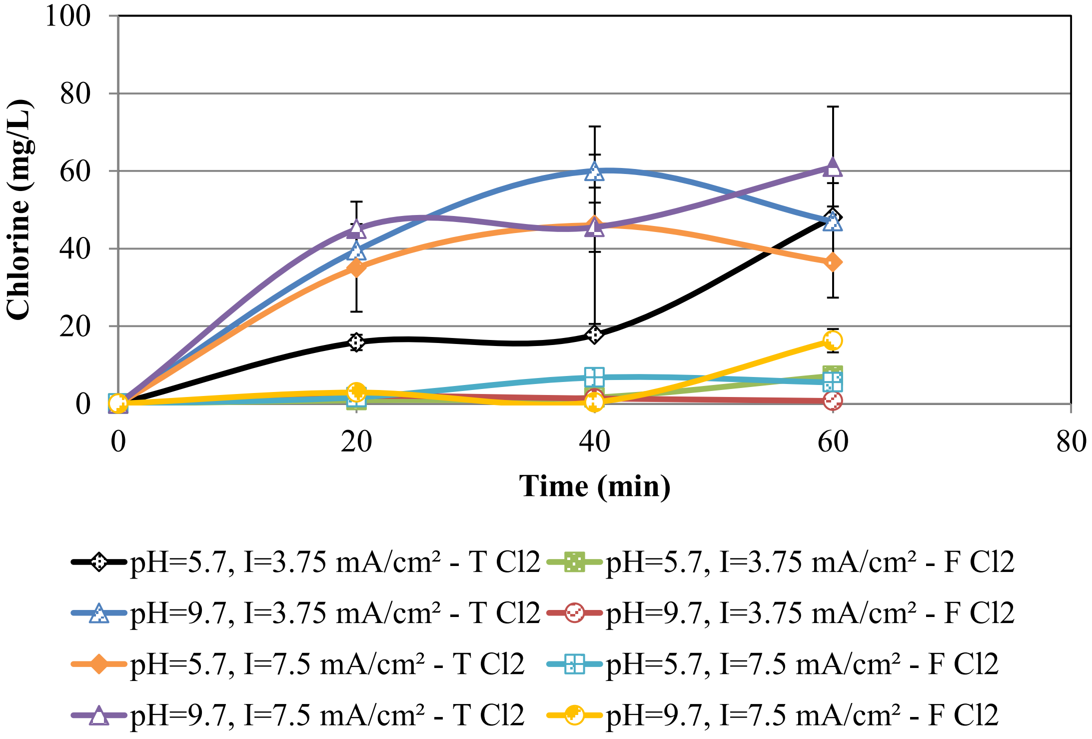

Figure 5-7 Total and free chlorine production through the electrolysis process at [Cl$^-$]=450 mg/L (Error bars represent standard deviation).

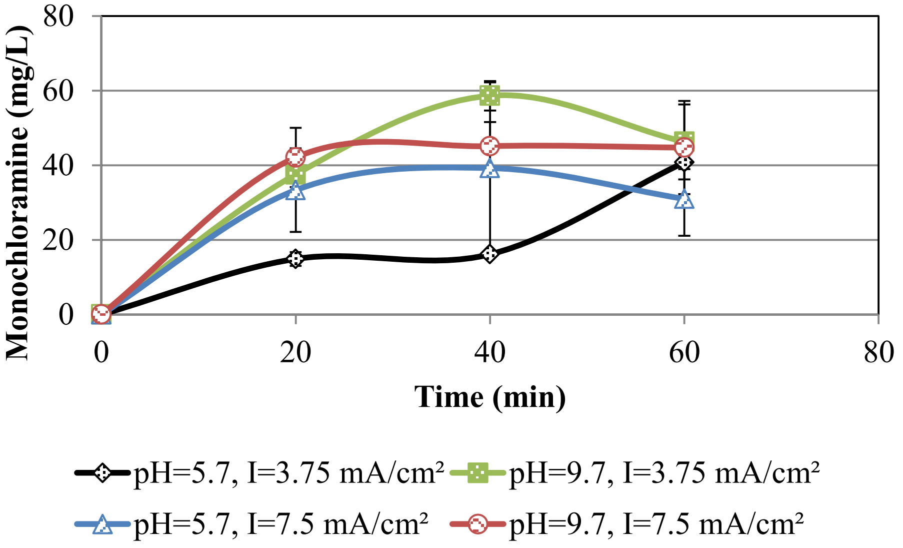

Figure 5-8 Monochloramine production through the electrolysis process at $[Cl^-]$=450 mg/L (Error bars represent standard deviation).

The results from this research differ from Li and Liu (2009) who reported free chlorine and monochloramine concentrations less than 2.1 mg/L and 3.0 mg-Cl_2/L in their system ($[NH_3$-$N]$=32 mg/L, Ti/RuO_2 anode at pH=7.0 with a current density of 15.4 mA/cm^2 and $[Cl^-]$=300 mg/L). The difference in initial ammonia and chloride concentrations could have resulted in this difference, as well as the reported loss of chlorine to chlorine gas in the system (Li and Liu, 2009).

Electrochemical Treatment of Aqueous Ammonia at $[Cl^-]$=4500 mg/L

Effect of pH

The influence of pH on aqueous ammonia and total nitrogen removal was investigated at two levels (5.7 and 9.7) with two current densities (20 and 40 mA/cm^2). Experiments were conducted with an initial ammonium concentration of 750 mg/L. The results are illustrated in Figure 5-9 and Figure 5-10 for aqueous ammonia and total nitrogen, respectively. The removal of aqueous ammonia and total nitrogen was achieved (at both current densities) with an elevated pH level of 9.7. With an initial pH=5.7 and a current density of 20 mA/cm^2, 50.78% removal of ammonium was observed after 80 minutes of electrolysis compared to 68.74% removal with initial pH=9.7. Independent t-test suggested a significant difference in treatment efficacy with pH ($p=0.047$). At a current density of 40 mA/cm^2 with an initial pH=5.7, 100% removal of ammonium (or close to the MDL) was observed after 80 minutes of electrolysis, compared to complete removal (or close to the MDL) with pH=9.7 after 60 minutes. An independent t-test confirmed a significance difference in treatment ($p=0.003$). The same trends were observed for total nitrogen removal, where a higher pH level resulted in higher removals.

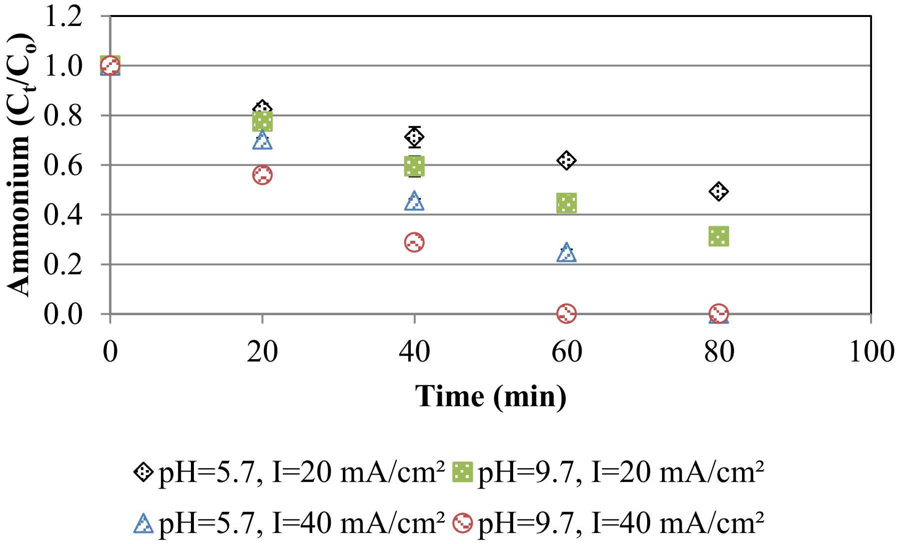

Figure 5-9 Effect of pH and current density on the electrolysis of ammonium at [Cl$^-$]=4500 mg/L (Error bars represent standard deviation).

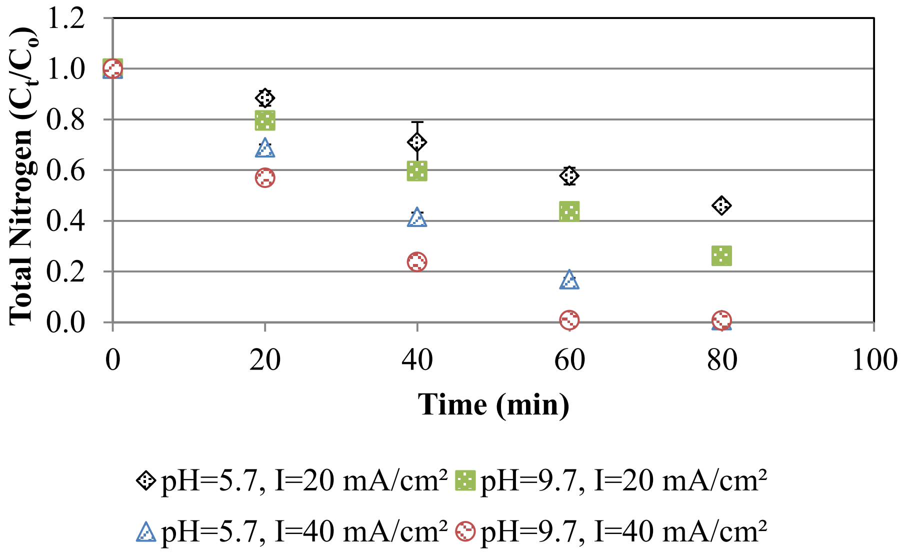

Figure 5-10 Effect of pH and current density on the electrolysis of total nitrogen at $[Cl^-]$=4500 mg/L (Error bars represent standard deviation).

The results are consistent with findings from the electrolysis of aqueous ammonia and total nitrogen at a chloride concentration of 450 mg/L. The increase in chloride concentration, from 450 mg/L to 4500 mg/L, was beneficial for higher removal rates. Previous research has reported the increase in efficiency for the removal of contaminants at higher chloride concentrations (Vlyssides et al., 2002; Vanlangendonck et al., 2005; Li and Liu, 2009). High chloride concentration increased the production of chlorine, which enhanced the indirect oxidation of the contaminant (Chen et al., 2007).

Effect of current density

Investigation of the influence of current density (20 and 40 mA/cm^2) on aqueous ammonia and total nitrogen removal was conducted at two pH levels (5.7 and 9.7). The influence of current density on aqueous ammonia and total nitrogen removal is illustrated in Figure 5-9 and Figure 5-10, respectively. Higher removal efficiencies for aqueous ammonia and total nitrogen were observed at a higher current density (40 mA/cm^2), regardless of the initial pH level (5.7 or 9.7).

After 80 minutes of electrolysis at an initial pH=5.7, complete removal of 750 mg/L of ammonium (or close to the MDL) was observed with a current density of 40 mA/cm^2, whereas only 50.78% removal was achieved with a current density of 20 mA/cm^2. An independent t-test suggested the treatments to be significantly different (p=0.02). With an initial pH=9.7, complete removal of ammonium (or close to the MDL) was observed with a current density of 40 mA/cm^2 after 60 minutes, whereas 68.73% of ammonia was removed after 80 minutes with a current density of 20 mA/cm^2. An independent t-test showed that the two treatments were significantly different (p=0.011). Total nitrogen removal followed the same trend as aqueous ammonia, where a higher current density (40 mA/cm^2) resulted in higher removal rates.

With increased current, higher removal efficiencies were observed for aqueous ammonia and total nitrogen. The results are consistent with the removal of aqueous ammonia and total nitrogen at a chloride concentration of 450 mg/L. The removal rates observed at a [Cl$^-$]=4500 mg/L were higher compared to a [Cl$^-$]=450 mg/L, where more concentration of contaminant was removed during the same treatment period. The increase in chloride concentration allowed for higher current densities, which further resulted in a higher production rate of chlorine, in accordance to Equation 5.2 (Kim et al., 2005; Chen et al., 2007).

The concentration of chloride dropped for all of the water matrices, due to the oxidation to chloride in accordance to Equation 5.2 (Figure 5-11), consistent with findings at [Cl$^-$]=450 mg/L. A F-test was conducted and determined all water matrices to undergo no statistical change in chloride concentration ($F_{cal}<F_{tab}$). In theory, the chloride ion acted as catalyst (Li and Liu, 2009; Liu et al., 2009).

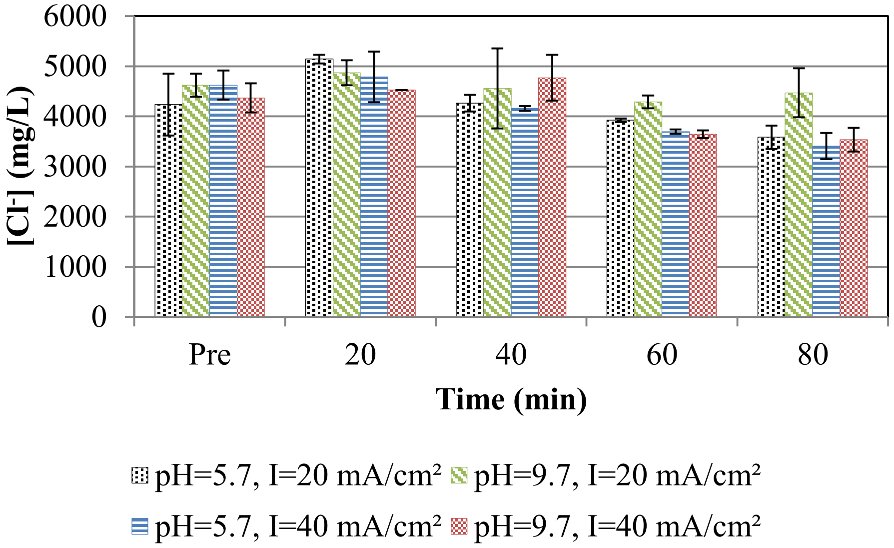

Figure 5-11 Variation in chloride concentration in various water matrices (Error bars represent standard deviation).

Variation in pH and production of chlorine species

The variation in pH through the electrolysis processes (pH levels 5.7 and 9.7, and current densities of 20 and 40 mA/cm^2) is illustrated in Figure 5-12. A drop in pH was observed in all water matrices, as H^+ ions were produced (Equation 5.3). In most water matrices, the pH dropped to around 2.5. At pH=5.7 with a current density of 40 mA/cm^2, the pH decreased to 2.46 after 20 minutes and stabilized in the same range (~2.5) until 60 minutes, where it gradually increased to 7.53. With pH=9.7 and 40 mA/cm^2, the pH dropped to 2.98 after 40 minutes and gradually increased to 8.9 after 60 minutes of electrolysis. The results suggest that HOCl was the dominant chlorine species in the solutions, except in some water matrices. In such matrices (pH=5.7 with 40 mA/cm^2, and pH=9.7 with 40 mA/cm^2), the active chlorine species was OCl^- when pH>7.4. This did not affect removal efficiencies because most of the contaminant was removed when pH was acidic (and HOCl was the dominant chlorine species), consisted with Xiao et al. (2009) who suggested that the pH turning point is an indicator that the ammonia has been depleted.

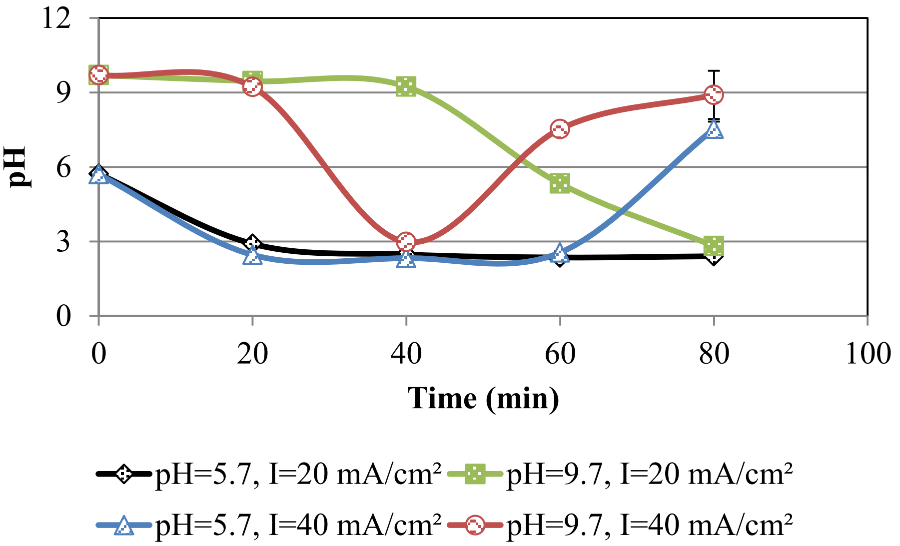

Figure 5-12 Variation in pH for various water matrices at [Cl$^-$]=4500 mg/L (Error bars represent standard deviation).

The concentration of produced chlorine (total and free) and monochloramine at both pH levels (5.7 and 9.7) and current densities (20 and 40 mA/cm^2) are illustrated in Figure 5-13 and Figure 5-14, respectively. A high current density (40 mA/cm^2) resulted in higher total chlorine concentrations. With 40 mA/cm^2 at pH=5.7 the total chlorine was 715 mg/L; whereas at pH=9.7 the total chlorine was 1620 mg/L after 80 minutes of electrolysis. Free chlorine concentrations were consistent with total chlorine, where a higher current density (40 mA/cm^2) resulted in higher concentrations. With 40 mA/cm^2 at pH=5.7 the free chlorine concentration was 520 mg/L; whereas at pH=9.7 the free chlorine was 1565 mg/L after 80 minutes of electrolysis. Low pH level (5.7) resulted in continuous production of monochloramine until 80 minutes of treatment. At the high pH level (9.7), a higher concentration of monochloramine was produced in the first 20 or 40 minutes, and then decreased and stabilized. The decrease in monochloramine concentration may be associated with the decay of monochloramine into dichloramine and trichloramine, and subsequently converted to non-toxic gases as observed by Xiao et al. (2009).

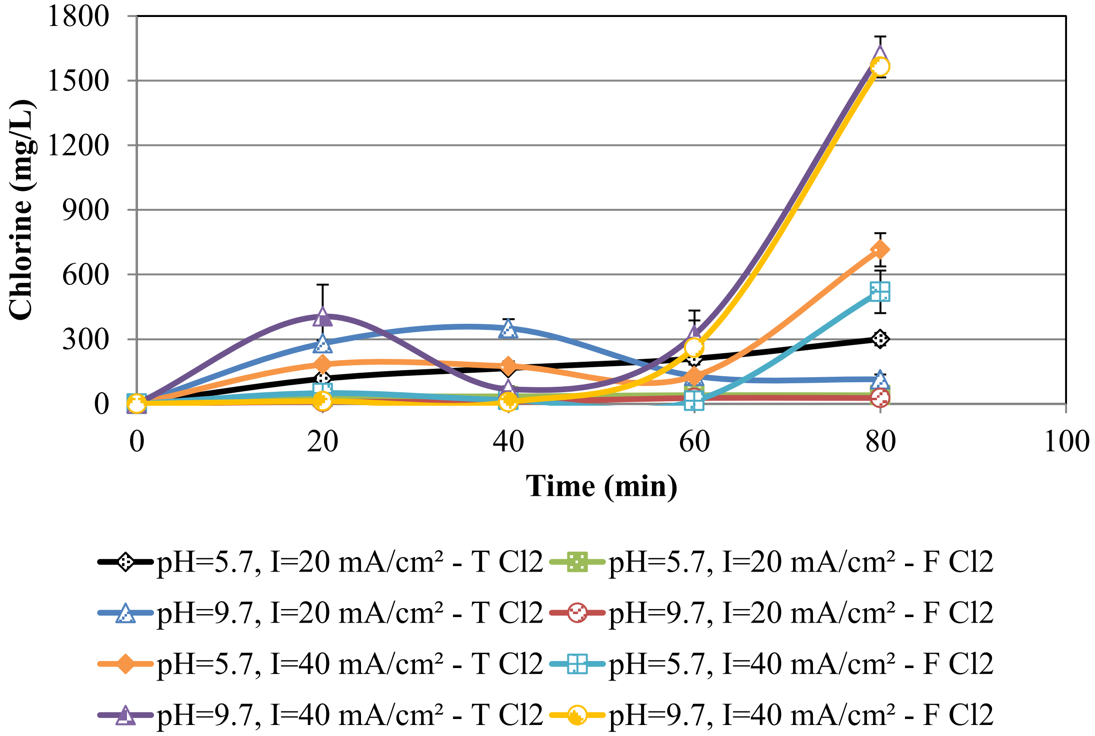

Figure 5-13 Total and free chlorine production through the electrolysis process at [Cl$^-$]=4500 mg/L (Error bars represent standard deviation).

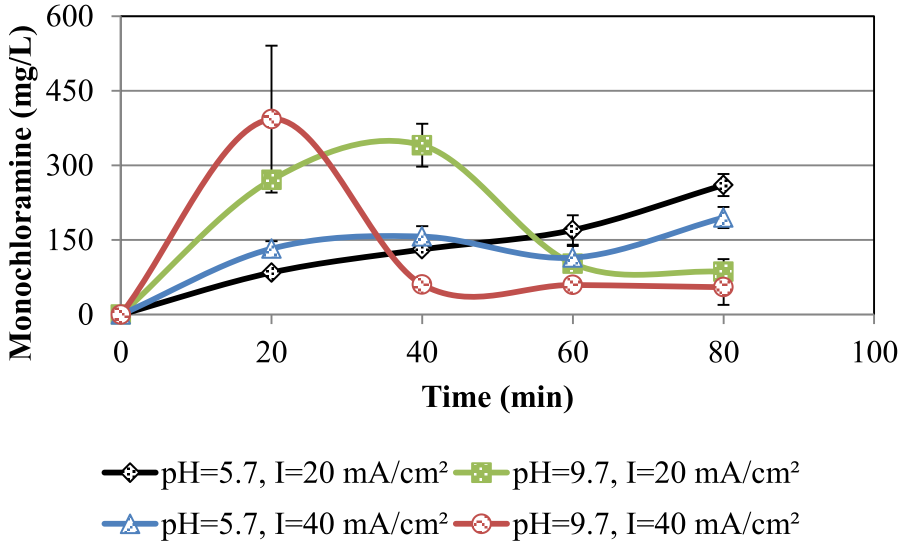

Figure 5-14 Monochloramine production through the electrolysis process at [Cl$^-$]=4500 mg/L (Error bars represent standard deviation).

Vlyssides et al. (2002) have also reported high concentrations of chlorine species during the electrolysis of domestic wastewater ($[NH_4^+\text{-}N]=150$ mg/L) with a Ti anode and a current density of 75 mA/cm^2, at various pH levels.

Degradation Pathway

In previous research, Vanlangendonck et al., (2005), Li and Liu (2009) and Xiao et al. (2009) have reported the electrolysis of ammonia using pseudo zero-order kinetics. However, Chen et al. (2007) and Hu et al. (2009) have reported the electrolysis of ammonia using pseudo first-order kinetics. In this research, pseudo first-order kinetics was only valid to describe some of the water matrices, and therefore pseudo zero-order kinetics was used for consistency. Rate constants were therefore calculated using pseudo-zero order reaction with respect to ammonium concentration (Equation 5.8):

$$\frac{d\left[NH_4^+\right]}{dt} = -k_{obs} \tag{5.8}$$

Solving Equation 5.8 yields the reaction rate constant, k_{obs}:

$$\left[NH_4^+\right] = -k_{obs}t + \left[NH_4^+\right]_{\bullet} \tag{5.9}$$

The values of the rate constants and correlation coefficients are presented in Table 5-1. The obtained rate constants were greater compared to research conducted by Xiao et al. (2009) but smaller than report by Liu et al. (2009), for Ti/RuO$_2$ and Ti/IrO$_2$ anodes. Rate constants increased with pH level, current density, and chloride concentration, consistent with the amount of contaminant removed. The rate constant obtained for the electrolysis of secondary wastewater effluent was the smallest as the concentration of the contaminant was smaller compared to the synthetic wastewater trials.

Table 5-1 Rate constants and correlation coefficient for the electrolysis of ammonium in various water matrices.

Water matrix	k (mg min^{-1} L^{-1})	R^2
[Cl$^-$]=450 mg/L, I=3.75 mA/cm^2, pH=5.7	0.475	0.993
[Cl$^-$]=450 mg/L, I=3.75 mA/cm^2, pH=9.7	0.529	0.932
[Cl$^-$]=450 mg/L, I=7.5 mA/cm^2, pH=5.7	0.885	0.977
[Cl$^-$]=450 mg/L, I=7.5 mA/cm^2, pH=9.7	1.238	0.989
[Cl$^-$]=4500 mg/L, I=20 mA/cm^2, pH=5.7	4.737	0.993
[Cl$^-$]=4500 mg/L, I=20 mA/cm^2, pH=9.7	5.902	0.976
[Cl$^-$]=4500 mg/L, I=40 mA/cm^2, pH=5.7	9.426	0.996
[Cl$^-$]=4500 mg/L, I=40 mA/cm^2, pH=5.7	11.460	0.985
Secondary municipal WW effluent (pH=10.0)	0.236	0.993

The results from this research suggest that nitrogen was removed electrochemically with a Ti/RuO$_2$ anode and a Ti cathode. The direct oxidation of ammonia has been reported to have low removal rates compared to indirect oxidation (Chen et al., 2007; Li and Liu, 2009; Wang et al., 2012). Therefore, aqueous ammonia can be indirectly oxidized by hydroxyl radicals produced in the bulk, or by HOCl formed in the electrochemical process (Chen et al., 2007; Li and Liu, 2009). The formation of hydroxyl radicals (OH·) was monitored via HPLC using pCBA as a probe compound, as detailed by Brunet et al. (2009). The results were inconclusive and suggested that the production of hydroxyl radicals by the Ti/RuO$_2$ anode had a negligible, or minimal, contribution to the indirect oxidization of aqueous ammonia in the process, which is consistent with other research (Feng et al., 2003; Li and Liu, 2009; Liu et al., 2009).

The removal mechanism observed in the electrochemical process was therefore attributed to the indirect oxidation of the contaminant. Aqueous ammonia was oxidized and converted to other sources of nitrogen (nitrate and nitrogen gas), according to the mechanism of breakpoint chlorination, in accordance to Equations 5.10 - 5.16 (Li and Liu, 2009; Liu et al., 2009; Gendel and Lahav, 2012; Wang et al., 2012):

At the cathode:

$$2H^{+} + 2e^{-} \rightarrow H_2 \tag{5.10}$$

At the anode:

$$2Cl^{-} \rightarrow Cl_2 + 2e^{-} \tag{5.11}$$

In the solution:

$$Cl_2 + H_2O \rightarrow HOCl + H^{+} + Cl^{-} \tag{5.12}$$

$$HOCl \rightarrow OCl^{-} + H^{+} \tag{5.13}$$

$$3HOCl + 2NH_3 \rightarrow N_2 + 3H_2O + 3H^{+} + 3Cl^{-} \tag{5.14}$$

$$3HOCl + 2NH_4^{+} \rightarrow N_2 + 3H_2O + 5H^{+} + 3Cl^{-} \tag{5.15}$$

$$4HOCl + NH_4^{+} \rightarrow NO_3^{-} + H_2O + 6H^{+} + 4Cl^{-} \tag{5.16}$$

Theoretically, no nitrite should be formed according to breakpoint chlorination (Hu et al., 2009). In order to quantify any concentration residual (due to background noise of the instrument) of nitrite or nitrate present in the samples before treatment, post treatment samples were adjusted to take into account the nitrate and nitrite residuals. Nitrite concentration was low, or close to the MDL (MDL of nitrite was 0.7 mg/L), through the electrochemical process for all water matrices which is consistent with other research (Kim et al., 2005; Hu et al., 2009; Wang et al., 2012). Nitrate was produced in the electrolysis process for most water matrices (Figure 5-15 and Figure 5-16), as expected from Equation 5.16, although some concentrations were low or close to the MDL (MDL of nitrate was 0.8 mg/L). At [Cl$^-$]=450 mg/L, the highest nitrate concentration was observed (3.33 mg/L) at pH=5.7 with 7.5 mA/cm^2. At [Cl$^-$]=4500 mg/L, nitrate concentration reached 7.95 mg/L at pH=9.7 with 40 mA/cm^2. Xiao et al. (2009) have also reported the production of 15.8 mg/L of nitrate when electrochemically treating 700 mg-N/L of ammonia at pH=5.7 with 40 mA/cm^2. However, Li and Liu (2009) have only reported 0.9 mg-N/L of nitrate when electrochemically treating 32 mg-N/L of ammonia at pH=7.0 with 15.4 mA/cm^2.

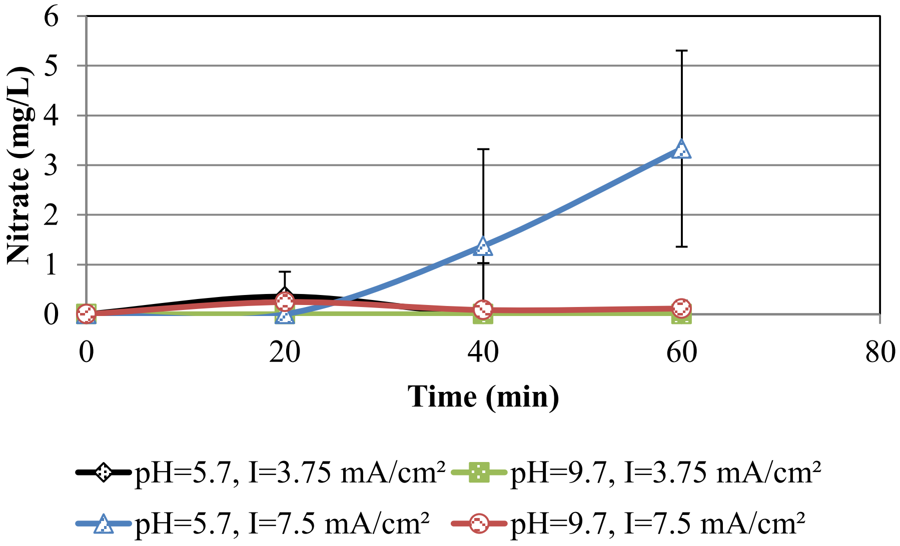

Figure 5-15 Nitrate production through the electrolysis process at [Cl$^-$]=450 mg/L (Error bars represent standard deviation).

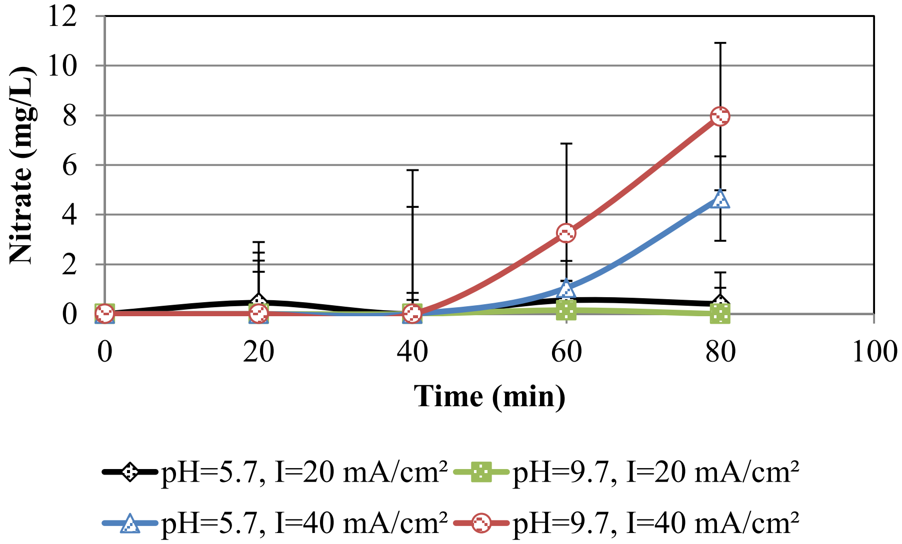

Figure 5-16 Nitrate production through the electrolysis process at [Cl$^-$]=4500 mg/L (Error bars represent standard deviation).

The production of nitrate in the electrolysis process is inconsistent in the literature, and data from this research suggests that there is no consistency in nitrate production for the various water matrices. It is suspected that in water matrices where no production of nitrate was observed, or close to the MDL, the nitrate was reduced to nitrogen gas at the cathode in accordance to Equation 5.17 (Kim et al., 2005):

$$NO_3^- + 3H_2O + 5e^- \rightarrow \frac{1}{2}N_2 + 6OH^- \qquad (5.17)$$

The production of nitrogen gas was not measured in this research. Other research (Kim et al., 2005; Li and Liu, 2009; Xiao et al., 2009) has previously reported the conversion of degraded ammonia to nitrogen gas in their respective electrochemical processes. It is suspected that the removed aqueous ammonia in this research is also converted to nitrogen gas, according to Equations 5.11 - 5.15.

Application to Wastewater

Secondary effluent (prior to UV disinfection) from MCWPCC was obtained and treated electrochemically. The wastewater was adjusted to an initial pH of 10.0, and not supplemented with chloride. Batch treatment was conducted in duplicate at three treatment times (20, 40 and 60 minutes), with a current density of 5 mA/cm^2.

A decrease in pH level was observed throughout treatment (from 10.0 to 9.77). This is consistent with findings from Li and Liu (2009), who reported a 0.5 pH level drop when electrochemically treating actual wastewater with a Ti/RuO$_2$ anode at a current density of 15.4 mA/cm^2 for two hours. Aqueous ammonia and total nitrogen were removed from the wastewater after 60 minutes of electrochemical treatment (Figure 5-17).

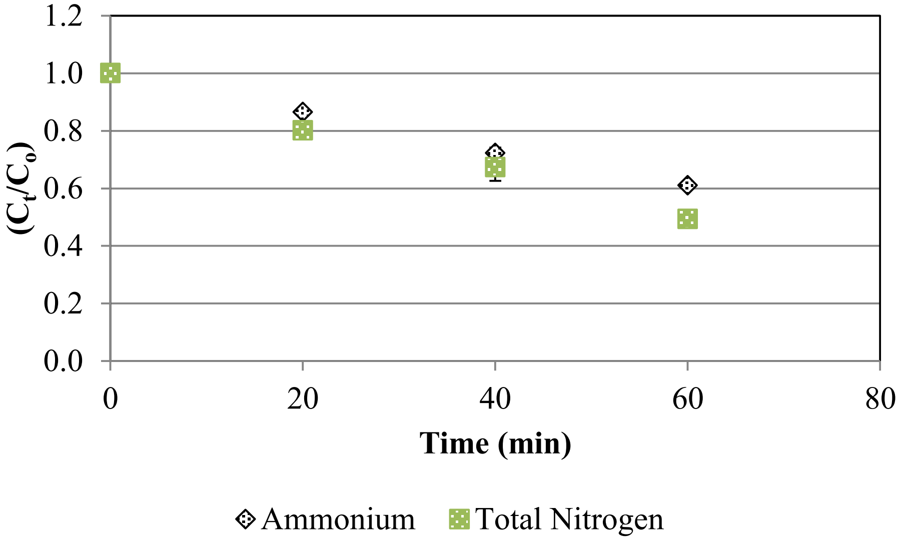

Figure 5-17 Electrolysis of nitrogen compounds in municipal wastewater (Error bars represent standard deviation).

Aqueous ammonia (39.04%) and total nitrogen (50.69%) were removed after 60 minutes of electrolysis. The rate constant obtained from the treatment of municipal wastewater was smaller compared to the synthetic wastewater trials. This is expected as both the initial concentration of the contaminant and the current density were smaller compared to the synthetic wastewater trials. The discrepancy in data, where total nitrogen is less than aqueous ammonia, was likely from analytical error of either instrument.

Little or no nitrite was formed in the process (or close to the MDL), whereas 2.54 mg/L of nitrate was formed after 60 minutes of electrolysis (Figure 5-18). The nitrate concentration observed was less than reports by Vlyssides et al. (2002), who reported 7.2 mg/L of nitrate from the electrochemical treatment of domestic wastewater at pH=9.0.

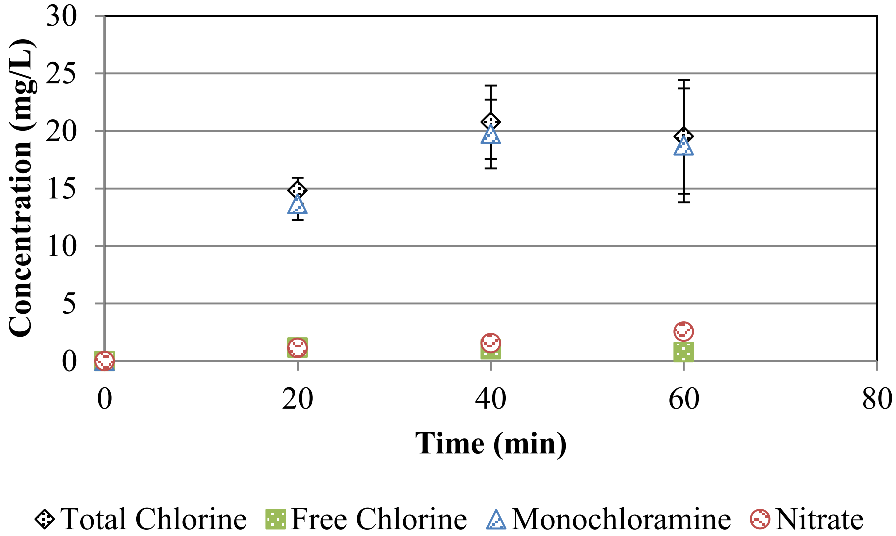

Figure 5-18 Production of chlorine (total and free), monochloramine, and nitrate in the electrolysis of municipal wastewater (Error bars represent standard deviation).

Chlorine (total and free) and monochloramine were produced during the process (Figure 5-18). Total chlorine reached a maximum (20.75 mg/L) after 40 minutes of electrolysis, and decreasaed to 19.5 mg/L at 60 minutes. Monochloramine concentration followed the same trend as total chlorine. Free chlorine produced was less than 1.2 mg/L at all times. The concentration of chlorine species observed in the electrochemical treatment of actual wastewater was smaller in magnitude compared to the synthetic wastewater trials. The water matrices used for the synthetic wastewater trials did not contain any organic matter; therefore the organic matter in the actual wastewater reacted with the chlorine species to form DBPs.

The concentration of DBPs (TTHMs and THAAs) in the electrolysis process was investigated, illustrated in Figure 5-19. TTHMs concentrations did not increase with treatment time, and reached a maximum of 36.7 µg/L after 40 minutes of treatment. THAAs concentration increased with treatment time, reaching a maximum of 205.6 µg/L after 60 minutes of treatment. Furthermore, a high correlation coefficient was observed between the concentration of THAAs and time (R^2=1.00), suggesting a steady production of THAAs with the process.

DBPs are currently not regulated in wastewater effluents, but should be of concern as more wastewater effluents are being recycled for drinking water supplies (Krasner et al., 2009; Song et al., 2010). Li and Ni (2012) have reported on the production of DBPs (chloroform, chlorate and perchlorate) in an electrochemical process, observing that the chloride concentration related to the chlorine produced and sub-sequentially to the concentration of DBPs. Diaz et al. (2011) have reported the production of THM compounds when electrochemically treating ammonia in aquaculture. The authors reported different concentrations of TTHMs with varying current densities, with a maximum concentration of 1.7 mg/L. The reported TTHMs concentration is significantly higher compared to the range in this research, where a maximum concentration of 205.6 µg/L was observed.

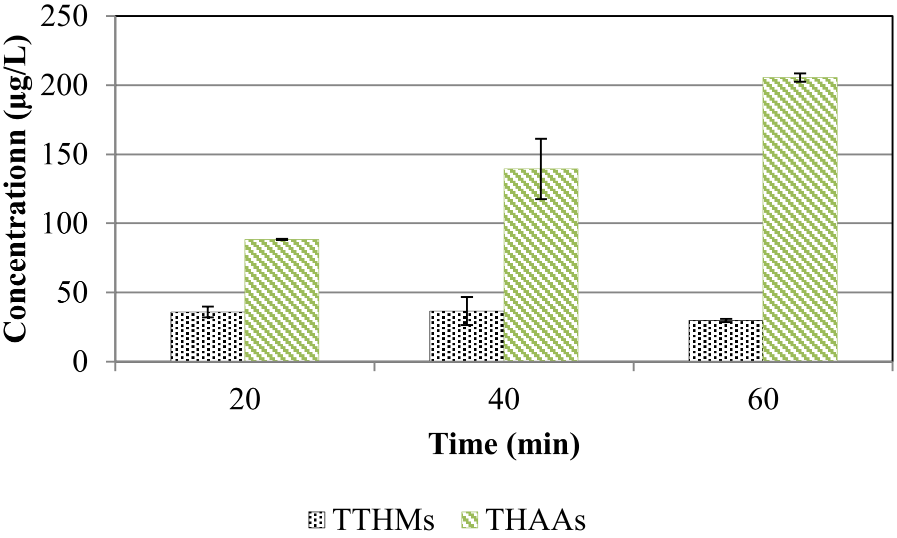

Figure 5-19 Production of TTHMs and THAAs in the electrolysis of municipal wastewater (Error bars represent standard deviation).

The release of metals was monitored through the electrolysis process, illustrated in Figure 5-20. Ruthenium was released, due to the oxidation of the Ti/RuO$_2$ anode, in accordance with either Equation 5.18 or 5.19 (Milazzo et al., 1978; Bard et al., 1985):

$$Ru(s) \rightarrow Ru^{2+} + 2e^- \tag{5.18}$$

$$Ru(s) + 4H_2O \rightarrow RuO_4 + 8H^+ + 8e^- \tag{5.19}$$

It is not clear what oxidation route the ruthenium took, and further investigation is required to confirm. However, based on the high standard reduction potential of Equation 5.19 (1.038 E°/V), it is suspected that ruthenium oxidation followed this path. The concentration of ruthenium gradually increased with time (R^2=0.83), and reached 7.56 µg/L after 40 minutes of treatment. No evidence of the release of titanium through the electrolysis process was evident. Titanium was present in the wastewater collected; therefore it is suspected that the varying concentrations observed are due to background concentration in the wastewater. At 40 minutes there was a spike of titanium concentration. This was probably due to an excess of titanium concentration in the wastewater used for that specific batch or from the oxidation of the anode (as it is composed of Ti/RuO_2), although further investigation is required to confirm the anomaly. The use of metals which are not toxic to the ecosystem is required in the electrochemical process, as metal corrosion is an un-intended consequence.

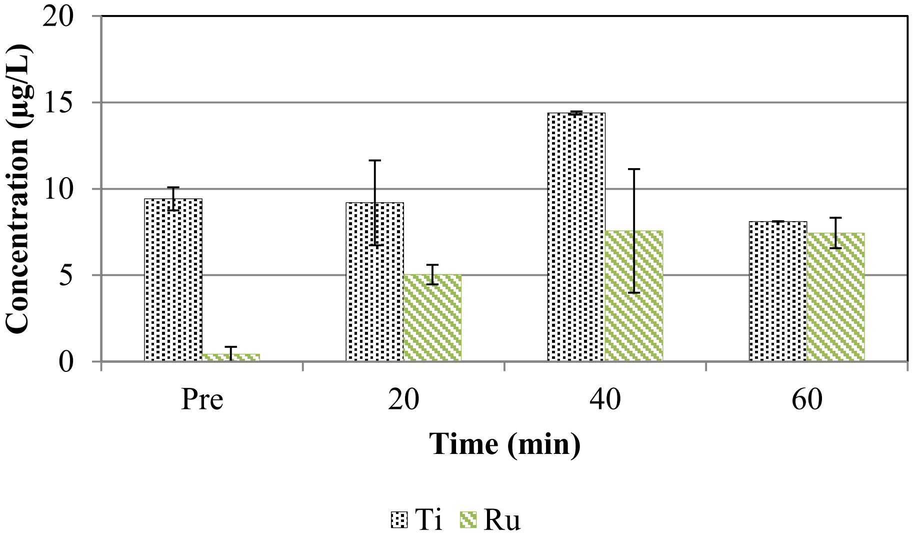

Figure 5-20 Metals release in the electrolysis of municipal wastewater (Error bars represent standard deviation).

5.4 Conclusion

- Electrochemical treatment of nitrogen compounds was investigated with a Ti cathode and a Ti/RuO_2 anode at two chloride concentrations ([Cl^-]=450 mg/L and [Cl^-]=4500 mg/L).
- Aqueous ammonia and total nitrogen degradation were affected by initial pH, chloride concentration, and current density. Removal efficiencies increased with chloride

concentration and current density. Elevated pH level (9.7) was found to be beneficial for aqueous ammonia and total nitrogen removal.

- The removal mechanism was attributed to the indirect oxidation of aqueous ammonia by the HOCl produced in the process. The indirect oxidation by hydroxyl radicals produced in the bulk water by the anode was considered minimal for the oxidation of aqueous ammonia. The final product of treatment was suspected to be nitrogen gas.
- Aqueous ammonia and total nitrogen of secondary wastewater effluent obtained from MCWPCC were removed. 39.04% and 50.69% of aqueous ammonia and total nitrogen, respectively, were removed after 60 minutes of electrolysis treatment.
- Production of TTHMs and THAAs were observed when electrochemically treating secondary wastewater. The maximum TTHMs and THAAs concentration observed were 36.7 µg/L and 205.6 µg/L, respectively.
- The results from this research suggest that nitrogen compounds can be electrochemically removed from wastewater, and produce nitrogen gas as a final product. However, care should be taken when employing such technology as it has un-intentional consequences, such as the production of DBPs and the release of metals. The addition of chloride ions in the treatment of municipal wastewater would also be beneficial to obtain higher removal rates and meet regulatory standards.

Chapter 6: Investigating Benefits of Employing UV Light in an Electrochemical Process

6.1 Introduction

Electrochemical processes have attracted interest in the past decade for the treatment of industrial and municipal wastewaters, leachate, and aquaculture wastewaters. Electrochemical processes are an easy to use technology, automated, have a rapid start-up time, and produce minimum secondary wastes (Dash and Chaudhari, 2005; Anglada et al., 2009; Liu et al., 2009; Diaz et al., 2011). Factors affecting the efficiency of electrochemically treating contaminants were found to be: pH, current density, initial contaminant concentration, chloride concentration, and material of the electrodes (Vanlangendonck et al., 2005; Diaz et al., 2011).

The electrochemical treatment of aqueous ammonia has been investigated in the literature for various electrode materials (Kim et al., 2005; Hu et al., 2009; Li and Liu, 2009; Liu et al., 2009). Aqueous ammonia can be removed either through the direct oxidation occurring at the anode, or through the indirect oxidation in the bulk solution. Indirect oxidation of aqueous ammonia occurs by hydroxyl radicals, or by HOCl formed in the process (Feng et al., 2003; Li and Liu, 2009).

In recent years, a number of researchers have investigated the effectiveness of employing UV light in the electrochemical process. Xiao et al. (2009) have reported faster degradation rates for ammonia when an electrochemical cell (with either a Ti/RuO_2 or Ti/IrO_2 anode) was supplemented with a low pressure UV light. Soltani et al. (2013) also reported synergistic effects for the removal of ammonium when combining an electrochemical process with a low pressure lamp while using sea water as an electrolyte. Furthermore, Soltani et al. (2013) have applied the photoelectrochemical process to treat high levels of ammonium in reject water from a sludge-dewatering unit. Xiao et al. (2013) have applied the photoelectrochemical process for the treatment of landfill leachate, observing synergistic effects.

Although both studies investigated the effectiveness of photoelectrochemically treating real wastewater, none reported the production of DBPs. Furthermore, Xiao et al. (2013) have reported ammonia degradation rates as pseudo zero-order kinetics; whereas Soltani et al. (2013) reported ammonia degradation rates as pseudo first-order kinetics. Therefore, there is conflicting understanding on the removal mechanism of ammonia with a photoelectrochemical process.

The objective of this research was to investigate synergistic effects when an electrochemical process was supplemented with UV light. A low pressure collimated UV beam was used. The electrodes used were a Ti cathode and a Ti/RuO_2 anode. The two processes were evaluated in parallel and the kinetics of removal was investigated for both processes. Furthermore, the efficiency of the processes and subsequent production of DBPs (TTHMs and THAAs) were assessed with secondary effluent wastewater obtained from MCWPCC, Bedford, NS.

6.2 Materials & Methods

Experimental Design

NH_4Cl and NaCl stock solutions were mixed with Milli-Q to produce synthetic wastewater. Batch experiments with synthetic wastewater were conducted to compare the removal efficiency of aqueous ammonia in an electrochemical process and in a photoelectrochemical process. Batch experiments with the two processes were evaluated in parallel. Experiments were conducted with the conditions reported by Xiao et al. (2009): [NH_3-N]=700 mg/L, pH=5.7, I=40 mA/cm^2 and [Cl^-]=5300 mg/L, a Ti cathode, and a Ti/RuO_2 anode. Samples were taken prior to and after treatment (20, 40, 60, and 80 minutes), and analyzed for the respective wastewater parameters (ammonium, total nitrogen, chlorine (total and free), monochloramine, nitrate, nitrite, TTHMs, THAAs, titanium, and ruthenium). All experiments were conducted in duplicates, at room temperature (20-23 °C), in a randomized order. Both treatment processes were used to treat secondary wastewater obtained from MCWPCC in Bedford, NS. Figure 6-1 illustrates a schematic of the experimental set-up.

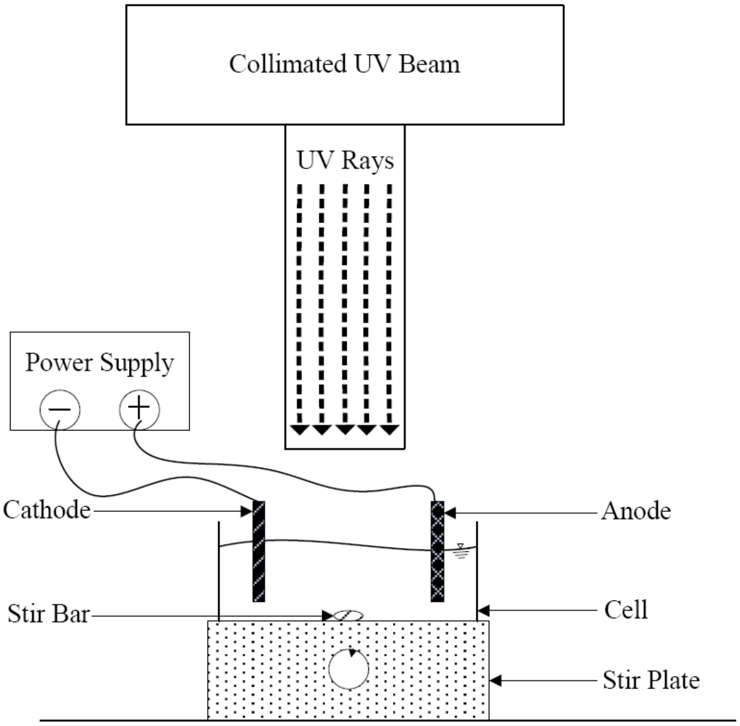

Figure 6-1 Experimental set-up for photoelectrochemical experiments.

Power Supply

A constant current (0-3 A) was supplied by a DC power source (GW Instek, Taiwan) by constantly changing the voltage (0-30 V). A titanium (Ti, Grade 2, commercially pure titanium, 98.9%) electrode was used as the cathode (BioSurface Technologies Corp, MT), with size 100 mm x 60 mm x 3 mm. An alloy of ruthenium dioxide and titanium (Ti/RuO_2) was used as the anode (Baoki Changli Special Metal Co. Ltd., China), with size 100 mm x 60 mm x 2 mm. The electrodes were spaced 6.0 cm, and each had a contact surface area of 30 cm^2.

Light Source

A LP UV collimated beam (Trojan Technologies, London, ON) emitting at 253.7 nm was used as a light source. The light intensity at the center of the beam was 0.274 mW/cm^2, measured with an ILT 1400-A radiometer photometer (International Light Technologies, Peadoby, MA). The UV light was employed as an additional treatment technology to the electrochemical process, therefore no UV fluence conditions were used. However, UV fluence conditions were calculated as described by Bolton and Linden (2003), and the treatment times of 20, 40, 60, and 80 minutes represented on average a UV fluence condition of 100, 200, 300, and 400 mJ/cm^2.

Chemical Preparation

Milli-Q (18.2 MΩ.cm, Millipore Corporation, MA) water was used for the preparation of all chemical solutions through this research. Laboratory grade detergent was used to wash all glassware, and washed glassware was triple rinsed with Milli-Q prior to the start of experiments. NH_4Cl and NaCl stock solutions were mixed with Milli-Q to produce synthetic wastewater at the desired concentrations. Additional chloride was added to the batches with NaCl stock solution. pCBA was used as a probe compound, and spiked into the synthetic wastewater batches to monitor the production of hydroxyl radicals. The adjustment of pH was achieved with the addition of 1.0 M NaOH and 0.1 M H_2SO_4.

Analytical Methods

As detailed in the Materials & Methods chapter.

Wastewater Collection

As detailed in the Materials & Methods chapter.

Statistical Analysis

Data was sorted, organized and plotted with Microsoft Excel 2010® (Redmond, WA). Statistical analyses (paired t-test) were computed with the aid of Mini-Tab ® 16 software (State College, PA). All statistical analysis was computed at a 95% significance level, unless stated otherwise.

6.3 Results & Discussion

Removal of Aqueous Ammonia and Total Nitrogen

Experimental conditions, as reported by Xiao et al. (2009) ([NH_3-N]=700 mg/L, pH=5.7, I=40 mA/cm^2, [Cl^-]=5300 mg/L, a Ti cathode, and a Ti/RuO_2 anode), were used to compare the removal efficiency of nitrogen compounds in a photoelectrochemical process to an electrochemical process. Although those were the target concentrations, the initial average ammonium concentration was measured at 762.84 ± 36.96 mg/L and the average initial chloride concentration was 5134.41 ± 191.67 mg/L.

The removal of ammonium and total nitrogen in the two processes are illustrated in Figure 6-2. Both processes were effective in complete removal of ammonium and total nitrogen (or close to their respective MDLs) with 80 minutes of treatment. No difference in removal efficiency was observed between the two processes, and each appeared to be equally efficient in removing the contaminants. A paired t-test conducted on the aqueous ammonia (p=0.92) and total nitrogen (p=0.855) data concluded that the two treatments were not statistically different.

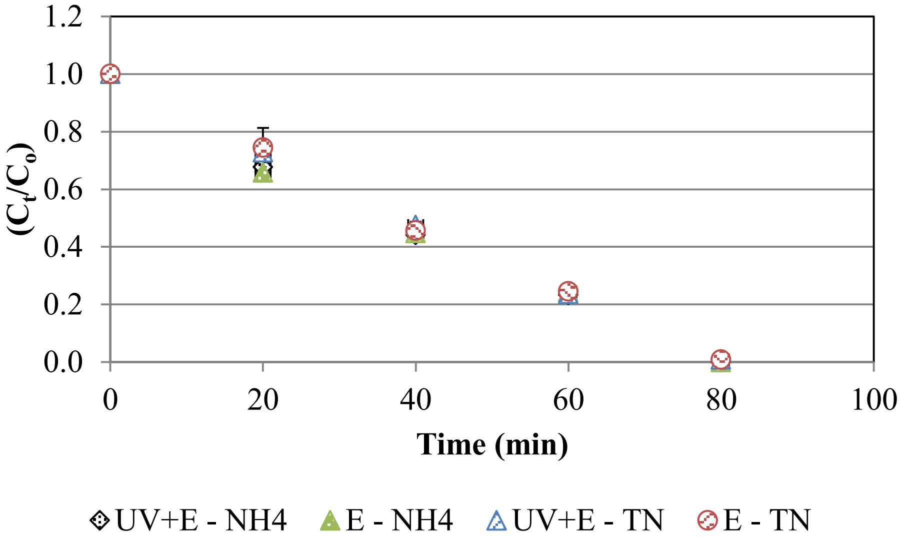

Figure 6-2 Removal of nitrogen compounds with a photoelectrochemical and electrochemical process (Error bars represent standard deviation).

In this research, the removal rate of aqueous ammonia was greater for both processes (electrochemical or photoelectrochemical) compared to the electrochemical process reported by Xiao et al. (2009) using the same electrodes. Furthermore, the results differed from Xiao et al. (2009) and Soltani et al. (2013) who reported faster degradation rates for aqueous ammonia with the introduction of UV light in an electrochemical process. The absence of synergistic effect for contaminant removal (for either aqueous ammonia or total nitrogen) observed in this research could be attributed to the lower light intensity of the UV light employed (0.274 mW/cm^2 for this research compared to 1.36 mW/cm^2).

However, some limitations were observed with the work conducted by Xiao et al. (2009). In their research, the authors do not report any statistics for the data and it is not clear whether batch experiments or flow-through experiments were conducted. The authors reported negligible NH_3 degradation in a photooxidation cell, which is inconsistent with findings from this research and other work in the literature (Zheng et al., 1998; Beckles and Diyamandoglu, 2006). Xiao et al. (2009) also conducted control experiments with a UV/H_2O_2 based AOP in order to investigate the effectiveness of $OH\cdot$ radicals to degrade NH_3. The authors reported negligible degradation of NH_3 with a UV/H_2O_2 based AOP, and concluded that $OH\cdot$ radials did not contribute to the degradation of the contaminant. This is inconsistent with other research in the literature which has investigated the effectiveness of UV/H_2O_2 based AOPs in removing NH_3 in various wastewaters (Huang et al., 2008; De Brito et al., 2008).

Variation in pH and Production of Chlorine

In an electrochemical process, the chloride ion loses electrons at the anode and subsequent chlorine production occurs in accordance to Equation 6.1 (Kim et al., 2005; De Lima et al., 2009). The produced chlorine is further hydrolyzed to HOCl and OCl^- (depending on the pH of the solution) in accordance to Equations 6.2 and 6.3 (Anglada et al., 2010; Wang et al., 2012):

$$2Cl^- \rightarrow Cl_2 + e^- \tag{6.1}$$

$$Cl_2 + H_2O \rightarrow HOCl + H^+ + Cl^- \tag{6.2}$$

$$HOCl \rightarrow OCl^- + H^+ \tag{6.3}$$

The concentration of chloride in both processes was monitored throughout the treatment processes (Figure 6-3). Chloride concentrations decreased with time for both processes, as chloride oxidized to chlorine (Equation 6.1). The drop in chloride concentration was caused by the accumulation of chlorine in the bulk or due to the escape of chlorine to the air (Li and Liu, 2009; Xiao et al., 2009; Anglada et al., 2010).

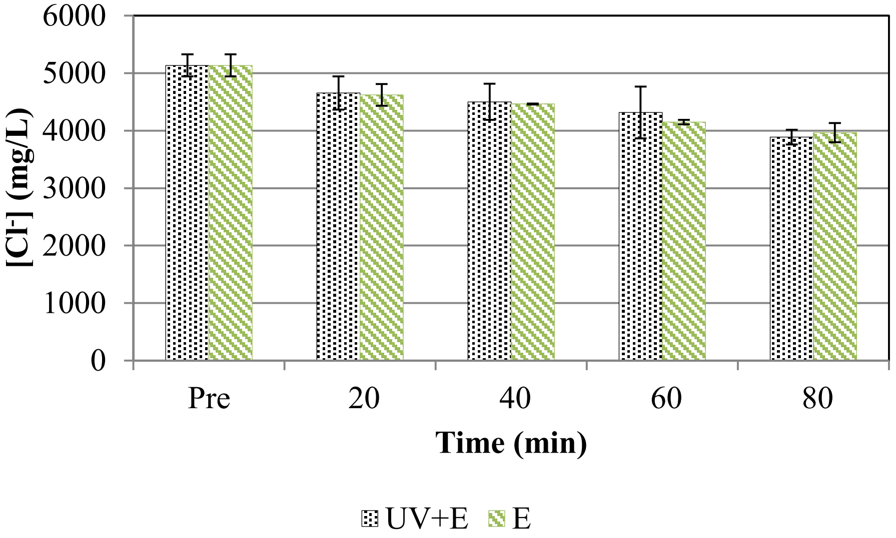

Figure 6-3 Variation in chloride concentration in the photoelectrochemical and electrochemical processes (Error bars represent standard deviation).

The variation in pH through both processes is illustrated in Figure 6-4. The pH dropped for both processes, as more H^+ ions were produced (Equation 6.2). For both processes, the pH dropped to around 2.5 until 80 minutes of treatment, when it gradually increased to 5.84 for the electrochemical process and to 4.20 for the photoelectrochemical process. The results suggest that HOCl is the main active chlorine species in both processes. The observed changes in pH level are consistent with report by Xiao et al. (2009), who observed a drop in pH at the beginning of treatment and a sequent increase in pH when the ammonia was depleted from the solution.

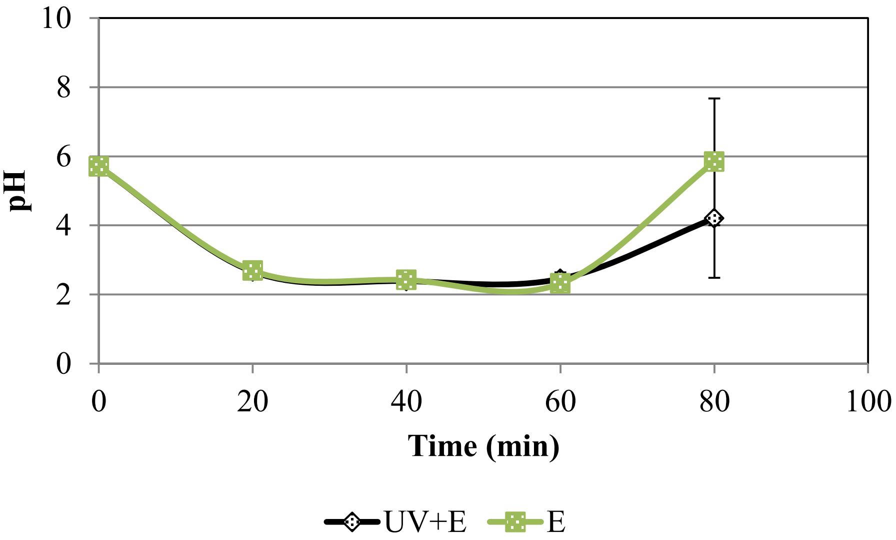

Figure 6-4 Variation of pH in the photoelectrochemical and electrochemical processes (Error bars represent standard deviation).

The interaction of ammonia and chlorine in various water matrices can be described with Equations 6.4 - 6.6 (Qiag and Adams, 2004; Gendel and Lahav, 2012):

$$HOCl + NH_3 \rightarrow NH_2Cl + H_2O \tag{6.4}$$

$$HOCl + NH_2Cl \rightarrow NHCl_2 + H_2O \tag{6.5}$$

$$HOCl + NHCl_2 \rightarrow NCl_3 + H_2O \tag{6.6}$$

In this research, chlorine (total and free) and monochloramine were measured. For both processes, the production of chlorine (total and free) and monochloramine are illustrated in Figure 6-5. On average, higher levels of chlorine species were observed in the electrochemical process compared to the photoelectrochemical process.

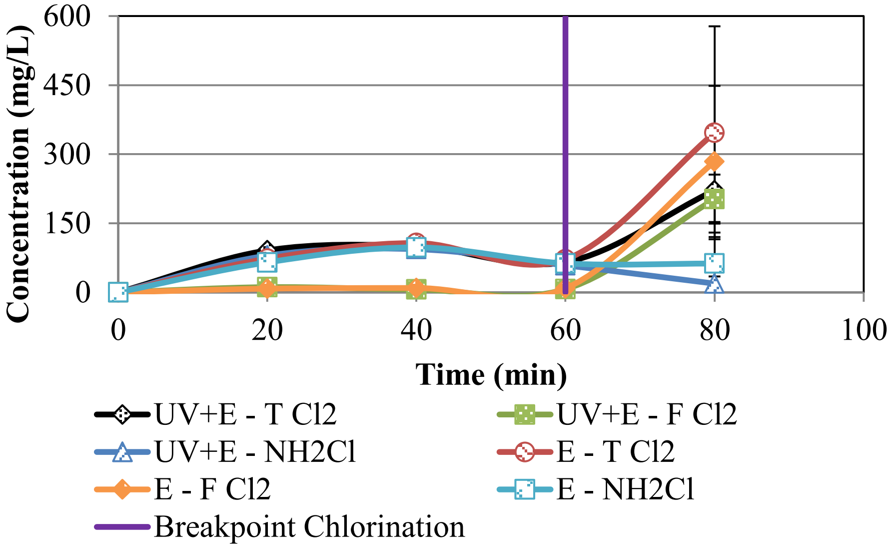

Figure 6-5 Production of chlorine (total and free) and monochloramine in the photoelectrochemical and electrochemical processes (Error bars represent standard deviation).

Both processes produced low levels of total chlorine until 80 minutes of treatment, when the concentration increased. This was attributed to the breakpoint chlorination of the water type, where chlorine was reacting with the contaminant and chloramines were being produced before the breakpoint (Figure 6-5). Theoretically, a chlorine concentration of 5800 mg/L would be required in order to achieve breakpoint chlorination (Cl_2:NH_3=7.6:1). After 80 minutes of treatment, the electrochemical process produced 346.5 mg/L of total chlorine compared to 221.5 mg/L from the photoelectrochemical process. The production of free chlorine followed the same trend as the total chlorine, where the electrochemical process produced 284 mg/L after 80 minutes of treatment compared to 202.5 mg/L with the photoelectrochemical process. Concentration of monochloramine in both processes peaked after 40 minutes, and then decreased. In the electrochemical process, monochloramine concentration reached a maximum (97.6 mg/L) after 40 minutes and then decreased to 62.5 mg/L after 80 minutes. In the photoelectrochemical process, monochloramine peaked to 93.75 mg/L after 40 minutes and then decreased to 19 mg/L after 80 minutes. The decrease in the monochloramine concentration observed could be caused by the conversion of monochloramine to dichloramine and trichloramine, and subsequently to non-toxic nitrogen gas as observed by Xiao et al. (2009).

The lower levels of chlorine species observed in the photoelectrochemical process are consistent with previous research. Ormeci et al. (2005) have previously reported the degradation of chlorine-based disinfectants (free chlorine and monochloramine) when exposed to UV light. It is suspected that the produced chlorine species in the protoelectrochemical process degraded due to the exposure to the UV light.

Production of OH· Radical

The electrochemical production of OH· radicals in the bulk by various anodes has been previously reported (Panizza and Cerisola, 2004; Basha et al., 2009; Li and Liu, 2009). The hydroxyl radicals are produced by the oxidation of the water molecule at the anode, in accordance to Equation 6.7 (Li and Goel, 2010; Talaat et al., 2010):

$$H_2O \rightarrow OH \cdot + H^+ + e^- \tag{6.7}$$

In the presence of chlorine, the photolysis of HOCl produces OH· and Cl· radicals in accordance to Equation 6.8 (Watts and Linden, 2007; Xiao et al., 2009):

$$HOCl + h\nu \rightarrow OH \cdot + Cl \cdot \tag{6.8}$$

In this research, the production of OH· radicals was monitored for both processes using pCBA as a probe compound with HPLC. pCBA samples were taken at all times through the experiments (at 20, 40, 60, and 80 minutes). The reaction of pCBA with the OH· radicals is expressed by Equation 6.9 (Cho et al., 2004; Watts and Linden, 2007):

$$\frac{-d[pCBA]}{dt} = k_{(OH,pCBA)}[OH]_{SS}[pCBA] \tag{6.9}$$

Solving Equation 6.9 results in:

$$-\ln\left(\frac{[pCBA]}{[pCBA]_{\bullet}}\right) = K_{\exp}t \tag{6.10}$$

Where:

$$K_{\exp} = k_{OH,pCBA}[OH]_{SS} \tag{6.11}$$

From Equation 6.10, the observed rate constant of pCBA (expressed as K_{exp}) was obtained. Furthermore, the steady state production of OH· radicals was calculated from Equation 6.11 with $k_{OH,pCBA} = 5 \times 10^{9}\ M^{-1}\ s^{-1}$ (Watts and Linden, 2007). Due to a constant degradation of pCBA (R^2>0.9), the pseudo-steady state assumption for the OH· radicals was valid (Elovitz and Gunten, 1999; Cho and Yoon, 2008).

The concentration of produced OH· radicals is illustrated in Figure 6-6 for both processes. None of the OH· radicals were consumed by the contaminant, as no synergistic effects was observed

(Figure 6-2), and therefore the concentration of OH· radicals observed is a representation of how much radical each process produced. The photoelectrochemical process resulted in higher concentrations of OH· radicals (8.54×10^{-10} mg/L), due to the additional OH· radicals produced from Equation 6.8, compared to the electrochemical process (4.44×10^{-10} mg/L). The results suggest that the contribution of OH· radicals (produced in the bulk by a Ti/RuO_2 anode or by the photolysis of HOCl) for the removal of contaminants was minimal, or negligible. This is consistent with other research that concluded negligible contribution by the OH· radical for the indirect oxidation of aqueous ammonia (Feng et al., 2003; Li and Liu, 2009; Xiao et al., 2009).

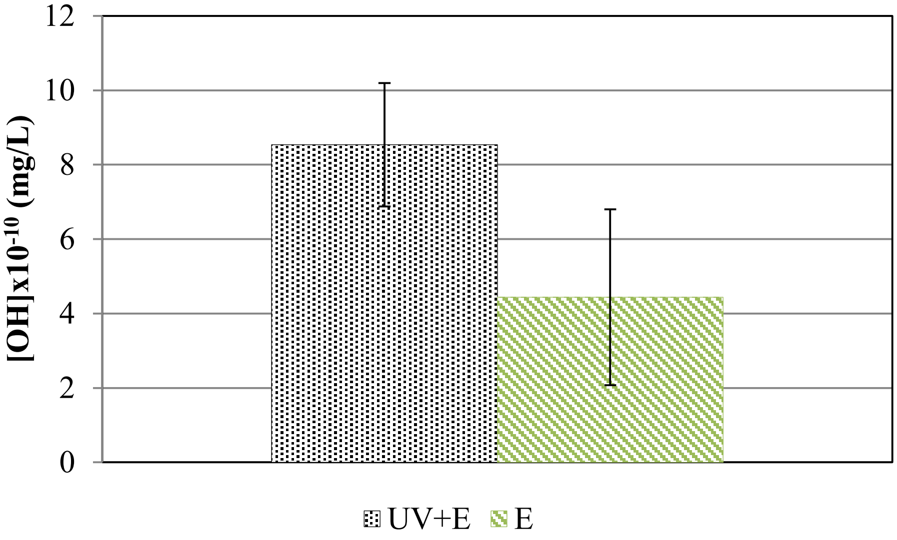

Figure 6-6 Production of OH· radicals in the photoelectrochemical and electrochemical processes (Error bars represent standard deviation).

Degradation Pathway

Pseudo zero and first-order kinetics have been previously used to describe the electrolysis and photoelectrolysis of ammonia. Vanlangendonck et al., (2005), Li and Liu (2009), and Xiao et al. (2009) reported the electrolysis of ammonia using pseudo zero-order kinetics. Xiao et al. (2009) have also reported the photoelectrochemical degradation of ammonia using pseudo zero-order kinetics. However, Soltani et al. (2013) have reported the photoelectrochemical degradation of ammonia using pseudo first-order kinetics. Chen et al. (2007) and Hu et al. (2009) have also reported the electrolysis of ammonia using pseudo first-order kinetics.

In this research, degradation of ammonium followed a linear trend with time. Therefore, rate constants were calculated using pseudo zero-order kinetics with respect to ammonium concentration, in accordance to Equation 6.12:

$$\frac{d\left[NH_4^+\right]}{dt} = -k_{obs} \tag{6.12}$$

Solving Equation 6.12 yields the reaction rate constant, k_{obs}:

$$\left[NH_4^+\right] = -k_{obs}t + \left[NH_4^+\right]_0 \tag{6.13}$$

The values of the rate constants and correlation coefficients are presented in Table 6-1. The obtained rate constants are greater compared to research by Xiao et al. (2009) for their systems (electrochemical and photoelectrochemical) with a Ti/RuO$_2$ anode. However, rate constants obtained from the electrochemical process were less than values reported by Liu et al. (2009) with a Ti/RuO$_2$ anode.

Table 6-1 Rate constants and correlation coefficients for ammonium in photoelectrochemical and electrochemical processes.

Treatment Process & Water Matrix	k (mg L^{-1} min^{-1})	R^2
UV + E - Synthetic	9.254	0.991
E - Synthetic	9.146	0.986
UV + E - Secondary municipal WW Effluent	0.281	0.995
E - Secondary municipal WW Effluent	0.236	0.993

The results from this research suggest that aqueous ammonia was removed with an electrochemical and photoelectrochemical process, although no difference in removal rate was observed. The removal mechanism for both processes was therefore assumed to be the same, following an electrochemical degradation pathway. Other research has previously reported the low removal rate due to the direct oxidation of ammonia compared to the indirect oxidation (Chen et al., 2007; Li and Liu, 2009; Wang et al., 2012). Subsequently, the indirect oxidation of ammonia was considered the main removal mechanism. Since the contribution of hydroxyl radicals was proven to be minimal, or negligible, the indirect oxidation of ammonia was only attributed to HOCl formed in the electrochemical process (Feng et al., 2003; Liu et al., 2009).

Aqueous ammonia was oxidized and converted to other sources of nitrogen (nitrate, and nitrogen gas), in accordance to Equations 6.14 - 6.19, following the mechanism of breakpoint chlorination (Li and Liu, 2009; Liu et al., 2009; Wang et al., 2012):

At the cathode:

$$2H^{+} + 2e^{-} \rightarrow H_2 \tag{6.14}$$

At the anode:

$$2Cl^{-} \rightarrow Cl_2 + 2e^{-} \tag{6.15}$$

In the solution:

$$Cl_2 + H_2O \rightarrow HOCl + H^+ + Cl^- \tag{6.16}$$

$$3HOCl + 2NH_3 \rightarrow N_2 + 3H_2O + 3H^+ + 3Cl^- \tag{6.17}$$

$$3HOCl + 2NH_4^+ \rightarrow N_2 + 3H_2O + 5H^+ + 3Cl^- \tag{6.18}$$

$$4HOCl + NH_4^+ \rightarrow NO_3^- + H_2O + 6H^+ + 4Cl^- \tag{6.19}$$

Accordingly, no nitrite should be formed in the process based on breakpoint chlorination (Hu et al., 2009). No concentration of nitrite or nitrate was detected in either process (or close to the MDL: 0.7 mg/L and 0.8 mg/L for nitrite and nitrate, respectively). The results are consistent with Soltani et al. (2013) who observed negligible production of nitrite and nitrate in their photoelectrochemical process. Negligible or little quantity of nitrite and nitrate production during the electrochemical treatment of aqueous ammonia has been previously reported in the literature (Kim et al., 2005; Hu et al., 2009; Kropp et al., 2009; Li and Liu, 2009). The results however, are not consistent with Xiao et al. (2009) who reported 15.8 mg/L and 2 mg/L of nitrate after 120 minutes in their electrochemical and photoelectrochemical processes, respectively. It is suspected that the nitrate produced in the process was reduced to nitrogen gas at the cathode, in accordance to Equation 6.20 (Kim et al., 2005):

$$NO_3^- + 3H_2O + 5e^- \rightarrow \frac{1}{2}N_2 + 6OH^- \tag{6.20}$$

In this research, the production of nitrogen gas was not measured. Xiao et al. (2009) have reported that more than 97% of the total nitrogen removed from their photoelectrochemical process was converted to nitrogen gas after 90 minutes. Li and Liu (2009) have also reported the conversion of 88% of the removed ammonia to nitrogen gas in their electrochemical process. It is suspected that the removed aqueous ammonia in this research is also converted to nitrogen gas, in accordance to Equations 6.15 - 6.18.

Application to Wastewater

Secondary wastewater effluent (prior to UV disinfection) was obtained from MCWPCC and treated photoelectrochemically and electrochemically. The wastewater was not supplemented with chloride, and adjusted to an initial pH of 10.0. Batch treatment was conducted in duplicate at three times (20, 40, 60 minutes), with a current density of 5 mA/cm^2 for both processes.

Aqueous ammonia and total nitrogen were removed partially from the wastewater after 60 minutes with both processes (Figure 6-7). 39.04% of aqueous ammonia was removed in the electrochemical process compared to 44.58% removal in the photoelectrochemical process. Total nitrogen was removed (50.69%) in the electrochemical process, compared to 54.74% removal in the photoelectrochemical process. A paired t-test suggested that the two treatments were not statistically different ($p=0.819$ and $p=0.427$ for aqueous ammonia and total nitrogen, respectively). The rate constants obtained (for both treatment processes) were smaller compared to the synthetic wastewater trial. This was expected as the both the initial concentration of contaminant and current density were lower compared to the synthetic wastewater trial. However, the rate constants obtained with the photoelectrochemical process were greater compared to the electrochemical process. There was a discrepancy in data, where total nitrogen was lower than aqueous ammonia, due to analytical error of the instrument.

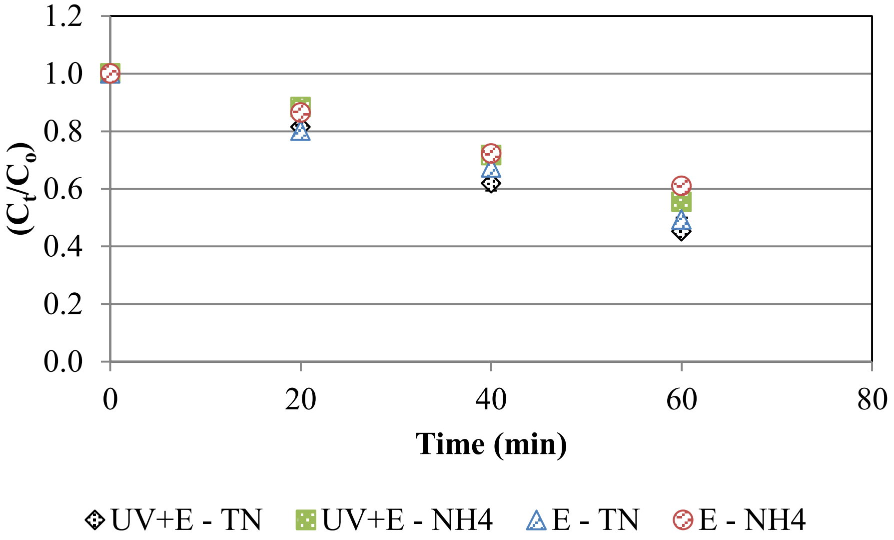

Figure 6-7 Removal of nitrogen compounds in the photoelectrochemical and electrochemical treatment of municipal wastewater (Error bars represent standard deviation).

No nitrite (or close to the MDL of 0.7 mg/L) was observed in the process. Nitrate was formed (Figure 6-8) throughout both treatment processes in accordance to Equation 6.19. The electrochemical process resulted in 2.54 mg/L of nitrate production compared to 4.01 mg/L in the photoelectrochemical process, after 60 minutes of treatment.

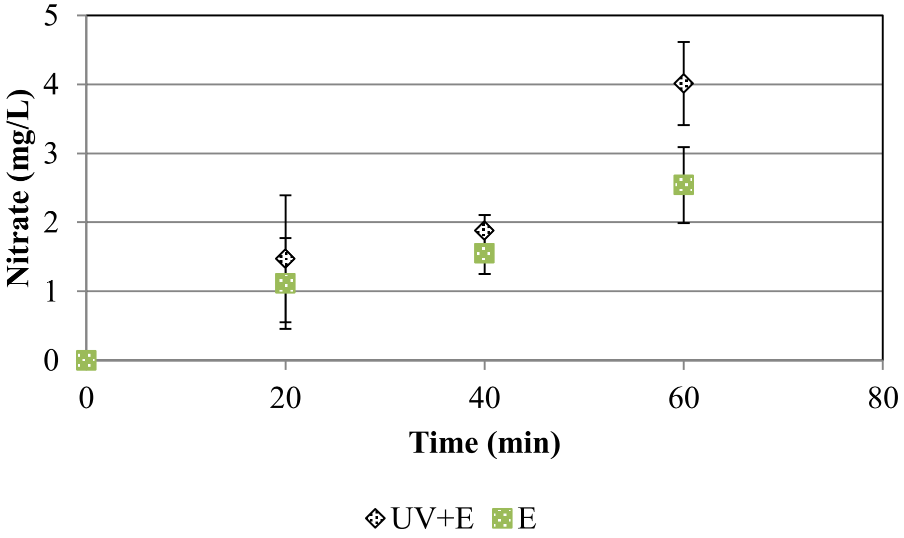

Figure 6-8 Production of nitrate throughout the photoelectrochemical and electrochemical treatment of municipal wastewater (Error bars represent standard deviation).

Production of chlorine (total and free) and monochloramine through the process is illustrated in Figure 6-9. Total chlorine reached a maximum of 18.5 mg/L with the photoelectrochemical process, compared to 20.75 mg/L for the electrochemical process. However, concentration of free chlorine was lower for the electrochemical process. Free chlorine concentration peaked after 20 minutes to 1.15 mg/L in the electrochemical process, and then decreased to 0.76 mg/L after 60 minutes of treatment. Free chlorine concentration for the photoelectrochemical process followed the same trend, but the concentration was higher. Free chlorine peaked after 20 minutes to 1.42 mg/L and then dropped to 1.41 mg/L after 60 minutes in the photoelectrochemical process. Monochloramine concentrations gradually increased for the photoelectrochemical process to 17.1 mg/L after 60 minutes of treatment. For the electrochemical process, monochloramine concentration peaked to 19.73 mg/L after 40 minutes and then dropped to 18.73 mg/L after 60 minutes. The observed chlorine species concentrations were lower compared to the synthetic wastewater trials. The synthetic wastewater did not contain organic matter, suggesting that the organics present in the actual wastewater reacted with the chlorine, producing DBPs.

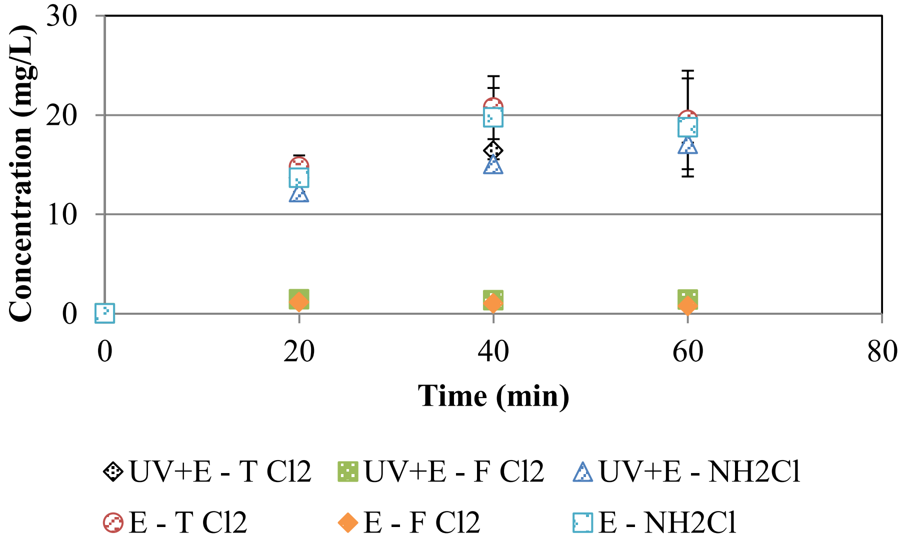

Figure 6-9 Production of chlorine and monochloramine throughout the photoelectrochemical and electrochemical treatment of municipal wastewater (Error bars represent standard deviation).

Therefore, the concentration of DBPs (TTHMs and THAAs) was investigated for both processes, illustrated in Figure 6-10. TTHMs concentrations did not increase with treatment time and were less for the electrochemical process compared to the photoelectrochemical process, except at 20 minutes of treatment. A paired t-test conducted on the data suggested that the two processes produced equivalent concentrations of TTHMs (p=0.293). However, THAAs concentrations increased gradually with time (R^2=1.00 and R^2=0.99 for the photoelectrochemical and electrochemical processes, respectively), and were lower for the photoelectrochemical process except at 40 minutes of treatment. A paired t-test suggested the two processes were not statistically different in the production of THAAs (p=0.684).

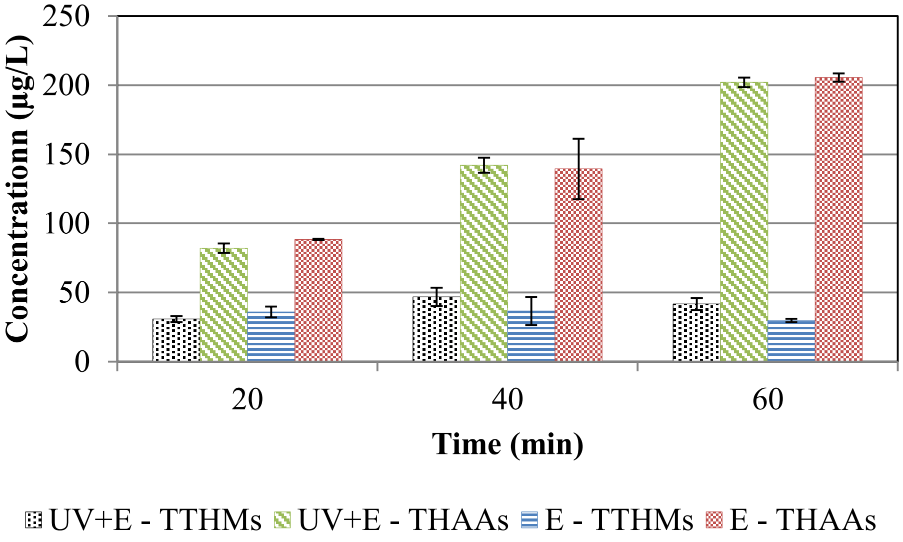

Figure 6-10 Production of TTHMs and THAAs throughout the photoelectrochemical and electrochemical treatment of municipal wastewater (Error bars represent standard deviation).

The release of metals (from the oxidation of the anode) was also monitored throughout the experimental duration, illustrated in Figure 6-11. The release of ruthenium was gradual with treatment time for both processes (R^2=0.98 and R^2=0.83 for the photoelectrochemical and electrochemical processes, respectively). The concentration of ruthenium was higher in the electrochemical process compared to the photoelectrochemical process. Titanium concentration was present in the wastewater before treatment, and it is suspected that the background concentration could account for the varying concentrations observed throughout both processes.

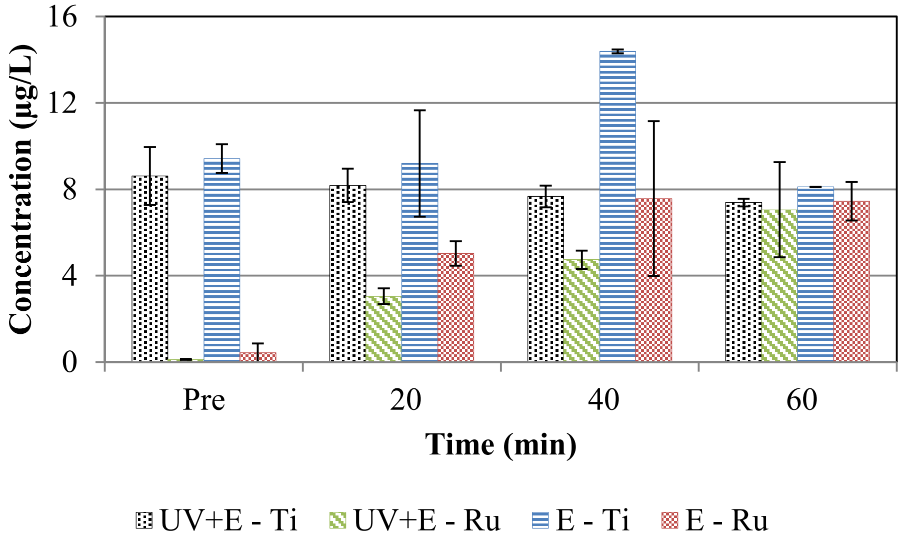

Figure 6-11 Release of metals throughout the photoelectrochemical and electrochemical treatment of municipal wastewater (Error bars represent standard deviation).

6.4 Conclusion

- The treatment of nitrogen containing compounds (aqueous ammonia and total nitrogen) was investigated with an electrochemical and a photoelectrochemical process.
- No synergistic effects for the removal of contaminants (aqueous ammonia or total nitrogen) were observed in the photoelectrochemical process. The absence of synergistic effect was attributed to the low intensity of the UV light used (0.274 mW/cm^2).
- The production of hydroxyl radicals by the anode, or by the photolysis of HOCl, proved to have minimal or negligible benefit for the degradation of aqueous ammonia in the process.

- The removal mechanism in both processes was attributed to the indirect oxidation of aqueous ammonia by HOCl produced in the process.
- Aqueous ammonia and total nitrogen were partially removed from secondary wastewater effluent obtained from MCWPCC with both processes. No synergistic effects for contaminant removal were observed in the photoelectrochemical process.
- The average production of TTHMs was lower for the electrochemical process, whereas THAAs were lower for the photoelectrochemical process. However, the concentration of produced THMs and HAAs were not statistically different in the two processes.
- Results from this research suggest that employing a UV light in an electrochemical process does not provide synergistic effects for the removal of nitrogen containing compounds. However, lower levels of chlorine species were detected with the photoelectrochemical process. This resulted in mixed data for the production of TTHMs and THAAs, where only THAAs were lower in the photoelectrochemical process compared to the electrochemical process.
- The addition of chloride ions or the use of higher intensity UV lamps would be beneficial to obtain higher removal rates, and to possibly meet regulatory standards.

Chapter 7: Conclusion

7.1 Synthesis

The work in this research was conducted in order to explore methods of removing nitrogen compounds, in particular aqueous ammonia, from wastewater. Two treatment technologies were considered: UV light and an electrochemical process. The two technologies were evaluated individually, as well as in combination.

Each treatment process was used to treat secondary wastewater effluent obtained from MCWPCC, Bedford, Nova Scotia. The direct photolysis of nitrogen compounds in municipal wastewater resulted in the removal of 70.1% total nitrogen with a UV fluence of 1000 mJ/cm^2 (corresponding to 277 minutes of treatment). Electrolysis and photoelectrolysis of municipal wastewater resulted in the removal of 50.69% and 54.74% total nitrogen after 60 minutes of treatment, respectively. Although the direct photolysis of nitrogen was observed, employing a UV light in an electrochemical process did not improve degradation rates. This was attributed to the low intensity of the UV light employed (0.274 mW/cm^2), as 277 minutes were required for the photolysis of 70.1% total nitrogen. The contribution of UV light in the photoelectrochemical process was therefore negligible, and the degradation pathway of nitrogen in the process was through the indirect oxidation of the contaminant as observed in the electrochemical process. However, the photoelectrochemical process resulted in lower chlorine residuals as the UV light degraded some of the chlorine. Lower levels of THAAs were therefore observed in the photoelectrochemical process compared to the electrochemical process.

Solely based on treatment efficacy with respect to time, the photoelectrochemical or electrochemical processes resulted in higher removal rates (although not statistically different in treatment efficacy). However, an energy audit would be required to assess the energy consumption of each process and to better assist the most suitable treatment.

7.2 Conclusions

The four main research questions for this research were:

1. What factors affect the direct photolysis of nitrogen compounds with a UV light?
2. What factors affect the electrolysis of nitrogen compounds with a Ti/RuO_2 anode?
3. Are there benefits in employing a UV light in an electrochemical process?
4. How effective is each technology for the treatment of municipal wastewater?

Photooxidation Treatment

The direct photolysis of nitrogen compounds was demonstrated with UV light. Treatment efficiency was affected by pH and initial concentration of contaminant, where an alkaline pH and a higher initial concentration of contaminant resulted in higher removal rates. The addition of chloride did not increase treatment efficiency. OH· radicals, produced from the direct photolysis of water, were responsible for the degradation of the contaminant. The direct photolysis of secondary municipal wastewater was also verified, although removal rates were low. The addition of oxidants (H_2O_2, O_3, TiO_2) would be beneficial to improve removal rates.

Electrochemical Treatment

The electrolysis of nitrogen compounds was demonstrated with a Ti/RuO_2 anode. The removal efficiency was affected by pH and current density. The increase in chloride concentration was beneficial, as higher removal rates were observed. The indirect oxidation of the contaminant by HOCl produced in the process, was attributed as the removal mechanism observed in the electrochemical process. The electrolysis of secondary wastewater effluent was conducted, and the production of DBPs (TTHMs and THAAs) reported. A maximum concentration of 36.7 µg/L and 205.6 µg/L for TTHMs and THAAs were observed through the process. The complete removal of nitrogen compounds in secondary wastewater effluent was not achieved however, and the addition of chloride ions would increase removal rates.

Photoelectrochemical Treatment

Synergistic benefits for the treatment of nitrogen compounds were not observed when a UV light was employed in an electrochemical cell, and this was attributed to the low intensity of the UV light (0.274 mW/cm^2) used in this research. However, lower levels of chlorine were detected in the photoelectrochemical process when compared to the electrochemical process. Therefore, the photoelectrolysis of secondary wastewater effluent resulted in lower THAAs (202.1 µg/L) when compared to an electrochemical process (205.6 µg/L).

In conclusion, technologies such as UV light and electrochemical cell are powerful technologies to be employed by wastewater utilities. These technologies could be used as a final treatment step in order to reduce nitrogen compounds in the effluents.

7.3 Recommendations

Future research paths were identified based on the results of this thesis. These were beyond the scope of this research, but are worth exploring. Overall, all processes should be investigated for the treatment of other wastewater parameters. An energy audit should be conducted to assess energy consumptions of each process. Quantitative bench scale experiments, or the use of continuous flow reactors, should be conducted in order to assess the results with stronger statistical tools. Enclosed cells should also be developed in order to monitor the production of gases in the processes. In specific, recommendations are presented for each treatment process:

- **Photooxidation**: other types of UV lamps, such as medium pressure (MP) or high pressure (HP), should be utilized to investigate differences in treatment efficacy.

- **Electrochemical**: other types of cathodes and anodes should be investigated for the process, as well as the chemistry of corrosion in the process. Other tools, such as Scanning Electron Microscopy (SEM) and Energy Dispersive X-Ray Spectroscopy (EDS), could be used to assess molecular changes on the electrodes. The production of other DBPs (in particular N-DBPs) should also be assessed.

- **Photoelectrochemical**: the use of MP and HP UV lamps should be investigated, as well as the use of other anodes or cathodes. The production of other DBPs (such as N-DBPs) and the use of sea water, as a natural electrolyte, should be investigated.

References

Adams, C. E. (1974) Removing nitrogen from wastewater. Environmental Science & Technology, 7(8), 696-701.

Ahmad, Z. (2006) Corrosion engineering and corrosion control. Elsevier Science & Technology Books, Amsterdam, Netherlands.

American Public Health Association (APHA), American Water Works Association (AWWA), Water Environment Federation (WEF) (2009) Standard Methods for the examination of water and wastewater.

Anglada, A., Ibanez, R., Urtiaga, A., and Ortiz, I. (2010) Electrochemical oxidation of saline industrial wastewaters using boron-doped diamond anodes. Catalysis Today, 151(1-2), 178-184.

Anglada, A., Urtiaga, A., and Ortiz, I. (2009) Contributions of electrochemical oxidation to waste-water treatment: fundamentals and review of applications. Journal of Chemical Technology and Biotechnology, 84(12), 1747-1755.

Anjaneyulu, Y., Chary, N. S., and Raj, D. S. S. (2005) Decolourization of industrial effluents–available methods and emerging technologies – a review. Reviews in Environmental Science and Bio/Technology, 4(4), 245-273.

Ashrafizadeh, S. N., and Khorasani, Z. (2010) Ammonia removal from aqueous solutions using hollow-fiber membrane contactors. Chemical Engineering Journal, 162(1), 242-249.

Ashrafizadeh, S. N., Khorasani, Z., and Gorjiara, M. (2008) Ammonia removal from aqueous solutions by Iranian natural zeolite. Seperation Science and Technology, 43(4), 960-978.

Badani, Z., Ait-Amar, H., Si-Salah, A., Brik, M., and Fuchs, W. (2005) Treatment of textile waste water by membrane bioreactor and reuse. Desalination, 185(1), 411-417.

Bard, A. J., Parsons, R., and Jordan, J. (1985) Standards potentials in aqueous solutions. Marcel Dekker, New York, USA.

Basha, C. A., Chithra, E., and Sripriyalakshmi, N. K. (2009) Electro-degradation and biological oxidation of non-biodegradable organic contaminants. Chemical Engineering Journal, 149(1-3), 25-34.

Beckles, Y., and Diyamandoglu, V. (2006) Interactions between Halide Ions and Ammonia in Water under UV Light from Low Pressure Mercury Lamps. In World Environmental and Water Resource Congress – Examining the Confluence of Environmental and Water Concerns – ASCE, 1-9.

Bhatkhande, D. S., Pangarkar, V. G., and Beenackers, A. A. (2002) Photocatalytic degradation for environmental applications – a review. Journal of Chemical Technology and Biotechnology, 77(1), 102-116.

Bolton, J. R., and Linden, K. G. (2003) Standardization of methods for fluence (UV dose) determination in bench-scale UV experiments. Journal of Environmental Engineering, 129(3), 209-215.

Brown, C. J., Knight, B. W., McMaster, M. E., Munkittrick, K. R., Oakes, K. D., Tetreault, G. R., and Servos, M. R. (2011). The effects of tertiary treated municipal wastewater on fish communities of a small river tributary in Southern Ontario, Canada. Environmental pollution, 159(7), 1923-1931.

Brunet, L., Lyon, D. Y., Hotze, E. M., Alvarez, P. J. J., and Wiesner, M. R. (2009) Comparative photoactivity and antibacterial properties of C_{60} fullerenes and titanium dioxide nanoparticles. Environmental Science & Technology, 43(12), 4355-4360.

Buxton, G. V., Greenstock, C. L., Helman, W. P., and Ross, A. B. (1988). Critical review of rate constants for reactions of hydrated electrons, hydrogen atoms and hydroxyl radicals. Journal of Physical and Chemical Reference Data, 17, 513-886.

Cabeza, A., Urtiaga, A., Rivero, M. J., and Ortiz, I. (2007) Ammonium removal from landfill leachate by anodic oxidation. Journal of hazardous materials, 144(3), 715-719.

Carlson, J. C., Anderson, J. C., Low, J. E., Cardinal, P., MacKenzie, S. D., Beattie, S. A., Challis, J. K., Bennet, R. J., Meronek, S. S., Wilks, R. P. A., Buhay, W. M., Wong, C. S., and Hanson, M. L. (2013) Presence and hazards of nutrients and emerging organic micropollutants from sewage lagoon discharges into Dead Horse Creek, Manitoba, Canada. Science of the Total Environment, 445, 64-78.

Catalkaya, E. C., and Kargi, F. (2007) Color, TOC and AOX removals from pulp mill effluent by advanced oxidation processes: A comparative study. Journal of hazardous materials, 139(2), 244-253.

Chen, J., Shi, H., and Lu, J. (2007) Electrochemical treatment of ammonia in wastewater by RuO_2-IrO_2-TiO_2/Ti electrodes. Journal of Applied Electrochemistry, 37(10), 1137-1144.

Chen, Y., Yang, S., Wang, K., and Lou, L. (2005) Role of primary active species and TiO_2 surface characteristic in UV-illuminated photodegradation of Acid Orange 7. Journal of Photochemistry and Photobiology A: Chemistry, 172(1), 47-54.

Cho, M., Chung, H., Choi, W., and Yoon, J. (2004) Linear correlation between inactivation of E. coli and OH radical concentration in TiO_2 photocatalytic disinfection. Water Research, 38(4), 1069-1077.

Cho, M., and Yoon, J. (2008) Measurement of OH radical C_t for inactivating Cryptosporidium parvum using photo/ferrioxalate and photo/TiO_2 systems. Journal of Applied Microbiology, 104(3), 759-766.

Chu, W., and Chan, K. H. (2007) Hybrid system to upgrade conventional Fenton's process by incorporating photo-fenton as a successive treatment process: Degradation of monuron. Industrial & engineering chemistry research, 46(5), 1505-1510.

Chung, Y. J., Choi, H. N., Lee, S. E., and Cho, J. B. (2004) Treatment of tannery wastewater with high nitrogen content using anoxic/oxic membrane bio-reactor (MBR). Journal of Environmental Science and Health, Part A, 39(7), 1881-1890.

Comeau, F., Surette, C., Brun, G. L., and Losier, R. (2008) The occurrence of acidic drugs and caffeine in sewage effluents and receiving waters from three coastal watersheds in Atlantic Canada. Science of the Total Environment, 396(2-3), 132-146.

Cong, Y., Wu, Z., and Li, Y. (2008) Electrochemical inactivation of coliforms by in-situ generated hydroxyl radicals. Korean Journal of Chemical Engineering, 25(4), 727-731.

Constable, M., Charlton, M., Jensen, F., McDonald, K., Craig, G., and Taylor, K. W. (2003) An ecological risk assessment of ammonia in the aquatic environment. Human and Ecological Risk Assessment, 9(2), 527-548.

Cooper, W. J., Cramer, C. J., Martin, N. H., Mezyk, S. P., O'Shea, K. E., and Sonntag, C. V. (2009) Free radical mechanisms for the treatment of methyl tert-butyl ether (MTBE) via advanced oxidation/reductive processes in aqueous solutions. Chemical reviews, 109(3), 1302-1345.

Crittenden, J. C., Hu, S., Hand, D. W., and Green, S. A. (1999) A kinetic model for H_2O_2/UV process in a completely mixed batch reactor. Water research, 33(10), 2315-2328.

Crouse, B. A., Ghoshdastidar, A. J., and Tong, A. Z. (2012) The presence of acidic and neutral drugs in treated sewage effluents and receiving waters in the Cornwallis and Annapolis River watersheds and the Mill Cove sewage treatment plant in Nova Scotia, Canada. Environmental Research, 112, 92-99.

Dash, B. P., and Chaudhari, S. (2005) Electrochemical denitrification of simulated ground water. Water Research, 39(17), 4065-4072.

De Brito, N. N., Paterniani, J. E. S., Brota, G. A., and Pelegrini, R. T. (2010) Ammonia removal from leachate by photochemical process using H_2O_2. Revista Ambiente & Agua – An interdisciplinary Journal of Applied Science, 5(2), 51-60.

De Gisi, S., Galasso, M., and De Feo, G. (2009) Treatment of tannery wastewater through the combination of a conventional activated sludge process and reverse osmosis with a plane membrane. Desalination, 249(1), 337-342.

De Lima, R. M. G., Da Silva, Wildhagen G. R., Da Cunha, J. W. S. D., and Afonso J. C. (2009) Removal of ammonium ion from produced waters in petroleum offshore exploitation by a batch single-stage electrolytic process. Journal of hazardous materials, 161(2), 1560-1564.

Deng, Y., and Englehardt, J. D. (2007) Electrochemical oxidation for landfill leachate treatment. Waste Management, 27(3), 380-388.

Diaz, V., Ibanez, R., Gomez, P., Urtiaga, A. M., and Ortiz, I. (2011) Kinetics of electro-oxidation of ammonia-N, nitrites and COD from recirculating aquaculture saline water system using BDD anodes. Water Research, 45(1), 125-134.

Droste, R. L. (1997) Theory and practice of water and wastewater treatment. John Wiley and Sons Inc., NY, USA.

Du, Q., Liu, S., Cao, Z., and Wang, Y. (2005) Ammonia removal from aqueous solution using natural Chinese clinoptilolite. Seperation and Purification Technology, 44(3), 229-234.

Elovitz, M. S. and Gunten, U. V. (1999) Hydroxyl radical/ozone rations during ozonation processes. I. The R_{ct} concept. Ozone Science & Engineering, 21(3), 239-360.

Environment Canada (2012) Wastewater Systems Effluent Regulations. Fisheries Act, P. C. 2012-942, published by the Minister of Justice, June 2012.

Environment Canada and Health Canada (2001) Priority substances list assessment report: ammonia in the aquatic environment. Canadian Environmental Protection Act, 1999.

Fang, H. Y., Chou, M. S., and Huang, C. W. (1993) Nitrification of ammonia-nitrogen in refinery wastewater. Water Research, 27(12), 1761-1765.

Farizoglu, B., Keskinler, B., Yildiz, E., and Nuhoglu, A. (2004) Cheese whey treatment performance of an aerobic jet loop membrane bioreactor. Process Biochemistry, 39(12), 2283-2291.

Feng, C., Sugiura, N., Shimada, S., and Maekawa, T. (2003) Development of high performance electrochemical wastewater treatment system. Journal of Hazardous Materials, 103(1-2), 65-78.

Gendel, Y., and Lahav, O. (2012) Revealing the mechanism of indirect ammonia oxidation. Electrochimica Acta, 63, 209-219.

Getoff, N. and Schenck, G. O. (1968) Primary products of liquid water photolysis at 1246, 1470 and 1849 A. Photochemistry and Photobiology, 8(3), 167-178.

Glaze, W. H., Kang, J. W., and Chapin, D. H. (1987) The chemistry of water treatment processes involving ozone, hydrogen peroxide and ultraviolet radiation. Ozone: Science & Engineering: The Journal of the Internal Ozone Association, 9(4), 335-352.

Gomes, A., and Fernandes, E. (2005) Fluorescence probes used for detection of reactive oxygen species. Journal of Biochemical and Biophysical Methods, 65(2-3), 45-80.

Halifax Water (2013) Correspondence and information obtained from the operator at Mill Cove Water Pollution Control Centre (MCWPCC).

Hansen, K. M. S., Willach, S., Antoniou, M. G., Mosbaek, H., Albrechtsen, H. J., and Andersen, H. R. (2012) Effect of pH on the formation of disinfection byproducts in swimming pool water – is less THM better? Water Research, 46(19), 6399-6409.

Hammer, M. J., and Hammer, M. J. Jr. (2012) Water and wastewater technology. 7th Edition, Prentice Hall, Pearson Education Inc., NJ, USA.

Hasanoglu, A., Romero, J., and Perez, B., and Plaza, A. (2010) Ammonia removal from wastewater streams through membrane contactors: experimental and theoretical analysis of operation parameters and configuration. Chemical Engineering Journal, 160(2), 530-537.

Hu, W., Gong, B., and Feng, C. (2009) Electrochemical oxidation of ammonia-containing wastewater using Ti/RuO_2-Pt electrode. Water Science and Engineering, 2(4), 103-109.

Hu, Z., and Gagnon, G. A. (2006) Factors affecting recirculating biofilters (RBFs) for treating municipal wastewater. Journal of Environmental Engineering and Science, 5(4), 349-357.

Huang, L., Li, L., Dong, W., Liu, Y., and Hou, H. (2008) Removal of ammonia by OH radical in aqueous phase. Environmental Science & Technology, 42(21), 8070-8075.

Huang, Y. K., Li, S., Wang, C., and Min, J. (2012) Simultaneous removal of COD and NH_3-N in secondary effluent of high-salinity industrial waste-water by electrochemical oxidation. Journal of Chemical Technology and Biotechnology, 87(1), 130-136.

Hued, A. C., Caruso, M. N., Wunderline, D. A., and Bistoni, M. A. (2006) Field and in vitro evaluation of ammonia toxicity on native fish species of the central region of Argentina. Bulleting of Environmental Contamination and Toxicity, 76(6), 984-991.

Holeton, C., Chambers, P. A., and Grace, L. (2011) Wastewater release and its impacts on Canadian waters. Canadian Journal of Fisheries and Aquatic Sciences, 68(10), 1836-1859.

Idelovitch, E., and Michail, M. (1981) Nitrogen removal by free ammonia stripping from high pH ponds. Journal (Water Pollution Control Federation), 53(9), 1391-1401.

Jung, J. Y., Chung, Y. C., Shin, H. S., and Son, D. H. (2004) Enhanced ammonia nitrogen removal using consistent biological regeneration and ammonium exchange of zeolite in modified SBR process. Water Research, 38(2), 347-354.

Kapalka, A., Cally, A., Neodo, S., Comninellis, C., Wachter, M., and Udert, K. M. (2010) Electrochemical behavior of ammonia at Ni/Ni(OH)$_2$ electrode. Electrochemistry Communications, 12(1), 18-21.

Khosravi, A., Esmhosseini, M., Jalili, J., and Khezri, S. (2012) Optimization of ammonium removal from waste water by natural zeolite using central composite design approach. Journal of Inclusion Phenomena & Macrocyclic Chemistry, 74(1-4), 383-390.

Khuntia, S., Majumder, S. K., and Ghosh, P. (2013) Removal of ammonia from water by ozone microbubbles. Industrial & Engineering Chemistry Research, 52(1), 318-326.

Kim, K. W., Kim, Y. J., Kim, I. T., Park, G. I., and Lee, E. H. (2005) The electrolytic decomposition mechanism of ammonia to nitrogen at an IrO$_2$ anode. Electrochimica Acta, 50(22), 4356-4364.

Krasner, S. W., Westerhoff, P., Chen, B., Rittmann B. E., and Amy, G. (2009) Occurrence of disinfection byproducts in United States wastewater treatment plant effluents. Environmental Science & Technology, 43(21), 8320-8325.

Kropp, R., Tompkins, D., Barry, T., Zeltner, W., Pepping, G., Anderson, M., and Barry, T. (2009) A device that converts aqueous ammonia into nitrogen gas. Aquaculture, 41(1), 28-34.

Kuo, J., Chen, C. L., and Nellor, M. (2003) Standardized collimated beam testing protocol for water/wastewater ultraviolet disinfection. Journal of Environmental Engineering, 129(8), 774-779.

Kurian, R., Acharya, C., Nakhla, G., and Bassi, A. (2005) Conventional and thermophilic aerobic treatability of high strength oily pet food wastewater using membrane-coupled bioreactors. Water research, 39(18), 4299-4308.

Kusic, H., Koprivanac, N., and Bozic, A. L. (2006). Minimization of organic pollutant content in aqueous solution by means of AOPs: UV-and ozone-based technologies. Chemical Engineering Journal, 123(3), 127-137.

Legrini, O., Oliveros, E., and Braun, A. M. (1993) Photochemical processes for water treatment. Chemical Reviews, 93(2), 671-698.

Li, H., and Ni, J. (2012) Electrogeneration of disinfection byproducts at a boron-doped diamond anode with resorcinol as a model substance. Electrochimica Acta, 69(1), 268-274.

Li, L., and Goel, R. K. (2010) Role of hydroxyl radical during electrolytic degradation of contaminants. Journal of hazardous materials, 181(1), 521-525.

Li, L. and Liu, Y. (2009) Ammonia removal in electrochemical oxidation: mechanism and pseudo-kinetics. Journal of Hazardous Materials, 161(2-3), 1010-1016.

Li, M., Feng, C., Zhang, Z., Lei, X., Chen, R., Yang, Y., and Sugiura, N. (2009a) Simultaneous reduction of nitrate and oxidation of by-products using electrochemical method. Journal of Hazardous Materials, 171(1-3), 724-730.

Li, M., Feng, C., Zhang, Z., Shen, Z., and Sugiura, N. (2009b) Electrochemical reduction of nitrate using various anodes and a Cu/Zn cathode. Electrochemistry Communications, 11(10), 1853-1856.

Liang, T., Wang, S., Cao, H., Zhang, X., Li, G., Li, H., Song, W., and Chong, Z. (2008) Estimation of ammonia nitrogen load from nonpoint sources in the Xitiao river catchment, China. Journal of Environmental Sciences, 20(10), 1195-1201.

Lin, H., Gao, W., Meng, F., Liao, B. Q., Leung, K. T., Zhao, L., Chen, J., and Hong, H. (2012) Membrane bioreactors for industrial wastewater treatment: a critical review. Critical Reviews in Environmental Science and Technology, 42(7), 677-740.

Lin, L., Chen, J., Xu, Z., Yuan, S., Cao, M., Liu, H., and Lu, X. (2009) Removal of ammonia nitrogen in wastewater by microvawe radiation: a pilot-scale study. Journal of Hazardous Materials, 168(2-3), 862-867.

Liu, H., Wang, C., Li, X., Xuan, X., Jiang, C., and Cui, H. N. (2007) A novel electro-Fenton process for water treatment: reaction-controlled pH adjustment and performance assessment. Environmental science & technology, 41(8), 2937-2942.

Liu, U., Li, L., and Goel, R. (2009) Kinetic study of electrolytic ammonia removal using Ti/IrO_2 as anode under different experimental conditions. Journal of Hazardous Materials, 167(1-3), 959-965.

Liu, X., Li, X. M., Yang, Q., Yue, X., Shen, T. T., Zheng, W., Luo, K., Sun, Y. H., and Zeng, G. M. (2012) Landfill leachate pretreatment by coagulation–flocculation process using iron-based coagulants: Optimization by response surface methodology. Chemical Engineering Journal, 200, 39-51.

Lopez, A., Pagano, M., Volpe, A., and Di Pinto A. C. (2004) Fenton's pre-treatment of mature landfill leachate. Chemosphere, 54(7), 1005-1010.

Melero, J. A., Martinez, F., Botas, J. A., Molina, R., and Pariente, M. I. (2009) Heterogeneous catalytic wet peroxide oxidation systems for the treatment of an industrial pharmaceutical wastewater. Water research, 43(16), 4010-4018.

Mikami, I., Aoki, S., and Miura, Y. (2010) Photocatalytic Oxidation of Aqueous Ammonia in the Presence of Oxygen over Platinum-loaded TiO_2. Chemistry Letters, 39(7), 704-705.

Miladinovic, N., and Weatherley, L. R. (2008) Intensification of ammonia removal in a combined ion-exchange and nitrification column. Chemical Engineering Journal, 135(1-2), 15-24.

Milazzo, G., Caroli, S., and Sharma, V. K. (1978) Tables of standard electrode potentials. Wiley, Chichester, 1978.

Min, K. S., Yu, J. J., Kim, Y. J., and Yun, Z. (2004) Removal of ammonium from tannery wastewater by electrochemical treatment. Journal of Environmental Science and Health, Part A, 39(7), 1867-1879.

Moazed, H. (2008) Ammonium ion removal from wastewater by a natural resin. Journal of Environmental Science and Technology, 1(1), 11-18.

Mousavi, S. A. R., Ibrahim, S., Aroua, M. K., and Ghafari, S. (2011) Bio-electrochemical denitrification – a review. International Journal of Chemical and Environmental Engineering, 2(2), 140-146.

Munter, R. (2001) Advanced oxidation processes–current status and prospects. Proceedings of the Estonian Academy of Sciences, Chemistry, 50(2), 59-80.

Munz, G., De Angelis, D., Gori, R., Mori, G., Casarci, M., and Lubello, C. (2009) The role of tannins in conventional and membrane treatment of tannery wastewater. Journal of hazardous materials, 164(2), 733-739.

National Research Council (NCR) (1977) Ammonia. Prepared for Health Effect Research Lab, November 1977, Washington, DC.

Nemoto, J., Gokan, N., Ueno, G., and Kaneko, M. (2007) Photodecomposition of ammonia to dinitrogen and dihydrogen on platinized TiO_2 nanoparticles in an aqueous solution. Journal of Photochemistry and Photobiology A: Chemistry, 185(2-3), 295-300.

Nishimura, F., Hidaka, T., Nakagawa, A., Yorozu, H., and Tsuno, H. (2012) Removal of high concentration ammonia from wastewater by a combination of partial nitrification and anammox treatment. Environmental Technology, 33(13), 1485-1489.

Ormeci, B., Linden, K., and Ducoste, J. (2005) UV disinfection of chlorinated water: impact on chlorine concentration and UV dose delivery. Journal of Water Supply: Research and Technology – AQUA, 54(3), 189-199.

Park, J. S., Choi, H., and Cho, J. (2004) Kinetic decomposition of ozone and para-chlorobenzoic acid (pCBA) during catalytic ozonation. Water Research, 38(9), 2285-2292.

Panizza, M. and Cerisola, G. (2004) Influence of anode material on the electrochemical oxidation of 2-naphthol - Part 2: Bulk electrolysis experiments. Electrochimica Acta, 49(19), 3221-3226.

Pressley, T. A., Bishop, D. F., and Roan, S. G. (1972) Ammonia-nitrogen removal by breakpoint chlorination. Environmental Sicence & Technology, 6(7), 622-628.

Qiag, Z., and Adams, C. D. (2004) Determination of monochloramine formation rate constants with stopped-flow spectrophotometry. Environmental Science & Technology, 38(5), 1435-1444.

Rand, J. L., and Gagnon, G. A. (2008) Loss of chlorine, chloramine or chlorine dioxide concentration following exposure to UV light. Journal of Water Supply: Research and Technology – AQUA, 57(2). 127-132.

Randall, D. J., and Tsui, T. K. N. (2002) Ammonia toxicity in fish. Marine Pollution Bulletin, 45(1), 17-23.

Reisz, E., Schmidt, W., Schuchmann, H. P., and von Sonntag, C. (2003) Photolysis of ozone in aqueous solutions in the presence of tertiary butanol. Environmental science & technology, 37(9), 1941-1948.

Rengifo-Herrera, J. A., Pierzchala, K., Sienkiewicz, A., Forro, L., Kiwi, J., and Pulgarin, C. (2009) Abatement of organics and Escherichia coli by N, S co-doped TiO_2 under UV and visible light. Implications of the formation of singlet oxygen ($^1O_2$) under visible light. Applied Catalysis B: Environmental, 88(3), 398-406.

Rezaee, A., Soltani, R. D. C., Khataee, A. R., and Godini, H. (2012) Optimization of combined photocatalytic involving immobilized ZnO nanoparticles and electrochemical processes for ammoniacal nitrogen removal from aqueous solutions. Journal of Materials and Environmental Science, 3(5), 955-966.

Rezakazemi, M., Shirazian, S., and Ashrafizadeh, S. N. (2012) Simulation of ammonia removal from industrial wastewater streams by means of a hollow-fiber membrane contactor. Desalination, 285(31), 383-392.

Roberts, P. J. W., Salas, H. J., Reiff, F. M., Libhaber, M., Labbe, A., and Thomson, J. C. (2011) Marine wastewater outfalls and treatment systems. IWA Publishing, London, UK.

Rosenfeldt, E. J., Linden, K. G., Canonica, S., and Gunten, U. V. (2006) Comparison of the efficiency of OH radical formation during ozonation and the advanced oxidation processes O_3/H_2O_2 and UV/H_2O_2. Water Research, 40(20), 3695-3704.

Saravanane, R., and Sundararaman, S. (2009) Effect of loading rate and HRT on the removal of cephalosporin and their intermediates during the operation of a membrane bioreactor treating pharmaceutical wastewater. Environmental technology, 30(10), 1017-1022.

Sarioglu, M. (2005) Removal of ammonium from municipal wastewater using natural Turkish (Dogantepe) zeolite. Seperation and Purification Technology, 41(1), 1-11.

Soltani, R. D. C., Rezaee, A., Godini, H., Khataee, A. R., and Hasanbeiki, A. (2013) Photoelectrochemical treatment of ammonium using seawater as a natural supporting electrolyte. Chemistry and Ecology, 29(1), 72-85.

Song, H., Addison, J. W., Hu, J., and Karanfil, T. (2010) Halonitromethanes formation in wastewater treatment plants effluents. Chemosphere, 79(2), 174-179.

Song, S., Xu, L., He, Z., Chen, J., Xiao, X., and Yan, B. (2007) Mechanism of the photocatalytic degradation of CI Reactive Black 5 at pH 12.0 using $SrTiO_3/CeO_2$ as the catalyst. Environmental science & technology, 41(16), 5846-5853.

Song, S., Xu, X., Xu, L., He, Z., Ying, H., Chen, J., and Yan, B. (2008) Mineralization of CI Reactive Yellow 145 in aqueous solution by ultraviolet-enhanced ozonation. Industrial & Engineering Chemistry Research, 47(5), 1386-1391.

Souza, B. M., Cerqueira, A. C., Sant'Anna Jr, G. L., and Dezotti, M. (2011) Oil-Refinery Wastewater Treatment Aiming Reuse by Advanced Oxidation Processes (AOPs) Combined with Biological Activated Carbon (BAC). Ozone: Science & Engineering, 33(5), 403-409.

Stasinakis, A. S. (2008) Use of selected advanced oxidation processes (AOPs) for wastewater treatment – a min review. Global NEST Journal, 10(3), 376-385.

Tai, C., Gu, X., Zou, H., and Guo, Q. (2002) A new simple and sensitive fluorometric method for the determination of hydroxyl radical and its application. Talanta, 58(4), 661-667.

Talaat, H. A., Ghaly, M. Y., Kamel, E. M., Ahmed, E. M., and Awad, A. M. (2010) Simultaneous Removal of Iron and Manganese from Ground Water by Combined Photo-Electrochemical Method. Journal of American Science, 6(12), 1-7.

Tanaka, J., and Matsumura, M. (2002) Kinetic studies of removal of ammonia from seawater by ozonation. Journal of Chemical Technology and Biotechnology, 77(6), 649-656.

Teel, A. L., Finn, D. D., Schmidt, J. T., Cutler, L. M., and Watts, R. J. (2007) Rates of trace mineral-catalyzed decomposition of hydrogen peroxide. Journal of Environmental Engineering, 133(8), 853-858.

Tetreault, G. R., Bennett, C. J., Shires, K., Knight, B., Servos, M. R., and McMaster, M. E. (2011) Intersex and reproductive impairment of wild fish exposed to multiple municipal wastewater discharges. Aquatic Toxicology, 104(3), 278-290.

Tezcanli-Guyer, G., and Ince, N. H. (2004) Individual and combined effects of ultrasound, ozone and UV irradiation: a case study with textile dyes. Ultrasonics, 42(1), 603-609.

Urtiaga, A., Ortiz, I., Anglada, A., Mantzavinos, D., and Diamadopoulos, E. (2012) Kinetic modeling of the electrochemical removal of ammonium and COD from landfill leachates. Journal of Applied Electrochemistry, 42(9), 779-786.

United States Environmental Protection Agency (US EPA) (1999) Method 300.1 – Determination of inorganic anions in drinking water by ion chromatography. Revision 1.0, National Exposure Research Laboratory, Office of Research & Development, USEPA, Cincinnati, USA.

United States Environmental Protection Agency (US EPA) (2009) National water quality inventory: 2004 report to congress. United States Environmental Protection Agency, EPA 841-R-08-001, January 2009.

Vanlangendonck, Y., Corbisier, D., and Van Lierde, A. (2005) Influence of operating conditions on the ammonia electro-oxidation rate in wastewaters from power plants (ELONITA technique). Water Research, 39(13), 3028-3034.

Vlyssides, A. G., Karlis, P. K., Rori, N., and Zorpas, A. A. (2002) Electrochemical treatment in relation to pH of domestic wastewater using Ti/Pt electrodes. Journal of Hazardous Materials 95(1-2), 215-226.

Vohra, M. S., Selimuzzaman, S. M., and Al-Suwaiyan, M. S. (2010) NH_4^+-NH_3 removal from simulated wastewater using UV-TiO_2 photocatalysis: effect of co-pollutants and pH. Environmental Technology, 31(6), 641-654.

Wang, Y., Guo, X., Li, J., Yang, Y., Lei, Z., and Zhang, Z. (2012) Efficient electrochemical removal of ammonia with various cathodes and Ti/RuO_2-Pt anode. Open Journal of Applied Sciences, 2(4), 241-247.

Watts, M. J., and Linden, K. G. (2007) Chlorine photolysis and subsequent OH radical production during UV treatment of chlorinated water. Water Research, 41(13), 2871-2878.

Wenjun, L., Di, W., Xin, S., Lixiong, W., and Lei, S. (2012) Removal of organic matter and ammonia nitrogen in azodicarbonamide wastewater by a combination of power ultrasound radiation and hydrogen peroxide. Energy, Resources and Environmental Technology, 20(4), 754-759.

Wicks, B. J., Joensen, R., Tang, Q., and Randall, D. J. (2002) Swimming and ammonia toxicity in salmonids: the effect of sub lethal ammonia exposure on the swimming performance of coho salmon and the acute toxicity of ammonia in swimming and resting rainbow trout. Aquatic toxicology, 59(1), 55-69.

Xiao, S., Peng, J., Song, Y., Zhang, D., Liu, R., and Zeng, P. (2013) Degradation of biologically treated landfill leachate by using electrochemical process combined with UV irradiation. Separation and Purification Technology, In Press.

Xiao, S., Qu, J., Zhao, X., Liu, H., and Wan, D. (2009) Electrochemical process combined with UV light irradiation for synergistic degradation of ammonia in chloride-containing solutions. Water Research, 43(5), 1432-1440.

Xianling, L., Jianping, W., Qing, Y., and Xueming, Z. (2005) The pilot study for oil refinery wastewater treatment using a gas–liquid–solid three-phase flow airlift loop bioreactor. Biochemical engineering journal, 27(1), 40-44.

Yang, X., Shang, C., and Huang, J. (2005) BDP formation in breakpoint chlorination of wastewater. Water Research, 39(19), 4755-4767.

Ye, J., Mu, Y., Cheng, X., and Sun, D. (2011) Treatment of fresh leachate with high-strength organics and calcium from municipal solid waste incineration plant using UASB reactor. Bioresource technology, 102(9), 5498-5503.

Zhang, F., Feng, C., Jin, Y., Li, W., Hao, G., and Cui, J. (2009) Photocatalytic degradation of ammonia nitrogen with suspsended TiO_2. In Bioinformatics and Biomedical Engineering, 3rd International Conference, 1-4.

Zhao, X., Qu, J., Liu, H., Wang, C., Xiao, S., Liu, R., Liu, P., Lan, H., and Hu, C. (2010) Photoelectrochemical treatment of landfill leachate in a continuous flow reactor. Bioresource technology, 101(3), 865-869.

Zheng, G. Y., Davies, J. A., and Edwards, J. G. (1998) Photooxidation of ammonia in aqueous basic solutions. Recent Research Developments in Physical Chemistry, Vol. 2, 1011-1027.

Zhu, X., Castleberry, S. R., Nanny, M. A., and Butler, E. C. (2005) Effects of pH and catalyst concentration on photocatalytic oxidation of aqueous ammonia and nitrite in titanium dioxide suspensions. Environmental Science & Technology, 39(10), 3784-3791.

Zhu, X., Nanny, M. A., and Butler, E. C. (2007) Effect of inorganic anions on the titanium dioxide-based photocatalytic oxidation of aqueous ammonia and nitrite. Journal of Photochemisty and Photobiology A: Chemistry, 185(2-3), 289-294.

Zhu, X., Nanny, M.A, and Butler, E. C. (2008) Photocatalytic oxidation of aqueous ammonia in model gray waters. Water Research, 42(10-11), 2736-2744.

Appendix A – Chapter 4 Raw Data

Table A-1 Total Nitrogen data investigating the effect of pH on the photolysis of nitrogen.

[TN]=	26 mg/L			
[Cl]=	500 mg/L		**TN (mg/L)**	
ID	**pH**	**UV (mJ/cm^2)**	**Pre**	**Post**
UV-A1	8	100	32.01	32.08
UV-A2	8	100	28.61	31.19
UV-A3	8	100	29.57	30.25
UV-G1	8	500	24.96	21.28
UV-G2	8	500	22.4	23.39
UV-I1	8	1000	21.56	22.32
UV-I2	8	1000	24.8	23.68
UV-B1	10	100	28.58	28.59
UV-B2	10	100	28.45	29.69
UV-B3	10	100	29.25	28.21
UV-H1	10	500	24.91	17.12
UV-H2	10	500	24.38	17.98
UV-J1	10	1000	23.64	10.75
UV-J2	10	1000	26.25	15.57
UV-AA1	12	100	26.36	24.01
UV-AA2	12	100	26.85	22.75
UV-AB1	12	500	26.11	16.52
UV-AB2	12	500	26.57	18.4
UV-AC1	12	1000	26.55	9.162
UV-AC2	12	1000	22.39	10.42

Table A-2 Total Nitrogen data investigating the effect of chloride concentration on the photolysis of nitrogen.

[TN]=	26 mg/L			
[Cl]=	60 mg/L		**TN (mg/L)**	
ID	**pH**	**UV (mJ/cm^2)**	**Pre**	**Post**
UV-Z1	10	100	35.97	32.95
UV-Z2	10	100	34.73	31.05
UV-Z3	10	500	32.75	20.56
UV-Z4	10	500	31.42	21.82
UV-Z5	10	1000	35.86	15.55
UV-Z6	10	1000	31.36	15.49
UV-Y1	12	100	29.66	29.46
UV-Y2	12	100	33.63	28.66
UV-Y3	12	500	31.79	18.55
UV-Y4	12	500	24.33	15.21
UV-Y5	12	1000	22.12	7.926
UV-Y6	12	1000	32.71	10.9

Table A-3 Total Nitrogen data investigating the effect of initial nitrogen concentration on the photolysis of nitrogen.

[TN]=	260 mg/L			
[Cl]=	650 mg/L		**TN (mg/L)**	
ID	**pH**	**UV (mJ/cm^2)**	**Pre**	**Post**
UV-W1	10	100	258.9	239.3
UV-W2	10	100	250.4	217.3
UV-W3	10	500	248.1	174.3
UV-W4	10	500	251.7	177.9
UV-W5	10	1000	245.8	140.1
UV-W6	10	1000	249.3	126.2
UV-X1	12	100	260.3	237.4
UV-X2	12	100	267.3	241.1
UV-X3	12	500	263.2	160
UV-X4	12	500	271	158
UV-X5	12	1000	265.5	98.83
UV-X6	12	1000	253.9	92.72

Table A-4 Ammonium nitrogen data investigating the effect of pH on the photolysis of nitrogen.

$[NH_4^+]$= 40 mg/L [Cl]= 500 mg/L			$[NH_4^+\text{-}N]$ (mg/L)	
ID	**pH**	**UV (mJ/cm^2)**	**Pre**	**Post**
UV-A1	8	100	36.31	35.32
UV-A2	8	100	34.04	33.95
UV-A3	8	100	35.10	33.19
UV-G1	8	500	37.64	36.13
UV-G2	8	500	34.90	35.48
UV-I1	8	1000	33.96	34.69
UV-I2	8	1000	35.01	33.57
UV-B1	10	100	34.48	31.40
UV-B2	10	100	35.61	32.80
UV-B3	10	100	34.67	31.98
UV-H1	10	500	34.81	26.21
UV-H2	10	500	36.38	26.02
UV-J1	10	1000	34.02	17.25
UV-J2	10	1000	32.90	22.05
UV-AA1	12	100	37.33	32.63
UV-AA2	12	100	37.09	31.75
UV-AB1	12	500	36.24	24.70
UV-AB2	12	500	35.77	26.37
UV-AC1	12	1000	36.23	16.76
UV-AC2	12	1000	38.08	15.67

Table A-5 Ammonium data for control experiments studying the volatilization of ammonium.

	$[NH_4^+]$ (mg/L)
pH=8.0, $[NH_4^+]$=40 mg/L, [Cl]=500 mg/L - T=10 min	44.07
pH=8.0, $[NH_4^+]$=40 mg/L, [Cl]=500 mg/L - T=30 min	42.61
pH=8.0, $[NH_4^+]$=40 mg/L, [Cl]=500 mg/L - T=50 min	43.37
pH=8.0, $[NH_4^+]$=40 mg/L, [Cl]=500 mg/L - T=70 min	40.73

Table A-6 Ammonium data for control experiments studying the volatilization of ammonium.

	$[NH_4^+]$ (mg/L)
pH=8.0, $[NH_4^+]$=40 mg/L, [Cl]=500 mg/L - T=Pre treatment	45.25
pH=8.0, $[NH_4^+]$=40 mg/L, [Cl]=500 mg/L - T=30 min	41.87
pH=8.0, $[NH_4^+]$=40 mg/L, [Cl]=500 mg/L - T=120 min	42.56
pH=8.0, $[NH_4^+]$=40 mg/L, [Cl]=500 mg/L - T=Post treatment	42.49

Table A-7 pH data investigating the effect of pH on the photolysis of nitrogen.

[TN]=	26 mg/L			
[Cl]=	500 mg/L		**pH**	
ID	**pH**	**UV (mJ/cm^2)**	**Pre**	**Post**
UV-A1	8	100	8.03	7.65
UV-A2	8	100	8	7.63
UV-A3	8	100	7.98	7.53
UV-G1	8	500	8.01	6.59
UV-G2	8	500	7.99	6.66
UV-I1	8	1000	8.02	6.66
UV-I2	8	1000	7.99	6.72
UV-B1	10	100	10.02	9.8
UV-B2	10	100	10.01	9.82
UV-B3	10	100	10.01	9.76
UV-H1	10	500	10.01	9.46
UV-H2	10	500	9.98	9.49
UV-J1	10	1000	10.01	9.01
UV-J2	10	1000	9.99	9.08
UV-AA1	12	100	12.01	11.89
UV-AA2	12	100	11.98	11.87
UV-AB1	12	500	11.99	11.71
UV-AB2	12	500	12	11.74
UV-AC1	12	1000	12.02	11.49
UV-AC2	12	1000	12	11.42

Table A-8 pH data investigating the effect of chloride concentration on the photolysis of nitrogen.

[TN]= 26 mg/L **[Cl]=** 60 mg/L			**pH**	
ID	**pH**	**UV (mJ/cm^2)**	**Pre**	**Post**
UV-Z1	10	100	10.04	9.79
UV-Z2	10	100	10.01	9.74
UV-Z3	10	500	9.99	9.45
UV-Z4	10	500	10.04	9.46
UV-Z5	10	1000	9.99	9.04
UV-Z6	10	1000	10.01	9.06
UV-Y1	12	100	11.99	11.9
UV-Y2	12	100	12.02	11.93
UV-Y3	12	500	12.02	11.74
UV-Y4	12	500	12.01	11.67
UV-Y5	12	1000	12.04	11.51
UV-Y6	12	1000	12.01	11.51

Table A-9 pH data investigating the effect of initial nitrogen concentration on the photolysis of nitrogen.

[TN]= 260 mg/L **[Cl]=** 650 mg/L			**pH**	
ID	**pH**	**UV (mJ/cm^2)**	**Pre**	**Post**
UV-W1	10	100	9.99	9.82
UV-W2	10	100	9.98	9.922
UV-W3	10	500	9.99	9.52
UV-W4	10	500	9.99	9.58
UV-W5	10	1000	9.99	9.28
UV-W6	10	1000	10.03	9.37
UV-X1	12	100	12	11.93
UV-X2	12	100	12.02	11.87
UV-X3	12	500	11.99	11.68
UV-X4	12	500	12.01	11.76
UV-X5	12	1000	12.02	11.48
UV-X6	12	1000	12.03	11.57

Table A-10 pCBA data investigating the effect of pH on the photolysis of nitrogen.

[TN]=	26 mg/L			
[Cl]=	500 mg/L		**pCBA (μM)**	
ID	**pH**	**UV (mJ/cm^2)**	**Pre**	**Post**
UV-A1	8	100	40.2105	39.839
UV-A2	8	100	47.096	46.526
UV-A3	8	100	35.9205	36.0445
UV-G1	8	500	43.6415	39.9385
UV-G2	8	500	45.267	40.7855
UV-I1	8	1000	46.7455	42.113
UV-I2	8	1000	49.7475	33.378
UV-B1	10	100	49.016	48.929
UV-B2	10	100	45.8005	46.2275
UV-B3	10	100	46.9635	45.718
UV-H1	10	500	51.2015	51.2445
UV-H2	10	500	40.4295	37.025
UV-J1	10	1000	52.061	44.156
UV-J2	10	1000	55.627	48.2685
UV-AA1	12	100	37.857	42.451
UV-AA2	12	100	50.1775	48.1085
UV-AB1	12	500	60.1635	57.4995
UV-AB2	12	500	51.0421	48.791
UV-AC1	12	1000	50.538	43.934
UV-AC2	12	1000	38.4215	34.6435

Table A-11 pCBA data investigating the effect of chloride concentration on the photolysis of nitrogen.

[TN]=	26 mg/L			
[Cl]=	60 mg/L		**pCBA (µM)**	
ID	**pH**	**UV (mJ/cm^2)**	**Pre**	**Post**
UV-Z1	10	100	48.801	46.729
UV-Z2	10	100	47.9615	46.051
UV-Z3	10	500	57.5365	53.3495
UV-Z4	10	500	49.989	46.99
UV-Z5	10	1000	40.676	36.498
UV-Z6	10	1000	51.033	44.9335
UV-Y1	12	100	56.7385	48.513
UV-Y2	12	100	47.9887	54.8715
UV-Y3	12	500	55.1525	53.61
UV-Y4	12	500	46.4555	45.7435
UV-Y5	12	1000	50.469	47.771
UV-Y6	12	1000	45.888	44.0235

Table A-12 pCBA data investigating the effect of initial nitrogen concentration on the photolysis of nitrogen.

[TN]=	26 mg/L			
[Cl]=	650 mg/L		**pCBA (µM)**	
ID	**pH**	**UV (mJ/cm^2)**	**Pre**	**Post**
UV-W1	10	100	49.0395	46.972
UV-W2	10	100	52.01	51.369
UV-W3	10	500	51.53	45.089
UV-W4	10	500	46.171	43.169
UV-W5	10	1000	52.5065	46.075
UV-W6	10	1000	50.845	44.1845
UV-X1	12	100	53.304	55.671
UV-X2	12	100	55.1375	56.8865
UV-X3	12	500	54.0755	51.4315
UV-X4	12	500	68.483	62.279
UV-X5	12	1000	52.7575	44.606
UV-X6	12	1000	63.819	47.345

Table A-13 pCBA data for control experiments investigating production of OH· radicals.

[pCBA]=	50 µM		**pCBA (µM)**	
ID	**pH**	**UV (mJ/cm^2)**	**Pre**	**Post**
OH-A1	8	100	17.8014	17.273
OH-A2	8	100	38.304	39.3785
OH-A3	8	500	41.701	38.4765
OH-A4	8	500	41.5385	39.835
OH-A5	8	1000	42.6305	38.397
OH-A6	8	1000	48.525	38.9555
OH-B1	10	100	52.204	55.48
OH-B3	10	500	47.836	41.596
OH-B4	10	500	57.037	50.266
OH-B5	10	1000	61.879	43.8855
OH-B6	10	1000	63.9775	49.926
OH-C1	12	100	42.1555	45.8715
OH-C2	12	100	59.286	57.3265
OH-C3	12	500	55.026	48.986
OH-C4	12	500	60.086	54.8089
OH-C5	12	1000	36.59	21.1445
OH-C6	12	1000	49.869	33.305

Table A-14 Total nitrogen data for the treatment of municipal wastewater.

			TN (mg/L)	
ID	**pH**	**UV (mJ/cm^2)**	**Pre**	**Post**
WW-UV-1	10	100	26.74	24.92
WW-UV-2	10	100	30.31	27.12
WW-UV-3	10	500	27.36	15.45
WW-UV-4	10	500	29.71	15.93
WW-UV-5	10	1000	30.17	8.926
WW-UV-6	10	1000	29.3	8.86

Figure A-1 pCBA degradation for [TN]=26 mg/L, [Cl$^-$]=500 mg/L.

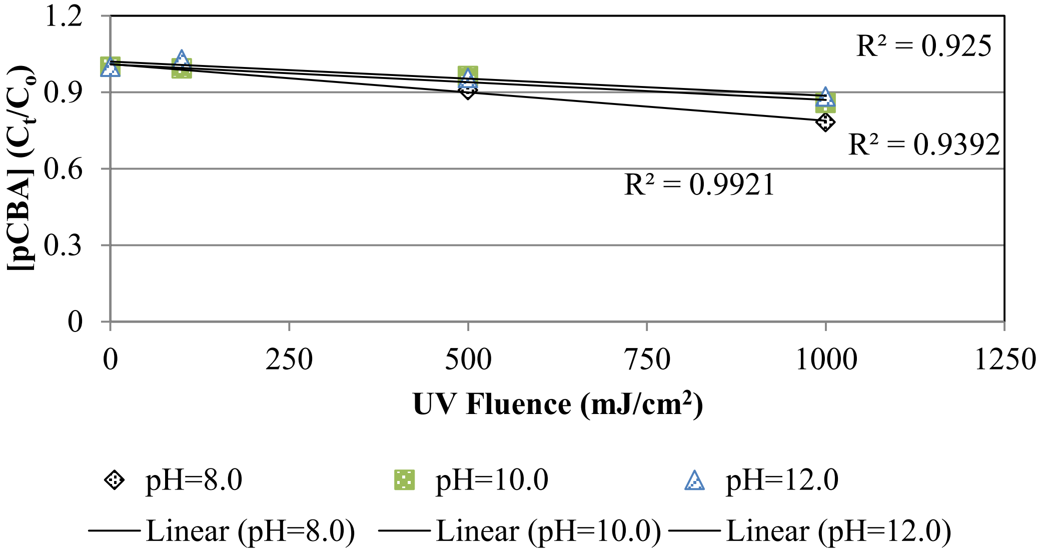

Figure A-2 pCBA degradation for [TN]=26 mg/L, [Cl$^-$]=60 mg/L.

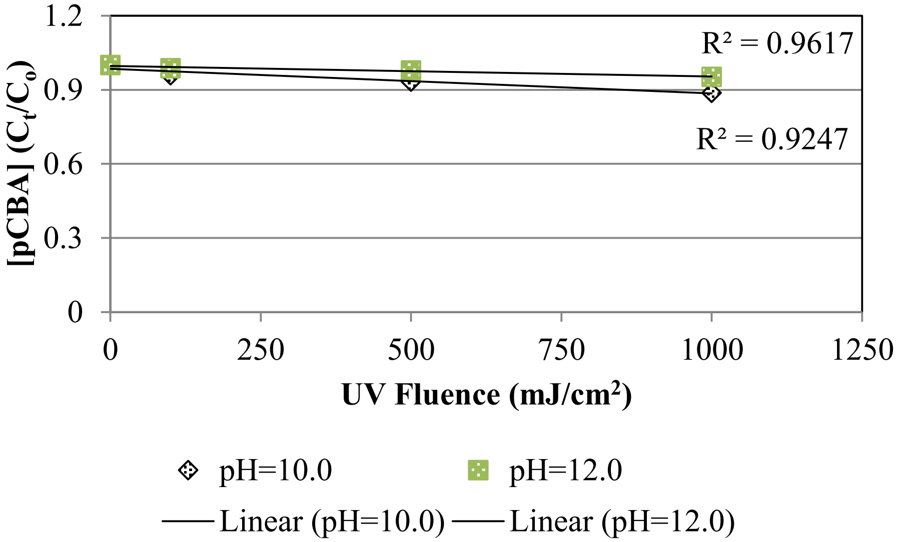

Figure A-3 pCBA degradation for [TN]=260 mg/L, [Cl$^-$]=650 mg/L.

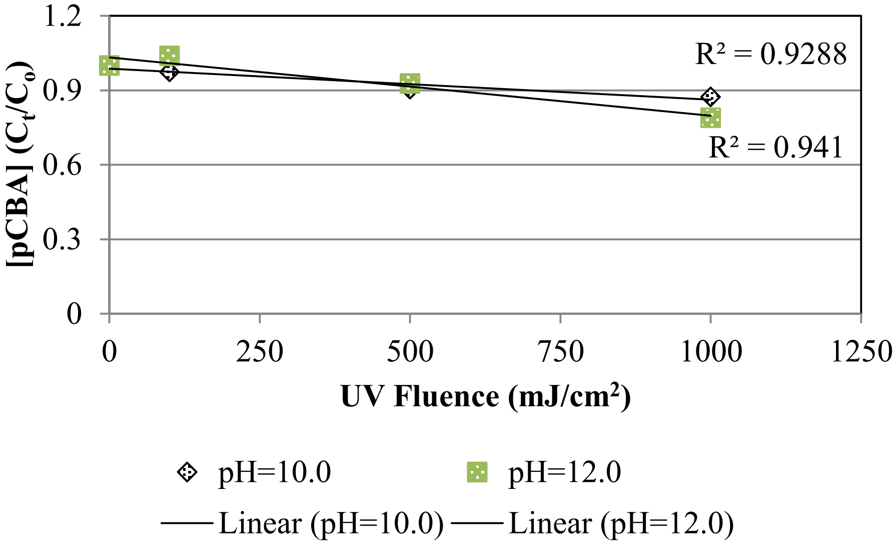

Figure A-4 pCBA degradation for control experiments investigating the production of OH· radicals.

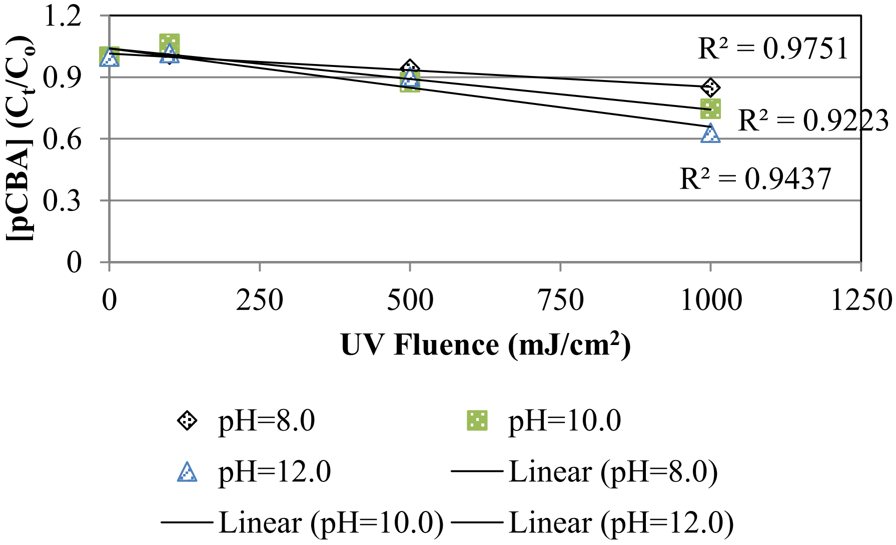

Appendix B – Chapter 5 Raw Data

Table B-1 Ammonium, total nitrogen, pH, nitrite, and nitrate data for synthetic wastewater trials at $[Cl^-]$=450 mg/L.

$[NH_4^+]$= **[Cl]=**	75 mg/L 450 mg/L			**$[NH_4^+]$ (mg/L)**		**TN (mg/L)**		**pH**		**$[NO_2^-]$ (mg/L)**		**$[NO_3^-]$ (mg/L)**	
ID	**Time (min)**	**pH**	**I (mA/cm^2)**	**Pre**	**Post**	**Pre**	**Post**	**Pre**	**Post**	**Pre**	**Post**	**Pre**	**Post**
AA1	20	5.7	3.75	74.1	61.58	50.22	42.67	5.73	3.71	0.17	0	0.17	0
AA2	20	5.7	3.75	72.555	62.405	48.64	39.93	5.71	3.84	0	0.71	0	0.71
AA3	40	5.7	3.75	78.515	56.275	44.01	32.67	5.73	3.34	2.89	1.46	2.89	1.46
AA4	40	5.7	3.75	72.455	52.205	47.73	37.8	5.71	3.33	0.21	0	0.21	0
AA5	60	5.7	3.75	71.55	44.105	46.49	28.48	5.74	3.25	0.21	0	0.21	0
AA6	60	5.7	3.75	73.94	45.43	46.96	27.53	5.69	3.31	0	0	0	0
CC1	20	9.7	3.75	75.48	57.955	50.87	36.16	9.71	9.63	0.18	0	0	0
CC2	20	9.7	3.75	75.42	63.345	50.77	42.49	9.72	9.57	0.63	0.11	0	0
CC3	40	9.7	3.75	76.745	48.555	52.54	29.51	9.69	9.34	0	0.72	0.19	0
CC4	40	9.7	3.75	74.235	47.195	51.38	31.71	9.73	9.31	0.76	0	0.44	0.2
CC5	60	9.7	3.75	76.53	42.9	47.67	27.28	9.71	9.03	0.75	0.37	0	0
CC6	60	9.7	3.75	77.15	46.93	49.54	29.58	9.73	9.14	0	0	0.36	0
DD1	20	5.7	7.5	74.91	52.825	51.27	36.09	5.73	3.25	0.65	0	0	0
DD2	20	5.7	7.5	72.2	48.47	49.51	31.16	5.73	3.29	0	0.74	0.2	0
DD3	40	5.7	7.5	77.895	38.96	46.15	21.42	5.68	3.18	0.23	0	0	2.75
DD4	40	5.7	7.5	76.43	33.635	46.14	18.27	5.7	3.14	0	0.3	0	0
DD5	60	5.7	7.5	76.94	25.32	45.7	12.8	5.69	3.11	0.31	0	0.28	2.29
DD6	60	5.7	7.5	77.795	18.345	46.01	8.13	5.7	3.2	0.27	0	0.43	5.08
BB1	20	9.7	7.5	74.75	45.135	47.37	28.32	9.69	9.22	0	0.24	0	0.28
BB2	20	9.7	7.5	72.6	46.005	46.33	28.38	9.69	9.32	0	0	0	0.21
BB3	40	9.7	7.5	73.475	18.1	49.38	10.74	9.7	3.91	0.39	0	0.49	0.25
BB4	40	9.7	7.5	74.275	18.29	45.33	10.56	9.72	3.82	0	0.18	0	0.17
BB5	60	9.7	7.5	74.23	0	42.05	1.572	9.71	3.59	0.16	0.16	0	0
BB6	60	9.7	7.5	74.82	0.745	45.45	1.614	9.71	3.55	0	0	0	0.23

Table B-2 Chlorine (total and free), chloride, and monochloramine data for synthetic wastewater trials at [Cl$^-$]=450 mg/L.

[NH$_4^+$]= 75 mg/L **[Cl]=** 450 mg/L				**T Cl$_2$ (mg/L)**	**F Cl$_2$ (mg/L)**	**NH$_2$Cl (mg/L)**	**[Cl$^-$] (mg/L)**	
ID	**Time (min)**	**pH**	**I (mA/cm^2)**	**Post**	**Post**	**Post**	**Pre**	**Post**
AA1	20	5.7	3.75	14.4	0.79	13.61	533.91	474.82
AA2	20	5.7	3.75	17.2	0.99	16.21	509.39	458.48
AA3	40	5.7	3.75	17.6	1.66	15.94	474.37	454.35
AA4	40	5.7	3.75	17.9	1.56	16.34	495.4	504.97
AA5	60	5.7	3.75	46	6.5	39.5	489.57	487.01
AA6	60	5.7	3.75	50	7.9	42.1	449.63	455.05
CC1	20	9.7	3.75	37	0.99	36.01	462.15	476.14
CC2	20	9.7	3.75	42	2.9	39.1	541.24	490.95
CC3	40	9.7	3.75	63	1.56	61.44	513.51	493.09
CC4	40	9.7	3.75	57	1.15	55.85	411.93	416.98
CC5	60	9.7	3.75	40	0.82	39.18	439.25	395.71
CC6	60	9.7	3.75	54	0.63	53.37	398.42	388.58
DD1	20	5.7	7.5	27	1.59	25.41	397.93	400.51
DD2	20	5.7	7.5	43	1.74	41.26	376.95	361.24
DD3	40	5.7	7.5	28	5	23	501.4	475.37
DD4	40	5.7	7.5	64	8.5	55.5	469.7	419.85
DD5	60	5.7	7.5	30	6	24	451.76	429.02
DD6	60	5.7	7.5	43	5	38	422.93	389.1
BB1	20	9.7	7.5	40	3.5	36.5	495.22	437.28
BB2	20	9.7	7.5	50	2.3	47.7	478.98	452.13
BB3	40	9.7	7.5	41	0.43	40.57	343.34	370.89
BB4	40	9.7	7.5	50	0.32	49.68	442.23	437.29
BB5	60	9.7	7.5	72	18.4	53.6	481.23	422.58
BB6	60	9.7	7.5	50	14.1	35.9	427.94	381.78

Table B-3 Ammonium, total nitrogen, pH, nitrite, and nitrate data for synthetic wastewater trials at $[Cl^-]$=4500 mg/L.

$[NH_4^+]$= 750 mg/L [Cl]= 4500 mg/L				$[NH_4^+]$ (mg/L)		TN (mg/L)		pH		$[NO_2^-]$ (mg/L)		$[NO_3^-]$ (mg/L)	
ID	**Time (min)**	**pH**	**I (mA/cm^2)**	**Pre**	**Post**	**Pre**	**Post**	**Pre**	**Post**	**Pre**	**Post**	**Pre**	**Post**
A1	20	5.7	20	775.15	625.15	509.5	439.45	5.76	2.89	0	2.1	2.6	3.9
A2	20	5.7	20	762.7	640.45	497.9	450.1	5.68	2.92	1	0	0.6	1.5
A3	40	5.7	20	779.1	532	518.2	397.15	5.69	2.49	1.6	0	2.6	1.5
A4	40	5.7	20	747	553.8	554.65	362.3	5.69	2.46	74	1.2	1.6	2.3
A5	60	5.7	20	758.3	463.1	511.55	306.75	5.72	2.36	3.9	0	1.2	0
A6	60	5.7	20	742.7	463.25	547.4	302.95	5.7	2.35	1.7	4.1	0	1.1
A7	80	5.7	20	744.7	363.65	512.55	229.75	5.76	2.31	0	0	1.2	0
A8	80	5.7	20	755.25	374.7	540.95	255.1	5.74	2.5	1	0	1	1.8
B1	20	9.7	20	690.75	533.75	526.2	407.55	9.69	9.44	1.9	1	2.4	0.7
B2	20	9.7	20	688.4	534.2	511.05	417.55	9.7	9.47	1	0	4.6	3.1
B3	40	9.7	20	703.35	398	506.25	300.9	9.71	9.25	1.3	3.3	0	0
B4	40	9.7	20	725.25	451.55	504.75	302.2	9.71	9.22	3.6	1.2	8.1	1.2
B5	60	9.7	20	697.25	309.4	493.95	220.9	9.68	5.19	0	1.8	7.2	0
B6	60	9.7	20	724.05	323.95	492.9	210.3	9.7	5.47	0.8	0	2.5	2.8
B7	80	9.7	20	747.3	248.55	552.2	153.6	9.68	2.67	1.8	1.1	6.2	1.5
B8	80	9.7	20	759.95	222.45	508.15	124.35	9.72	2.96	0	1.1	2.4	0
D1	20	5.7	40	750.75	524.05	527.7	359.1	5.69	2.47	0	1.2	0	3.5
D2	20	5.7	40	766.8	542.45	524.2	366.05	5.72	2.45	0	0	0	0
D3	40	5.7	40	799.75	361.95	558.6	225.2	5.68	2.37	0	0	0	0
D4	40	5.7	40	793.2	365.8	532.95	227.85	5.7	2.29	16.9	0	16.9	6.1
D5	60	5.7	40	762.2	195.75	531.6	92.425	5.71	2.52	3.1	3	3.1	1.7
D6	60	5.7	40	779.05	188.05	544.8	90.345	5.72	2.59	0	0	0	2.1
D7	80	5.7	40	737.2	0	522.15	3.9185	5.69	7.74	1.1	2.4	1.1	15.5
D8	80	5.7	40	790.4	0	533.25	4.133	5.73	7.33	8.6	3.7	8.6	17.9
C1	20	9.7	40	698.55	397.55	522.05	300.65	9.69	9.24	2.4	0.7	2.8	5.7
C2	20	9.7	40	701.85	385.9	518.2	292.2	9.68	9.2	2.8	1.1	2.3	1.6
C3	40	9.7	40	696.6	189.75	526.9	133.95	9.69	2.99	3.8	0	0	8.2
C4	40	9.7	40	763.7	230.85	523.2	115.05	9.7	2.97	0	0	9.3	0
C5	60	9.7	40	695.65	0	511.6	4.4465	9.69	7.67	4.4	3.7	1.3	16.4
C6	60	9.7	40	687.75	0	485.4	3.7215	9.71	7.39	0	1.1	4.8	11.3
C7	80	9.7	40	699.15	0	522.3	2.9995	9.73	9.59	1	2.6	2.2	13.3
C8	80	9.7	40	689.05	0	513.5	4.0775	9.69	8.22	0	2.4	1.6	17.5

Table B-4 Chlorine (total and free), chloride, and monochloramine data for synthetic wastewater trials at [Cl$^-$]=4500 mg/L.

[NH$_4^+$]= 750 mg/L **[Cl]=** 4500 mg/L				**T Cl$_2$ (mg/L)**	**F Cl$_2$ (mg/L)**	**NH$_2$Cl (mg/L)**	**[Cl$^-$] (mg/L)**	
ID	**Time (min)**	**pH**	**I (mA/cm^2)**	**Post**	**Post**	**Post**	**Pre**	**Post**
A1	20	5.7	20	120	30	90	5455.4	5079.3
A2	20	5.7	20	112	33	79	4574	5203.2
A3	40	5.7	20	157	31	126	4305	4380
A4	40	5.7	20	174	38	136	4233.3	4146.8
A5	60	5.7	20	190	41	149	4403.9	3947.6
A6	60	5.7	20	230	39	191	3896	3898.5
A7	80	5.7	20	320	44	276	3383.7	3748.8
A8	80	5.7	20	280	35	245	3630.4	3417.5
B1	20	9.7	20	290	8.6	281.4	4965.4	5043.7
B2	20	9.7	20	270	9.9	260.1	4879.3	4693.5
B3	40	9.7	20	320	10.1	309.9	4759.9	5120.4
B4	40	9.7	20	380	9.1	370.9	4023.9	3993.7
B5	60	9.7	20	116	21	95	5348	4376.7
B6	60	9.7	20	142	32	110	3994.7	4198.2
B7	80	9.7	20	97	29	68	4760.9	4122.6
B8	80	9.7	20	129	25	104	4231.9	4817
D1	20	5.7	40	186	43	143	5237.7	5143.1
D2	20	5.7	40	178	56	122	4845.2	4429.1
D3	40	5.7	40	159	17	142	4461.3	4125.5
D4	40	5.7	40	190	18.2	171.8	4445.4	4191.1
D5	60	5.7	40	142	10.9	131.1	4646.8	3725.3
D6	60	5.7	40	114	16.2	97.8	4565.7	3665.1
D7	80	5.7	40	770	590	180	4187.7	3222.1
D8	80	5.7	40	660	450	210	4598.9	3590.1
C1	20	9.7	40	300	11.6	288.4	4724.6	4524.6
C2	20	9.7	40	510	12.6	497.4	4526	4523.4
C3	40	9.7	40	77	8.4	68.6	4175.4	4445.1
C4	40	9.7	40	59	6.8	52.2	4834.4	5092.6
C5	60	9.7	40	240	171	69	3984.5	3587.1
C6	60	9.7	40	400	350	50	4779.8	3697.4
C7	80	9.7	40	1560	1530	30	4052.3	3702.3
C8	80	9.7	40	1680	1600	80	3860	3368.4

Table B-5 pH, chlorine (total and free), monochloramine, titanium, and ruthenium data for the electrolysis of municipal wastewater.

				pH		T Cl_2 (mg/L)	F Cl_2 (mg/L)	NH_2Cl (mg/L)	Ti (µg/L)		Ru (µg/L)	
ID	**Time (min)**	**pH**	**I (mA/cm^2)**	**Pre**	**Post**	**Post**	**Post**	**Post**	**Pre**	**Post**	**Pre**	**Post**
WW1	20	10	5	10.01	9.86	15.6	0.96	14.64	10.945	7.452	1.482	4.62
WW2	20	10	5	9.97	9.88	14	1.34	12.66	6.662	10.93	0.366	5.428
WW3	40	10	5	10.07	9.79	18.5	0.88	17.62	12.514	14.453	0.269	10.09
WW4	40	10	5	10.03	9.84	23	1.15	21.85	7.744	14.325	0.203	5.04
WW5	60	10	5	9.96	9.77	16	0.76	15.24	9.565	8.11	0.147	6.816
WW6	60	10	5	10.02	9.78	23	0.77	22.23	9.07	8.1	0.11	8.069

Table B-6 Ammonium, total nitrogen, nitrate, and nitrite data for the electrolysis of municipal wastewater.

				[NH_4^+] (mg/L)		TN (mg/L)		[NO_2^-] (mg/L)		[NO_3^-] (mg/L)	
ID	**Time (min)**	**pH**	**I (mA/cm^2)**	**Pre**	**Post**	**Pre**	**Post**	**Pre**	**Post**	**Pre**	**Post**
WW1 – E	20	10	5	36.714	32.032	19.62	15.48	0.17	0.13	0.11	0.76
WW2 – E	20	10	5	36.162	30.97	18.79	15.28	0.16	0.33	0.13	1.71
WW3 – E	40	10	5	38.044	28.016	19	13.41	0.15	0.2	0.87	2.63
WW4 – E	40	10	5	38.246	27.064	19.15	12.26	0.3	0.13	1.48	2.82
WW5 – E	60	10	5	38.006	23.278	18.91	9.228	1.23	0.25	1.29	4.22
WW6 – E	60	10	5	37.354	22.662	18.11	9.022	0.22	0	1.29	3.44

Table B-7 TTHMs and THAAs data for the electrolysis of municipal wastewater.

ID	**Time (min)**	**pH**	**I (mA/cm^2)**	**TTHMs (µg/L)**	**THAAs (µg/L)**
WW1 – E	20	10	5	38.693	87.976
WW2 – E	20	10	5	33.079	88.754
WW3 – E	40	10	5	29.496	123.877
WW4 – E	40	10	5	43.913	154.931
WW5 – E	60	10	5	28.98	203.415
WW6 - E	60	10	5	30.745	207.72

Appendix C – Chapter 6 Raw Data

Table C-1 pH, chlorine (total and free), and monochloramine data for synthetic wastewater trials with the photoelectrochemical and electrochemical processes.

$[NH_4^+]$: 760 mg/L **$[Cl^-]$:** 5100 mg/L				**pH**			**T Cl_2 (mg/L)**		**F Cl_2 (mg/L)**		**NH_2Cl (mg/L)**	
ID	**Time (min)**	**pH**	**I (mA/cm^2)**	**Pre**	**UV+E**	**E**	**UV+E**	**E**	**UV+E**	**E**	**UV+E**	**E**
L1	20	5.7	40	5.68	2.64	2.65	92	61	11.4	8	80.6	53
L2	20	5.7	40	5.71	2.69	2.73	90	85	11.1	7.9	78.9	77.1
L3	40	5.7	40	5.69	2.41	2.44	99	110	6	8.7	93	101.3
L4	40	5.7	40	5.73	2.37	2.4	101	104	6.5	10.1	94.5	93.9
L5	60	5.7	40	5.71	2.32	2.23	81	61	8.8	8.2	72.2	52.8
L6	60	5.7	40	5.68	2.59	2.41	50	82	5	9.2	45	72.8
L7	80	5.7	40	5.73	2.99	7.14	270	510	240	400	30	110
L8	80	5.7	40	5.69	5.42	4.54	173	183	165	168	8	15

Table C-2 Ammonium and total nitrogen data for synthetic wastewater trials with the photoelectrochemical and electrochemical processes.

$[NH_4^+]$: 760 mg/L **$[Cl^-]$:** 5100 mg/L				**$[NH_4^+]$ (mg/L)**			**TN (mg/L)**		
ID	**Time (min)**	**pH**	**I (mA/cm^2)**	**Pre**	**UV+E**	**E**	**Pre**	**UV+E**	**E**
L1	20	5.7	40	741.6	508.45	484.85	380.95	281.5	301.95
L2	20	5.7	40	740.8	494.85	489.75	389.9	279.1	271.3
L3	40	5.7	40	818.25	365.6	374.6	395.5	184.55	181.2
L4	40	5.7	40	816.65	355.75	357.75	398.75	192.75	181.85
L5	60	5.7	40	776.05	177.65	191	392.1	90.035	100.565
L6	60	5.7	40	731.05	173.55	174.65	403.35	98.035	94.555
L7	80	5.7	40	730.5	0	0	460.65	3.595	4.253
L8	80	5.7	40	747.8	0	0	430.45	3.973	3.3205

Table C-3 Nitrite and nitrate data for synthetic wastewater trials with the photoelectrochemical and electrochemical processes.

$[NH_4^+]$:	760 mg/L								
$[Cl^-]$:	5100 mg/L			**$[NO_2^-]$ (mg/L)**			**$[NO_3^-]$ (mg/L)**		
ID	**Time (min)**	**pH**	**I (mA/cm^2)**	**Pre**	**UV+E**	**E**	**Pre**	**UV+E**	**E**
L1	20	5.7	40	0	3.5	0	0	0	0
L2	20	5.7	40	0	1.3	0	0	0	0
L3	40	5.7	40	0	0	0	2.1	189	0
L4	40	5.7	40	0	0	0	0	204	0
L5	60	5.7	40	0	1.2	1.1	0	0	0
L6	60	5.7	40	0	0	3	0	0	0
L7	80	5.7	40	0	0	0	0	14.9	0
L8	80	5.7	40	0	0	0.8	0	181.9	0

Table C-4 Chloride and pCBA data for synthetic wastewater trials with the photoelectrochemical and electrochemical processes.

$[NH_4^+]$:	760 mg/L								
$[Cl^-]$:	5100 mg/L			**$[Cl^-]$ (mg/L)**			**pCBA (µM)**		
ID	**Time (min)**	**pH**	**I (mA/cm^2)**	**Pre**	**UV+E**	**E**	**Pre**	**UV+E**	**E**
L1	20	5.7	40	4819.2	4861.1	4488	48.8295	37.4705	40.398
L2	20	5.7	40	4910.1	4452.1	4756.8	49.387	37.1235	42.2275
L3	40	5.7	40	5488.8	4724.4	4458.3	48.594	32.101	45.1485
L4	40	5.7	40	5146.6	4278.3	4467.9	53.9805	19.1495	40.0895
L5	60	5.7	40	5441.5	4635	4120	45.549	17.7745	33.5945
L6	60	5.7	40	4928.8	3995.3	4176.2	45.001	16.136	19.9485
L7	80	5.7	40	4869.2	3794.4	3847.2	45.34	17.1715	29.781
L8	80	5.7	40	5471.1	3975.2	4085.2	46.733	13.905	20.613

Table C-5 pH, chlorine (total and free), monochloramine data for the photoelectrochemical and electrochemical treatment of municipal wastewater.

				pH		pH		T Cl_2 (mg/L)		F Cl_2 (mg/L)		NH_2Cl (mg/L)	
ID	**Time (min)**	**pH**	**I (mA/cm^2)**	**Pre**	**UV+E**	**Pre**	**E**	**UV+E**	**E**	**UV+E**	**E**	**UV+E**	**E**
WW1	20	10	5	9.94	9.82	10.01	9.86	13.1	15.6	1.26	0.96	11.84	14.64
WW2	20	10	5	9.97	9.9	9.97	9.88	14.2	14	1.58	1.34	12.62	12.66
WW3	40	10	5	10.03	9.88	10.07	9.79	16.5	18.5	1.1	0.88	15.4	17.62
WW4	40	10	5	10.05	9.91	10.03	9.84	16.3	23	1.58	1.15	14.72	21.85
WW5	60	10	5	9.96	9.77	9.96	9.77	19.4	16	1.72	0.76	17.68	15.24
WW6	60	10	5	10.05	9.69	10.02	9.78	17.6	23	1.1	0.77	16.5	22.23

Table C-6 Chloride and nitrite data for the photoelectrochemical and electrochemical treatment of municipal wastewater.

				$[Cl^-]$ (mg/L)		$[Cl^-]$ (mg/L)		$[NO_2^-]$ (mg/L)		$[NO_2^-]$ (mg/L)	
ID	**Time (min)**	**pH**	**I (mA/cm^2)**	**Pre**	**UV+E**	**Pre**	**E**	**Pre**	**UV+E**	**Pre**	**E**
WW1	20	10	5	171.954	188.56	126.88	167.4	0.494	0.5	0.17	0.13
WW2	20	10	5	224.968	187.134	193.62	157.67	0.384	0.63	0.16	0.33
WW3	40	10	5	75.926	163.962	160.09	168.89	0.592	0.512	0.15	0.2
WW4	40	10	5	216.834	188.748	173.2	166.14	0.402	0.662	0.3	0.13
WW5	60	10	5	217.08	201.456	145.66	171.73	0.37	0.732	1.23	0.25
WW6	60	10	5	226.524	182.236	175.72	129.78	0.58	0.678	0.22	0

Table C-7 Nitrate and ammonium data for the photoelectrochemical and electrochemical treatment of municipal wastewater.

				$[NO_3^-]$ (mg/L)		$[NO_3^-]$ (mg/L)		$[NH_4^+]$ (mg/L)		$[NH_4^+]$ (mg/L)	
ID	**Time (min)**	**pH**	**I (mA/cm^2)**	**Pre**	**UV+E**	**Pre**	**E**	**Pre**	**UV+E**	**Pre**	**E**
WW1	20	10	5	1.304	2.126	0.11	0.76	36.954	33.18	36.714	32.032
WW2	20	10	5	0.024	2.146	0.13	1.71	37.816	32.842	36.162	30.97
WW3	40	10	5	0.922	2.962	0.87	2.63	38.644	27.124	38.044	28.016
WW4	40	10	5	1.772	3.486	1.48	2.82	38.246	27.956	38.246	27.064
WW5	60	10	5	1.524	5.962	1.29	4.22	38.006	22.554	38.006	23.278
WW6	60	10	5	1.638	5.226	1.29	3.44	37.354	19.232	37.354	22.662

Table C-8 Total nitrogen, TTHMs, and THAAs data for the photoelectrochemical and electrochemical treatment of municipal wastewater.

				TN (mg/L)		TN (mg/L)		TTHMs (µg/L)		THAAs (µg/L)	
ID	Time (min)	pH	I (mA/cm^2)	Pre	UV+E	Pre	E	UV+E	E	UV+E	E
WW1	20	10	5	19.47	15.74	19.62	15.48	29.168	38.693	79.797	87.976
WW2	20	10	5	19.39	15.91	18.79	15.28	32.346	33.079	84.465	88.754
WW3	40	10	5	19.75	11.87	19	13.41	51.643	29.496	145.962	123.877
WW4	40	10	5	19.27	12.26	19.15	12.26	42.131	43.913	138.231	154.931
WW5	60	10	5	18.78	8.549	18.91	9.228	38.604	28.98	204.554	203.415
WW6	60	10	5	19.4	8.728	18.11	9.022	44.662	30.745	199.611	207.723

Table C-9 Titanium and ruthenium data for the photoelectrochemical and electrochemical treatment of municipal wastewater.

				Ti (µg/L)		Ti (µg/L)		Ru (µg/L)		Ru (µg/L)	
ID	Time (min)	pH	I (mA/cm^2)	Pre	UV+E	Pre	E	Pre	UV+E	Pre	E
WW1	20	10	5	9.289	8.730	10.945	7.452	0.164	3.306	1.482	4.625
WW2	20	10	5	8.376	7.626	6.662	10.930	0.140	2.785	0.366	5.428
WW3	40	10	5	7.523	8.027	12.514	14.453	0.120	5.042	0.269	10.099
WW4	40	10	5	6.803	7.314	7.745	14.325	0.114	4.440	0.203	5.040
WW5	60	10	5	10.294	7.263	9.565	8.114	0.108	8.606	0.147	6.816
WW6	60	10	5	9.369	7.506	9.078	8.100	0.098	5.491	0.110	8.069

Figure C-1 pCBA degradation for synthetic wastewater trials with the photoelectrochemical and electrochemical processes.